2007

Investigating the Spring Bloom in San Francisco Bay: Links between Water Chemistry, Metal Cycling, Mercury Speciation, and Phytoplankton Community Composition

Allison C. Luengen
University of San Francisco, aluengen@usfca.edu

UNIVERSITY OF CALIFORNIA

SANTA CRUZ

INVESTIGATING THE SPRING BLOOM IN SAN FRANCISCO BAY: LINKS BETWEEN WATER CHEMISTRY, METAL CYCLING, MERCURY SPECIATION, AND PHYTOPLANKTON COMMUNITY COMPOSITION

A dissertation submitted in partial satisfaction
of the requirements for the degree of

DOCTOR OF PHILOSOPHY

in

ENVIRONMENTAL TOXICOLOGY

by

Allison Christine Luengen

June 2007

The Dissertation of Allison Christine Luengen
is approved:

Professor A. Russell Flegal, Chair

Professor Kenneth W. Bruland

Professor Raphael M. Kudela

Professor Peter T. Raimondi

Lisa C. Sloan
Vice Provost and Dean of Graduate Studies

TABLE OF CONTENTS

LIST OF TABLES

LIST OF FIGURES

ABSTRACT

Allison Christine Luengen

Investigating the spring bloom in San Francisco Bay: Links between water chemistry, metal cycling, mercury speciation, and phytoplankton community composition

This dissertation addresses the relationship between two problems facing estuaries nationwide: nutrient enrichment and metal contamination. The focus is on the southern reach of San Francisco Bay, where high nutrient concentrations can control the magnitude of the predictably occurring spring phytoplankton bloom. The bloom in this study, in spring 2003, was one of the largest blooms on record, exceeding 150 $\mu g\ L^{-1}$ of chlorophyll *a*. As the bloom grew, diatoms (e.g. *Thalassiosira punctigera*) depleted dissolved nutrients from the water column, including the silicate required for their frustules. Along with nutrients, the bloom depleted dissolved Mn, Ni, Pb, and methyl mercury (MeHg). That depletion was statistically significant when the water chemistry data were reduced into three factors by principal component analysis, and the effect of those factors on trace metal concentrations was examined. Algal uptake of trace metals could entrain those metals within the estuary and affect their bioavailability to higher trophic levels through bloom dilution. Consistent with bloom dilution, we calculated that MeHg concentrations in phytoplankton decreased when the bloom peaked. However, that decrease was a transient event, caused by depletion of MeHg from the water column. Concentrations of MeHg and other dissolved metals returned to pre-bloom values, and even exceeded those values, as phytoplankton decayed. The decomposition of

phytoplankton presumably caused suboxic conditions in surficial sediments and led to release of trace metals from historically contaminated sediments. Because sediments contain large reservoirs of metals, the most important impact of the recently observed increase in algal biomass in the estuary could be release of metals from sediments during algal decomposition. As the diatoms decayed following nutrient depletion, small phytoplankton (e.g., *Synechocystis sp.*) increased. Statistical analyses (multidimensional scaling) found significant spatial and temporal differences in phytoplankton communities. Those community patterns were linked to water temperature and dissolved ammonium concentrations, demonstrating the myriad effects of nutrient enrichment in this system. However, algal community composition was not related to dissolved metal concentrations. This research shows that nutrient enrichment affects the magnitude of the bloom and thereby alters metal cycling, but the relationship is unidirectional because metals do not shape algal community composition.

ACKNOWLEDGMENTS

The text of this dissertation includes a reprint of the following previously published material: Luengen, A. C., P. T. Raimondi, and A. R. Flegal. 2007. Contrasting biogeochemistry of six trace metals during the rise and decay of a spring phytoplankton bloom in San Francisco Bay. *Limnology and Oceanography* **52:** 1112-1130. The co-authors listed in this publication directed and supervised the research which forms the basis for the dissertation.

In addition to my co-authors, I would like to thank the researchers at the United States Geological Survey (USGS) who made this project possible by donating the ship time and in-kind analyses: Jim Cloern, Steve Hagar, Amy Little, Cary Lopez, and Tara Schraga. I am also grateful to Scott Conard and Byron Richards, the crew members of the R/V *Polaris.*

My committee members and my advisor also helped shape this research. I acknowledge Ken Bruland, Russ Flegal, Raphael Kudela, Sam Luoma, and Pete Raimondi. My advisor Russ Flegal gave me the freedom to pursue my own research interests. The resulting interdisciplinary approach was made possible by the guidance of my committee members and their diverse backgrounds. I am grateful to Pete Raimondi for teaching me the statistical techniques to analyze my data and to my other committee members for working with me as I learned how to present the results in a meaningful format.

My colleagues in the WIGS group at the University of California at Santa Cruz (UCSC) helped me tremendously during this project. I thank Frank Black, Christopher Conaway, J.R. Flanders, Celine Gallon, Mari Gilmore, Ana Gonzalez, Sharon Hibdon, Brian Johnson, Mary Langsner, Fiona Morris, Charley Rankin, Mara Ranville, Genine Scelfo, and Hans Schwing. I owe a special thanks to Christopher Conaway for his support during this project, including our numerous predawn trips over the hill for sampling and conferences.

For the analytical parts of this project, I am in debt to Rob Franks for his assistance with mass spectrometry and optical emission spectrometry. In addition, Nicolas Bloom, Studio Geochemistry, opened the doors of his laboratory to me for the methyl mercury analyses. His insights also made it possible for me to replicate his setup in our lab. My trip to his lab was made possible by a student research award from the Northern California Society of Environmental Toxicology and Chemistry.

Other sources of funding that made this research possible included: a Dissertation Year Fellowship Award from the Graduate Division at UCSC, a grant from the University of California Water Resources Center, a Center for the Dynamics and Evolution of the Land-Sea Interface (CDELSI) Travel Award, a STEPS Institute for Innovation in Environmental Research Graduate Research Award, a Friends of the Long Marine Lab Student Research and Education Award, and a University of California at Santa Cruz Dean's Fellowship.

Last, but perhaps most importantly, I thank my friends and family for their support. My parents, Stephen and Sheila Luengen, were there for me when I needed

them most. My fiancé, Dan Yang gave me the strength to finish this work. My friend Katie Greene was instrumental in helping me translate my thoughts into writing. Fellow graduate students Susi Altermann and Meredith Armstrong provided moral support over lunch. My friends Chris Pluhar and Kellie Townsend listened to my trials and provided some of the best distractions. The encouragement of all of my friends and family members was critical to completing this work.

INTRODUCTION

Every spring, as terrestrial plant life blooms, a similar phenomenon occurs in many marine systems: microscopic phytoplankton rapidly increase in abundance. This rapid increase, relative to background conditions, is called the spring phytoplankton bloom. The spring bloom has been recognized since the late 1800s, when German botanist Franz Schütt described phytoplankton abundance in the Baltic Sea (Mills 1989, p. 125):

> "One form appears, grows and vanishes yet again from the surface waters and makes way for another form, which now asserts its dominance for its own time, yet again to fade away, and this play repeats itself year after year with the same regularity as every spring the trees turn green and in autumn lose their leaves; with just such absolute certainty as the cherries bloom before the sunflowers, so *Skeletonemas* arrive at their yearly peak earlier than the *Ceratiums*."

Schütt described a classic spring bloom that begins with diatoms, or eukaryotic algae characterized by siliceous cell walls. Since that time, it has been recognized that phytoplankton blooms can occur at any time of year and that many different types of phytoplankton can bloom (Cloern 1996). Some of these phytoplankton blooms produce harmful toxins and have been termed harmful algal blooms or red tides for those blooms that discolor the water (with or without toxins). However, this research focuses on a classic spring diatom bloom, composed of species that are generally not toxic to humans.

Although classic spring blooms have not received as much media attention as harmful algal blooms, they are important for several reasons. Spring blooms play an important ecological role as a food source (Smayda 1997). As the first step in the food chain, phytoplankton can serve as a vector for transfer of pollutants from water to higher trophic levels (Cloern et al. 2006). Those pollutants include methyl mercury, which is a toxic form of mercury that bioaccumulates in the food chain (Mason et al. 1996). In addition to pollutants, phytoplankton accumulate nutrients that are needed for cellular processes, such as nitrate, phosphate, silicate, and some trace metals (Morel et al. 2004). Phytoplankton utilize enough of these nutrients to alter concentrations in the surface waters of the oceans (Bruland et al. 1991). Thus, quantifying the uptake of nutrients and metals by blooms may help us understand the movement and partitioning (cycling) of nutrients and trace metals in the environment.

Finally, studying blooms in estuaries, which are unique and highly productive habitats where rivers meet the ocean, may provide insights into the effects of anthropogenic nutrient enrichment. Between 1960 and 1990, nutrient inputs have increased dramatically in many estuaries (Cloern 2001). The resulting ecological impacts and biogeochemical changes are broadly defined as eutrophication (Cloern 2001). One obvious effect of eutrophication is algal growth and subsequent depletion of dissolved oxygen, but effects can also include subtle changes in biological species composition, changes in the timing or magnitude of blooms, and alterations in the biogeochemical cycling of nutrients and metals (Cloern 2001).

Understanding these myriad effects of eutrophication is especially important at our field site, in the southern reach of San Francisco Bay (South Bay), because recent research shows that phytoplankton biomass has increased throughout the estuary (Cloern et al. 2006). Chlorophyll *a* concentrations in the estuary were relatively low (< 10 μm L^{-1} under non-bloom conditions) until the late 1990s, despite multiple anthropogenic stressors (Cloern et al. 2006). Those stressors include fresh water diversions, introduction of exotic species, habitat losses, additions of contaminants, and inputs of nutrients from wastewater treatment plants (Cloern 1996; Nichols et al. 1986; Smith and Hollibaugh 2006). There is now a need to understand how the increase in algal abundance will interplay with the existing stressors in the estuary, particularly metal contamination.

Cobalt, copper, nickel, lead, mercury, and zinc are enriched in the estuary due to anthropogenic activities (Conaway et al. 2003; Flegal et al. 2005). In South Bay, historically contaminated sediments are a source of all of these metals (Flegal et al. 2005; Gee and Bruland 2002; Rivera-Duarte and Flegal 1997). Many of these metals also have current sources, such as inputs from wastewater treatment plants (e.g., cobalt, copper, nickel, and zinc) or slow release from contaminated watersheds (e.g., lead and mercury) (Flegal et al. 2005; Steding et al. 2000; Tovar-Sánchez et al. 2004). However, some of these metals (e.g., copper) are complexed to organic ligands, which limits their bioavailability to phytoplankton and diminishes their potential to alter the ecosystem (Beck et al. 2002; Buck and Bruland 2005; Buck et al. in press).

Of the metals in the estuary, mercury is the chief concern due to its potential impacts on human health and wildlife. There are currently fish consumption advisories in the estuary because methyl mercury bioaccumulates in fish to levels that exceed the human health screening value of 0.23 parts per million (Thompson et al. 2000). Those elevated concentrations may affect fetal brain development and result in neuromotor, visual, and sensory impairments in children (Mahaffey 2000). Methyl mercury is also a threat to the endangered California Clapper Rail (*Rallus longirostris obsoletus)* because it decreases its egg viability. The last ~1000 breeding individuals live in the tidal marshes of the estuary, with about 600 in South Bay (Schwarzbach et al. 2006). To protect people and wildlife, it is useful to look at processes affecting methyl mercury transfer between water and phytoplankton because most of the bioaccumulation occurs at that level (Mason et al. 1995).

This study is the first to consider how the recent increase in algal biomass in the estuary will affect the transfer of mercury and other metals to the food chain. To address that question, this research combines trace metal chemistry with a study of the ecology of the bloom. Because both the metals and the bloom are anthropogenically perturbed, this work also explores the connection between multiple environmental disturbances. The three chapters to follow will explore the interrelationship between nutrient inputs, trace metal enrichment, mercury pollution, and phytoplankton community structure.

The first chapter, *Contrasting biogeochemistry of six trace metals during the rise and decay of a spring phytoplankton bloom in San Francisco Bay,* sets the stage

for the rest of the work by characterizing the environmental conditions surrounding the bloom. That characterization consisted of using principal component analysis (PCA) to reduce the water chemistry data into three composite factors: 1) a bloom factor that described growth of the bloom, 2) a sorbent factor that characterized the amount of material available for metal sorption, and 3) a decay factor that described the decomposition of the bloom. The chapter details how the unique biogeochemistries of each metal explained their differing responses to the bloom, the amount of sorbent, and the decay. The effects of phytoplankton on trapping metals within the estuary were also quantified by calculating that about 75% of the nickel discharged annually to the lower South Bay cycles through the phytoplankton. Overall, the observed alterations in metal concentrations were evidence of eutrophication in South Bay and indicated that changes in phytoplankton biomass affect metal cycling.

The second chapter, *Depletion of dissolved methyl mercury by a phytoplankton bloom in San Francisco Bay*, shows that dissolved methyl mercury concentrations in the water column significantly decreased during the bloom, indicating that phytoplankton assimilated methyl mercury. Calculated concentrations of methyl mercury in phytoplankton decreased at the peak of the bloom. That result was consistent with the bloom dilution hypothesis (Pickhardt et al. 2002), which states that high algal biomass decreases algal mercury concentrations. However, in this study, the decrease in dissolved methyl mercury was only transitory.

The most important aspect of an increase in algal biomass may be the decay of that material. During bloom decay, dissolved methyl mercury concentrations increased. Presumably some of that increase was due to the production of methyl mercury in surface sediments under the low oxygen conditions created by decaying phytoplankton. Accordingly, the decay of the bloom could be a source of methyl mercury to overlying waters. The decay of the bloom also enhanced the partitioning of total mercury onto particles, potentially retaining that mercury within the estuary where it could be later methylated. These changes in partitioning and dissolved methyl mercury concentrations indicate that the decay of the bloom an important period of mercury mobilization in the estuary.

The third chapter, *Fine scale changes in phytoplankton community composition and water chemistry during a spring bloom in San Francisco Bay,* examines how the phytoplankton community changes temporally and spatially by using a statistical approach called multidimensional scaling. The focus is not on large-scale drivers of biomass, but instead it is on understanding the composition of the entire community, including small and less abundant species. The chapter then explores the links between phytoplankton community composition, water chemistry data, and trace metal concentrations. The results show that the concentration of dissolved trace metals does not directly shape algal communities. However, there are spatial and temporal changes in the phytoplankton communities that could affect which phytoplankton species are most exposed to trace metals. Those spatial and temporal changes in phytoplankton communities are explained in part by temperature

and dissolved ammonium concentrations. The importance of temperature and ammonium is an example of phytoplankton communities both modifying and responding to their environment.

Overall, this work examines the links between phytoplankton, nutrients, and trace metal concentrations during the 2003 spring bloom in South San Francisco Bay. The bloom, which was one of the largest on record for South Bay, began with growth of centric diatoms, such as *Thalassiosira punctigera*. As it grew, the bloom depleted some metals, including methyl mercury, from the water column. After depleting all of the nutrients, the diatoms crashed and the community changed to favor cyanobacteria and cryptophytes. Simultaneously, concentrations of dissolved manganese, cobalt, zinc, lead, and methyl mercury rapidly increased and were thus potentially available to those phytoplankton species. Although this work does not address the impact of these changes in metal concentrations on higher trophic levels, it may begin to illuminate the complexity of eutrophication in an estuary. This study also serves as a reminder that looking at only a single component of the ecosystem cannot fully uncover the impact that myriad anthropogenic stressors have upon estuaries.

Limnol. Oceanogr., 52(3), 2007, 1112–1130

Contrasting biogeochemistry of six trace metals during the rise and decay of a spring phytoplankton bloom in San Francisco Bay

Allison C. Luengen[1]
Environmental Toxicology Department, WIGS Group, University of California at Santa Cruz, 1156 High Street, Santa Cruz, California 95064

Peter T. Raimondi
Ecology and Evolutionary Biology Department, University of California at Santa Cruz, 1156 High Street, Santa Cruz, California 95064

A. Russell Flegal
Environmental Toxicology Department, WIGS Group, University of California at Santa Cruz, 1156 High Street, Santa Cruz, California 95064

Abstract

The spring 2003 phytoplankton bloom in South San Francisco Bay (South Bay) affected the cycling of Mn, Co, Zn, Ni, and Pb, but not Cu. We followed this diatom bloom for 2 months, capturing a peak in chlorophyll *a* (Chl *a*) of >150 $\mu g\ L^{-1}$ and then an increase in dissolved organic carbon of >400 $\mu mol\ L^{-1}$ as phytoplankton decomposed. To determine how the stages of the bloom affected metal concentrations, we used principal component analysis to reduce our 15 water chemistry variables into a bloom factor, a sorbent factor, and a decay factor. Increasing values of the bloom factor, which was a composite of dissolved oxygen, Chl *a*, and other variables, significantly accounted for reductions in dissolved Mn, Ni, and Pb. We attributed those declines to microbial oxidation, phytoplankton uptake, and sorption onto phytoplankton, respectively. In contrast, dissolved Cu concentrations were not explained by either the bloom or decay factors, consistent with previous studies showing its strong organic complexation and limited bioavailability in South Bay. The decay factor significantly accounted for increases in dissolved Mn, Co, Zn, and Pb. Decomposing bloom material presumably caused suboxic conditions in surface sediments, resulting in release of metals to overlying waters during reductive dissolution of Mn and Fe (hydr) oxides. These alterations in metal cycling during a nutrient-enriched bloom were evidence of eutrophication. Annually, phytoplankton productivity has the potential to affect metal retention in the estuary; in 2003, 75% of Ni discharged into lower South Bay by wastewater treatment plants was cycled through phytoplankton.

Metal contamination and eutrophication, or biological changes that result from excessive nutrient inputs, are two interrelated problems affecting many estuaries, including San Francisco Bay (Cloern 2001; Flegal et al. 2005). The Bay (Fig. 1), which is one of the largest estuaries on the western coast of North America, is an ideal field site to investigate the interaction between metal cycling and phytoplankton blooms for several reasons. The southern reach of the estuary (South Bay) is contaminated with trace metals, including Co, Zn, Cu, Ni, and Pb (Flegal et al. 2005). The South Bay also has a predictable, nutrient-enriched spring phytoplankton bloom, which has been well characterized (Cloern 1996). During the bloom, phytoplankton can take up some metals, thereby increasing metal bioavailability to the food chain and trapping those metals within the estuary (Lee and Luoma 1998; Luoma et al. 1998).

South Bay has seasonally high concentrations of many trace metals (Flegal et al. 1991). Metals such as Co, Ni, Cu, Zn, and Pb are elevated as a result of diagenetic remobilization from contaminated sediments (Rivera-Duarte and Flegal 1997; Squire et al. 2002) and desorption from resuspended sediments (Gee and Bruland 2002). Metal concentrations typically peak in summer, when freshwater flow from the Sacramento and San Joaquin Rivers is low (Flegal et al. 1991). Those rivers empty into the northern reach of the estuary (Fig. 1) and

[1] Corresponding author (luengen@etox.ucsc.edu).

Acknowledgments

Jim Cloern, U.S. Geological Survey (USGS), and his lab group, including Amy Little, Cary Burns Lopez, and Tara Schraga, provided the shipboard measurements and boat time that made this project possible. We thank the crew of the R/V *Polaris*, and we thank Steve Hager, USGS, for his nutrient analyses. Jeanne DiLeo, USGS, contributed the map used in Fig. 1. Rob Franks, University of California at Santa Cruz (UCSC), provided invaluable assistance with ICP-MS and ICP-OES. Sara Tanner, Moss Landing Marine Laboratories, analyzed the dissolved organic carbon samples. Richard Looker, California Regional Water Quality Control Board, supplied wastewater treatment plant data. Helen Cole, UCSC, assisted with the graphics. We thank members of the WIGS group at UCSC for help with collecting and preparing samples, particularly Christopher Conaway, Sharon Hibdon, Mari Gilmore, and Genine Scelfo. We are grateful to Raphael Kudela and Ken Bruland, UCSC, and Sam Luoma, USGS, for their many comments on methods and drafts. We thank Kristen Buck, UCSC, and two anonymous reviewers for valuable comments on the manuscript.

The University of California Center for Water Resources partially funded this project.

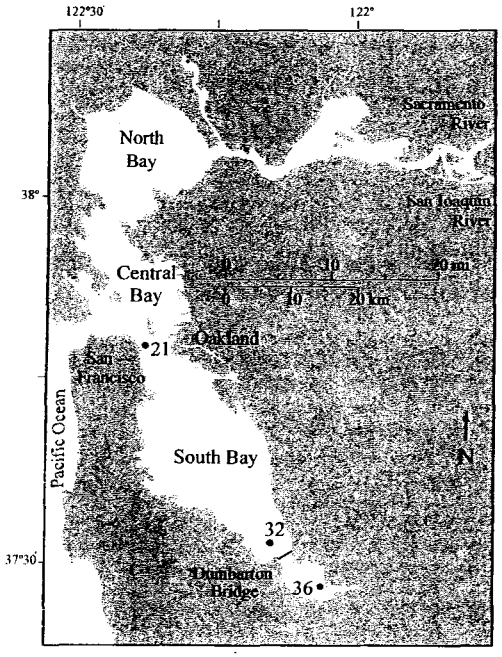

Fig. 1. The USGS stations in South San Francisco Bay (South Bay) that we sampled during this study were site 21 (Bay Bridge), site 32 (Ravenswood Point), and site 36 (Calaveras Point).

exchange with South Bay only during periods of high river flow.

Although South Bay has elevated metal concentrations, the bioavailability of some metals can be limited by complexation to organic ligands, as described in the free ion model developed by Sunda and Huntsman (1998). In that model, the free metal ion (e.g., Cu^{2+}) is the form equilibrating with cellular receptors. Metals complexed to charged organic ligands do not dissociate rapidly enough for the free metal ion to be complexed to receptor sites and then transported into the cell (Sunda and Huntsman 1998). Thus, most organically complexed metals are not readily bioavailable to phytoplankton. For example, Cu is strongly complexed to organic ligands in South Bay (Buck and Bruland 2005; Hurst and Bruland 2005). As a result of that complexation, dissolved Cu was not depleted from South Bay water by a spring bloom in 1994 (Luoma et al. 1998) or by a laboratory simulation of the South Bay bloom (Beck et al. 2002).

The South Bay bloom occurs predictably every spring (February–April), although its timing and magnitude vary annually on the basis of freshwater input, winds, tides, and nutrient concentrations (Cloern 1996). In early spring, freshwater input and warm, calm weather stratify the water column and create conditions for the bloom by isolating phytoplankton from benthic grazers and increasing light exposure (Cloern 1996). The bloom is dominated by diatoms, including *Thalassiosira rotula, Thalassiosira hendeyi, Thalassiosira punctigera, Chaetoceros socialis, Chaetoceros debilis, Skeletonema costatum, Ditylum brightwellii,* and *Coscinodiscus oculus-iridis* (Cloern and Dufford 2005). The bloom typically occurs during neap tides when reduced mixing both helps maintain stratification and prevent phytoplankton from being advected out of the estuary. The magnitude of the bloom may also be affected by the amount of nutrients, which have elevated concentrations in the heavily urbanized South Bay as a result of wastewater treatment plant inputs (Hager and Schemel 1996). Previous phytoplankton blooms in South Bay have been observed to crash after depletion of nutrients from the water (Hager and Schemel 1996; Grenz et al. 2000).

Along with nutrients, trace metals have also been depleted by blooms in South Bay (Luoma et al. 1998), the Scheldt estuary (Zwolsman and van Eck 1999), coastal waters (Schoemann et al. 1998; Ingri et al. 2004), and laboratory mesocosm studies (Beck et al. 2002; Riedel and Sanders 2003; Wang et al. 2005). In South Bay, the 1994 spring bloom depleted dissolved Cd, Ni, and Zn (but not Cu) from the water (Luoma et al. 1998). Similarly, Zwolsman and van Eck (1999) observed a depletion of dissolved Cd and Zn^- but not Cu^- during a bloom in the Scheldt estuary. Studies in coastal waters have shown that metals (e.g., Mn or Fe) can then be remobilized as blooms decay (Thamdrup et al. 1994; Schoemann et al. 1998). However, the number of such studies is limited by both the difficulty of capturing a bloom in the field and attributing any observed changes in metal concentrations to bloom processes (Luoma et al. 1998). Because of these difficulties, some researchers have used mesocosm studies (Beck et al. 2002; Riedel and Sanders 2003; Wang et al. 2005) or large field enclosures (Muller et al. 2005) to study the effect of phytoplankton blooms on metal concentrations.

In addition to previous bloom studies, we used the oceanic distributions of our trace elements to determine how the metals were likely to be affected by bloom processes. For example, the oceanic profile of dissolved Mn is shaped by geochemical scavenging and redox activity (Bruland et al. 1991). Maximum concentrations of dissolved Mn in surface waters are maintained by photoreduction of manganese oxides and photoinhibition of bacteria, which oxidize dissolved Mn to particulate Mn (Sunda and Huntsman 1988). On the basis of this cycling of Mn between dissolved and particulate forms and a past study (Beck et al. 2002) indicating that bacteria can oxidize dissolved Mn during South Bay blooms, we expected that dissolved Mn would by depleted by microbial oxidation during our bloom. Because Co is oxidized by the same microbial pathway as dissolved Mn (Moffett and Ho 1996), we also hypothesized that dissolved Co would be depleted by bacterial oxidation.

On the basis of the oceanic distributions of Zn, Ni, and Pb, we hypothesized that those metals would also be depleted during a phytoplankton bloom. Both Zn and Ni have nutrient-type distributions characterized by depletion in surface oceanic waters as a result of phytoplankton uptake (Bruland and Lohan 2004). We expected those two

metals to be assimilated by phytoplankton during our bloom, unless they were highly complexed to organic ligands. In contrast, because Cu is strongly complexed in South Bay (Buck and Bruland 2005), we hypothesized that the bloom would not deplete that metal from the water. Finally, because Pb is a scavenged-type element (Kozelka et al. 1997; Bruland and Lohan 2004), we hypothesized that it would decrease because of sorption to phytoplankton.

For those metals that were likely to be depleted by the bloom (Mn, Co, Zn, Ni, and Pb), we developed quantitative hypotheses to determine how much metal could be taken up by a theoretical bloom that reached 65 μL^{-1} of chlorophyll *a* (Chl *a*). A bloom of that magnitude (which was the average Chl *a* at our sites 32 and 36) would result in a decrease of 0.19 mmol C L^{-1} in water, given a [C]:[Chl *a*] ratio of 35 (Cloern et al. 1995), as shown below:

$$\left(\frac{65\ \mu g\ Chl\ a}{L}\right)\left(\frac{35\ \mu g\ C}{\mu g\ Chl\ a}\right)\left(\frac{1\ mol\ C}{12\ g\ C}\right) = \frac{0.19\ mmol\ C}{L}$$

By multiplying 0.19 mmol C L^{-1} by [metal]:[C] ratios, we calculated the potential depletion of each metal by phytoplankton during the bloom (Table 1). Then, to determine how the bloom affected those metals, we collected water samples at weekly intervals from mid-February to the beginning of May.

By combining frequent field sampling with principal component analysis (PCA), we were able to address the challenge of following the biogeochemical cycling of metals during a bloom in the field. With these approaches, we sought to (1) distinguish the effect of bloom growth versus decay, (2) determine whether the bloom depleted dissolved Ni given previous conflicting results (Luoma et al. 1998; Beck et al. 2002) regarding the bioavailability of Ni in the South Bay, (3) make the first measurements of Co and Pb during a South Bay bloom, and (4) contrast the cycling of these metals to elucidate their differing biogeochemistries. To explore these objectives, we focused on representative metals with nutrient, scavenged, and hybrid profiles (Bruland and Lohan 2004; Morel et al. 2004) and different degrees of organic complexation.

Methods

Sampling design—Water samples were collected at three sites in the central channel of South Bay (Fig. 1) during cruises designed to capture the spring 2003 phytoplankton bloom. During the first cruise on 19 February, all parameters shown in Table 2 were measured, except dissolved organic carbon (DOC). Beginning 24 February, all parameters listed in Table 2, as well as dissolved (<0.45 μm) and total (unfiltered) trace metals, were measured. Cruises on 24 February, 04 March, 12 March, and 27 March captured trace metal concentrations and associated water chemistry during a period of high phytoplankton biomass. The 01 April, 17 April, 23 April, and 01 May cruises traced the decline of the bloom. The 27 August cruise was timed to provide a low phytoplankton

Table 1. Potential algal drawdown of each metal (Me) from the water column on the basis of a bloom of 65 $\mu g\ L^{-1}$ Chl *a*, a depletion of 5.16 nmol L^{-1} P, and [Me]:[C] and [Me]:[P] ratios for phytoplankton. By using Monterey Bay and Southern Ocean phytoplankton data to calculate the potential depletion of metals by our bloom, we were able to estimate how much of our observed changes in metal concentrations (average of sites 32 and 36) could be explained by phytoplankton assimilation. When our changes in dissolved metal concentrations far exceeded those predicted for phytoplankton activity (e.g., Mn), we considered other processes (e.g., diagenetic remobilization from sediments).

	Monterey Bay phytoplankton*		High-Fe Southern Ocean diatoms†		Potential algal drawdown calculated from		Highest-lowest average dissolved	Possible contribution of phytoplankton to Me
Element	Me:P (mmol mol^{-1})	Me:C (μmol mol^{-1})	Me:P (mmol mol^{-1})	Me:C (μmol mol^{-1})	Me:C (nmol L^{-1})	Me:P (nmol L^{-1})	Me concentration (nmol L^{-1})‡	concentration (%)‡
Mn	0.39	3.7	0.28	4.5	0.70–0.86	1.4–2	1,600	0.04–0.1
Co	<0.07	<0.6			<0.1	<0.4	4.0	3–10
Zn	0.84	7.9	6.2	71	1.5–13	4.3–32	15	10–100
Cu	0.18	1.7			0.32	0.93	No change	
Ni	0.21	2.0	0.73	8.5	0.38–1.6	1.1–3.8	5.8	7–70
Pb	0.04	0.3			0.06	0.2	0.08	70–100

* Martin and Knauer 1973. Martin and Knauer (1973) collected Monterey Bay phytoplankton samples during a diatom bloom in conditions where suspended sediment concentrations were low. To further minimize contamination by suspended sediments, Bruland et al. (1991) selected Mn, Zn, Cu, and Ni data from that study for low Al concentrations. Following Bruland's protocol, we selected data for Co and Pb. Lead is shown for the one low-Al sample in which it was detected, and Co is shown as less than the detection limit.

† Twining et al. 2004. We used phytoplankton data from the Southern Ocean (Twining et al. 2004) because the authors measured metal concentrations in individual cells, which eliminated the suspended sediments that often confounded other field studies.

‡ This study.

Table 2. Parameters measured during the spring 2003 bloom.

Variable	Explanation
Chl *a*	Chl *a* measured from discrete sample
Phaeo	Phaeophytin measured from discrete sample
Chl ratio	Chl *a*/(Chl *a* + Phaeo)
SPM	Suspended particulate matter calculated from optical backscatter
Salinity	Salinity
DO	Percentage of dissolved oxygen that would be present if in atmospheric equilibrium
T	Temperature
σ_t	Water density
DOC	Dissolved organic carbon
DRP	Dissolved reactive phosphate
DSi	Dissolved silicate
DIN	Dissolved inorganic nitrogen (nitrate, nitrite, and ammonium)
UFFe	Total (unfiltered iron)
UFMn	Total (unfiltered manganese)
Tide	Tidal amplitude

biomass contrast to the spring data. All samples were taken aboard the U.S. Geological Survey (USGS) R/V *Polaris*.

Vertical profiles of the water column were taken with a Sea-Bird Electronics (SBE) underwater unit (SBE-9 plus) according to established methods (Caffrey et al. 1998). The instrument package included SBE conductivity–temperature–depth (CTD) sensors, biospherical photosynthetically active radiation (PAR) light sensor, SCUFA fluorometer, SBE-43 dissolved oxygen sensor, and D&A Instruments optical backscatter for suspended particulate matter (SPM). The latter three sensors were calibrated each cruise with discrete samples (from 2 m depth via the ship's flow-through system) at six USGS sites, including sites 21, 32, and 36, where the samples for this study were collected. For Chl *a* discrete samples, duplicate aliquots were filtered onto GFF filters. The filters were then frozen immediately, stored at −80°C, acetone-extracted, and analyzed with a Turner TD700 fluorometer (Parsons et al. 1984). Dissolved oxygen (DO) samples were analyzed by Winkler titration (Granéli and Granéli 1991). SPM was measured by gravimetric analysis of samples collected onto 0.45-μm polycarbonate filters (Hager 1994).

Surface (1 m) water was collected with the use of two peristaltic pumps equipped with acid-cleaned Teflon tubing attached to an aluminum pole extended out from the boat, as per the methods that the WIGS group (University of California at Santa Cruz) had previously used in San Francisco Bay (Flegal et al. 1991). The metal samples were collected with clean techniques into 1-liter acid-cleaned low-density polyethylene bottles. Additional samples were collected for nutrients, DOC, Chl *a*, and phaeophytin (Phaeo). Filtered (0.45 μm) water for dissolved metals was obtained by attaching an acid-cleaned Osmonics polypropylene filter (Calyx Capsule) to the tubing of one pump. The second pump was used to collect unfiltered water for total metal samples.

Trace metal analyses—Trace metal samples (both dissolved and total) were acidified in the laboratory approximately 3 months before analysis by addition of 4 mL of 6 mol L^{-1} high-purity (Optima®) hydrochloric acid (HCl) to a 1-liter sample. A 30-mL aliquot of acidified sample was then ultraviolet (UV) digested (Ndung'u et al. 2003). Concentrations of Co, Cu, Ni, Zn, and Pb were measured by high-resolution inductively coupled plasma magnetic sector mass spectrometry (ICP-MS) with a Finnigan Element ICP-MS and a Finnigan microsampler, according to established methods (Ndung'u et al. 2003). These methods included an online preconcentration step with a chelating resin (AF-Chelate 650M) to concentrate and remove the metals from the saltwater matrix (Warnken et al. 2000). National Research Council Canada certified reference materials (CRMs) CASS-4, SLEW-2, and SLEW-3 for trace elements in water were used to quantify recoveries (Table 3).

Acidified (pH < 1) samples were analyzed for dissolved and total Mn and total Fe by inductively coupled plasma optical emission spectrometry (ICP-OES) with a Perkin-Elmer 4300DV in radial mode. CRMs SLEW-2 and SLRS-1 were analyzed concurrently to quantify accuracy (Table 3).

Particulate metal concentrations were calculated as the difference between the total and dissolved samples. The

Table 3. Trace metal analyses figures of merit, showing mean ± 1 standard deviation.*

Element†	Material type	Co (nmol L^{-1})	Ni (nmol L^{-1})	Cu (nmol L^{-1})	Zn (nmol L^{-1})	Pb (nmol L^{-1})	Fe (nmol L^{-1})	Mn (nmol L^{-1})
DL (3σ)		0.048	2.0	0.21	0.56	0.001	.43	7.1
CASS-4	Measured	0.39±0.02	4.9±0.6	9.5±0.3	6.9±0.5	0.050±0.005		
	Certified	0.44±0.03	5.35±0.26	9.32±0.43	5.83±0.44	0.047±0.009		
SLEW-2	Measured		13.1±0.9	26.8±1.0	19.5±0.9	0.11±0.02		298±2
	Certified		12.1±0.5	25.5±0.9	16.8±1.1	0.13±0.01		311±10
SLEW-3	Measured	0.76±0.03	21.8±0.6	26.4±0.4	2.5±0.3	0.035±0.005		
	Certified	0.71±0.08	21.0±0.6	24.4±0.9	3.07±0.28	0.043±0.003		
SLRS-1	Measured						633±32	32±1
	Certified						564±19	32±0.2

* All measured and certified values were within one standard deviation of each other, except SLEW-2 for Zn, SLEW-3 for Cu, and SLRS-1 for Fe. Those values were within two standard deviations of each other.

† DL, detection limit; CASS-4, SLEW-2, SLEW-3, and SLRS-1 are certified reference materials provided by the National Research Council of Canada for ocean water, estuarine water, and river water, respectively.

distribution coefficient, K_d, was then given as moles of particulate metal per gram of SPM divided by the concentration of dissolved metals. Accordingly, K_d values were given in units of liters per kilogram.

Nutrients and DOC—Dissolved reactive phosphate (DRP), dissolved inorganic nitrogen (DIN), and dissolved silica (DSi) were analyzed with a Technicon Autoanalyzer II, according to established colorimetric methods (Hager 1994). DIN was the sum of NO_3^-, NO_2^-, and NH_4^+. Most samples were frozen and thawed overnight before analysis.

DOC samples were analyzed with a Dohrmann DC-190 (Rosemount Anaytical, temperature 680°C, catalyst 0.5% $PtAl_2O_3$) according to established methods (Sharp et al. 1993). Typical precision was 2.5–4.5 μmol L^{-1} (SD) or 1–5% of the certified value. The detection limit was 2.9 μmol L^{-1}.

Data analyses—Results from the concurrent vertical profiles (e.g., Chl *a*, SPM, salinity) can be found on the USGS web site at http://sfbay.wr.usgs.gov/access/wqdata. Instrument results for SPM and DO were used rather than discrete samples because instrument data were available at 1 m, the depth at which the trace metal samples were collected. Results from discrete Chl *a* samples collected from the peristaltic pump were used in the data analyses instead of USGS discrete or instrumental data.

An additional variable, tidal amplitude, was calculated with data from Yerba Buena Island, Dumbarton Bridge, and Calaveras Point corresponding to sites 21, 32, and 36 from WWW Tide and Current Predictor (http://tbone.biol.sc.edu/tide/). On the basis of the time at which samples were collected, tidal amplitude was calculated as the absolute value of the difference between the nearest high and low tide. Then, outgoing tides were given a negative value and incoming tides a positive value for statistical analyses.

PCA—To address the challenge of characterizing the bloom in the field, we employed PCA (with Systat Version 10.2.05, SPSS) to develop composite factors that described bloom processes. A similar approach was used by Osenberg et al. (1992) to derive factors that described the spatial variability of infaunal taxa in relation to distance from a produced water outfall. We first log-transformed SPM, DOC, DRP, Chl *a*, and Phaeo to satisfy assumptions of normal statistics. Then we used PCA to reduce the 15 variables (Table 2) to a bloom factor, a sorbent factor, and a decay factor (Table 4). The correlation between original variables and derived factors was given by the component loadings (Table 4). Original variables with component loadings ≥0.6 or ≤−0.6 were interpreted according to Tabachnick and Fidell's (2001) discussion of cutoffs for loadings.

General linear models—To determine whether the three PCA factors and the categorical variable (site) affected dissolved metal concentrations, an analysis of covariance (ANCOVA) was performed with a general linear model (GLM) routine. These analyses illustrate the power of PCA in GLMs because all factors are, by definition, independent. In contrast, original variables are commonly collinear, which would violate assumptions of any GLM model. All dissolved metals were normally distributed, except Mn and Zn. Those two dependent variables were square root and log transformed, respectively. With the use of GLMs, the four-way interaction between the categorical variable (site) and the three covariates (PCA factors) was tested for homogeneity of surfaces and removed when its probability was >0.05.

Table 4. Three PCA factors were formed by the water chemistry variables. The water chemistry variables that composed each factor are listed and their loadings are given in parentheses.

Bloom factor*	Sorbent factor†	Decay factor‡
DO(0.703)	log SPM(0.748)	log DOC(−0.657)
T(−0.622)	σ_t(−0.646)	log Phaeo(0.697)
Salinity(−0.620)	log DRP(0.832)	
DIN(−0.607)	UFFe(0.819)	
DSi(−0.834)	UFMn(0.775)	
log Chl *a*(0.864)		

* High values of the bloom factor corresponded to high values of both Chl *a* and DO and low values of DIN, DSi, T, and salinity. Those low T and salinity values were probably the result of cold freshwater from fluvial inputs.

† High values of the sorbent factor characterized high concentrations of SPM, DRP (which is particle reactive), and Fe and Mn (hydr)oxides. Additionally, the sorbent factor included water density, which was inversely related to that factor likely because fluvial inputs contained high particulate concentrations.

‡ Decreasing values of the decay factor corresponded with increasing DOC

A model-building approach was used to select models that were most predictive of dissolved metal concentrations and that used the fewest number of variables. In that approach, we ran backward models that first included all three covariates and the categorical variable, site. Variables with $p > 0.15$ were then successively dropped. The r^2 values from different models were also used to assess the effect of dropping variables. In some models, site, the only categorical variable, was removed, and GLMs were then used to perform multiple linear regression. In the final models (Table 5), mean square errors or t values were used as estimates of the relative contribution of different factors.

A model-building approach was also used to determine the best predictors of distribution coefficients (K_d values) for all metals except Mn. Because total Mn was incorporated into the sorbent factor, we could not look at the effect of the PCA factors on Mn partitioning. Our model-building approach used both backward and forward models. In contrast to backward models that sequentially remove variables, forward models successively add variables. When the forward and backward models did not converge, the model with the highest r^2 value was selected (Table 6).

Resulting models often contained multiple predictor variables. To graphically represent multiple linear regression results for dissolved metals, we ran the model with all but one of the factors and then plotted the residuals against the missing factor (partial residual plots). We repeated this

Table 5. Reduced models for dissolved metal concentrations. These results were generated by running general linear models with the categorical variable (site) and the three PCA factors (bloom, sorbent, and decay). Then, a model-building approach was used to reduce the models to include only the independent variables that best predicted dissolved metal concentrations.*

Effect	Coefficient	SE	Std Coef	Tolerance	*t*	*p* (two-tail)
Reduced model for square root Mn $r^2 = 0.72$						
Constant	0.607	0.044	0.000		13.8	<0.01
Sorbent factor	0.245	0.045	0.582	1	5.46	<0.01
Decay factor	−0.255	0.045	−0.605	1	−5.68	<0.01
Bloom factor	−0.090	0.045	−0.213	1	−2.00	0.058
Reduced model for Co $r^2 = 0.77$						
Constant	4.10	0.194	0.000		21.2	<0.01
Sorbent factor	1.39	0.198	0.697	1	7.04	<0.01
Decay factor	−1.08	0.198	−0.538	1	−5.44	<0.01
Reduced model for log Zn $r^2 = 0.66$						
Constant	0.927	0.028	0.000		33.5	<0.01
Sorbent factor	0.107	0.028	0.463	1	3.78	0.001
Decay factor	−0.153	0.028	−0.664	1	−5.43	<0.01
Reduced model for Pb, $r^2 = 0.93$						
Constant	0.135	0.00492	0.000		27.4	<0.01
Sorbent factor	0.049	0.00501	0.547	1	9.79	<0.01
Decay factor	−0.068	0.00501	−0.758	1	−13.5	<0.01
Bloom factor	−0.022	0.00501	−0.240	1	−4.30	<0.01
Source	Sum of squares	df	Mean square	*F*-ratio	*p*	
Reduced model for Cu $r^2 = 0.86$						
Site	3247	2	1623	69.4	<0.01	
Decay factor	114	1	114	4.88	0.038	
Error	515	22	23.4			
Reduced model for Ni, $r^2 = 0.92$						
Site	1742	2	871	98.5	<0.01	
Decay factor	36.9	1	36.9	4.18	0.054	
Bloom factor	261	1	261	29.5	<0.01	
Error	186	21	8.84			

* Std Coef, standard coefficient; df, degrees of freedom.

Table 6. Reduced models for K_d, the distribution coefficient between the dissolved and solid phases. A model-building approach that included both forward and backward stepwise approaches was used to generate these reduced models.*

Source	Sum of-squares	df	Mean square	*F*-ratio	*p*	
Reduced backwards model for log Co K_d, $r^2 = 0.55$						
Site	1.05	2	0.525	12.7	<0.01	
Error	0.865	21	0.0412			
Reduced backward model for log Cu K_d, $r^2 = 0.45$						
Site	2.68	2	1.34	8.42	0.002	
Error	3.34	21	0.159			
Reduced forward model for log Ni K_d, $r^2 = 0.63$						
Site	0.259	2	0.130	7.64	0.004	
Sorbent factor	0.0761	1	0.0761	4.49	0.049	
Decay factor	0.108	1	0.108	6.37	0.022	
Bloom factor	0.0481	1	0.0481	2.84	0.110	
Error	0.288	17	0.0170			
Reduced backward model for log Pb K_d, $r^2 = 0.73$						
Site	0.963	2	0.481	17.7	<0.01	
Decay factor	0.118	1	0.118	4.36	0.051	
Bloom factor	0.160	1	0.160	5.90	0.026	
Error	0.489	18	0.027			
Effect	Coefficient	SE	Std Coef	Tolerance	*t*	*p* (two-tail)
Reduced forward model for log Zn K_d, $r^2 = 0.35$						
Constant	5.20	0.0389	0		133	<0.01
Sorbent factor	−0.0850	0.0379	−0.406	1	−2.24	0.036
Decay factor	0.0909	0.0396	0.415	1	2.30	0.033

* Std Coef, standard coefficient; df, degrees of freedom.

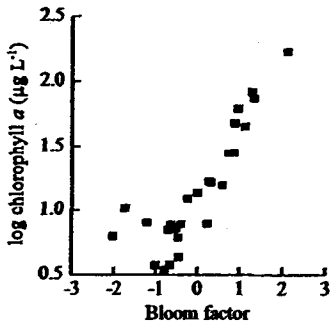

Fig. 2. The bloom factor was correlated with log Chl *a* (linear regression $F_{1,24} = 71$, $p < 0.01$, $r^2 = 0.75$).

process until each factor was individually plotted against the other sets of partial residuals. The resulting graphs showed how the omitted factor explained variation in the data and hence its contribution to the model. The slope of the relationship showed whether the factor negatively or positively affected metal concentrations. The relative contribution of the factors was indicated by the range of the *y*-axis, which showed the number of standard deviations of variation explained by that factor.

Results

PCA factors—The 15 water chemistry variables (Table 2) clearly separated into three PCA factors (Table 4). The separation of original variables into derived factors illustrates the utility of PCA for these types of analyses; groups of assorted original variables make up derived factors that often relate to ecological (or other) phenomena. The three derived factors collectively explained 77% of the variance.

The first PCA factor was a bloom factor, comprising log Chl *a* (+), DIN (−), DSi (−), DO (+), temperature (−), and salinity (−) (Table 4). The bloom factor was directly correlated with Chl *a*, our proxy for phytoplankton biomass (Fig. 2). However, it was a more complete representation of the rise of the bloom than Chl *a* alone because it included other variables.

The second PCA factor was a sorbent factor that represented the amount of particulate material, including SPM and Fe and Mn (hydr)oxides, available for metal sorption (Table 4). We use the term sorption to include metals that were adsorbed onto SPM, coprecipitated with Fe and Mn (hydr)oxides, or incorporated into organic matrices surrounding particles, as per Morel and Hering's (1993, p. 556) definition of sorption: "the partitioning of solutes between the solution and the whole of a particulate phase." In our sorbent factor, SPM and water density (σ_t) were inversely related, most likely because SPM increased with freshwater inputs that simultaneously decreased water density. DRP, which is particle reactive, also increased as SPM increased.

The third PCA factor was a decay factor. Declining values of that factor represented decomposition of phytoplankton. As the algae decayed, Phaeo decreased and DOC increased. The former was a particulate measure of Chl *a* breakdown, whereas the latter increased as organic material was remineralized into the dissolved phase.

Models describing metal concentrations—Table 5 shows which terms best explained the dissolved metal concentrations. Spatial terms (the categorical variable, site, or the sorbent factor) were part of the models for all metals. In many ways, the variable site and the sorbent factor modeled the same variance structure; the amount of particulates often accounted for the observed differences in metal concentrations between the sampling locations. However, the variable site predicted dissolved Ni and Cu concentrations better than the sorbent factor. Thus, some site-specific parameters not measured in this study contributed to variations in dissolved Ni and Cu concentrations.

The bloom factor accounted for variability in the concentrations of only three dissolved metals: Mn, Pb, and Ni (Table 5). The bloom factor did not affect dissolved Cu concentrations. That result was consistent with our hypothesis that organic complexation would limit algal uptake of dissolved Cu. Contrary to our hypothesis that Co and Zn would be depleted, concentrations of those two metals were not affected by the bloom factor. A subsequent discussion addresses three possible reasons for that lack of depletion.

The decay factor was an important variable governing concentrations of dissolved Mn, Co, Zn, and Pb, as demonstrated by the mean square error or *t* values (Table 5). Because the mean square error was an estimate of the variance attributable to the term of interest (e.g., the decay factor), it can be used to roughly assess the contribution of the term to the model fit. For example, in the dissolved Ni and Cu models, the relatively low mean square error indicated that the decay factor was comparatively unimportant relative to the other terms in those models. Similar to the mean square error, the *t* value indicated the variance explained by individual variables in a multiple linear regression model. In the dissolved Mn model, the *t* value for the decay factor was −5.68, whereas for the bloom factor, it was −2.00 (Table 5), indicating that the decay factor explained more of the variability in dissolved Mn concentrations than the bloom factor.

K_d *values*—Our log K_d values (L kg^{-1}, mean ± SD) were 5.01 ± 0.63 for Mn, 4.68 ± 0.29 for Co, 5.21 ± 0.22 for Zn, 4.11 ± 0.51 for Cu, 4.54 ± 0.19 for Ni, and 5.93 ± 0.28 for Pb. The log K_d values for Zn were consistent with the value (~5.3 L kg^{-1}) given by Luoma et al. (1998) for spring bloom particles but higher than the value (4.52 L kg^{-1}) measured by Gee and Bruland (2002) for their South Bay samples. Gee and Bruland (2002) also measured K_d values for Ni and Cu in South Bay of 3.65 and 3.88 L kg^{-1}, respectively, which were lower than our values. However, our comparatively high K_d values were consistent with reports (Gee and Bruland 2002) of higher

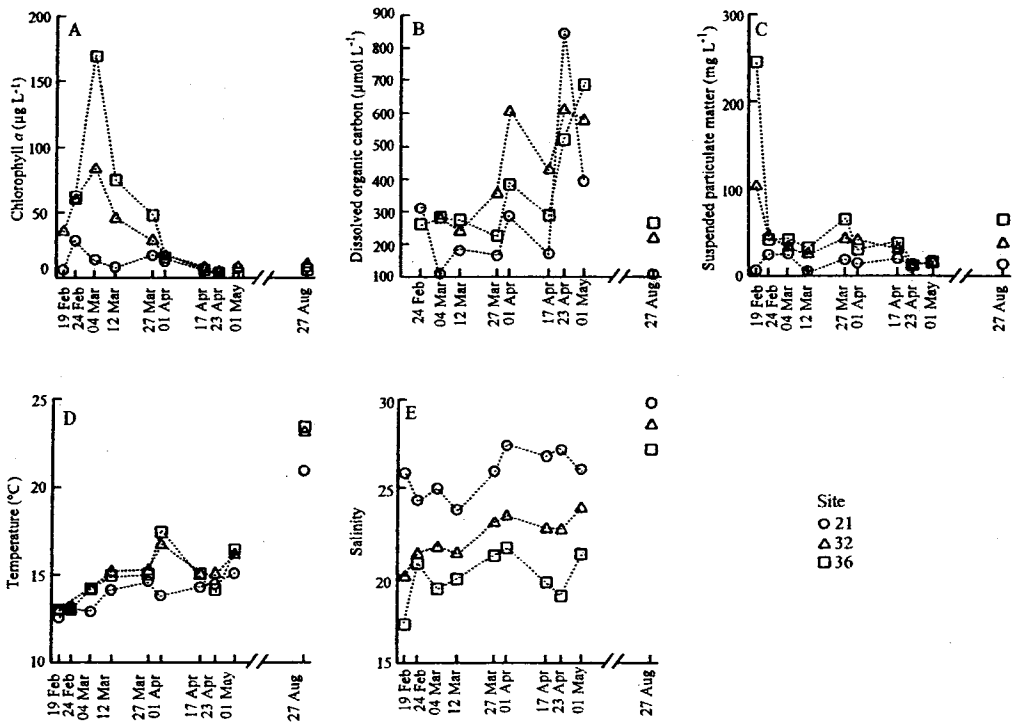

Fig. 3. Parameters measured during the spring 2003 bloom at sites 36, 32, and 21. (A) Chl *a* peaked at site 36 at >150 μg L^{-1} on 04 March. (B) DOC began to increase at the beginning of April after Chl *a* declined. Although the 23 April DOC value at site 21 was unusually high, we did not dismiss that datum because high NH_4^+ was also observed, and both observations might have been the result of wastewater treatment plant inputs. (C) SPM was high on 19 February but decreased once trace metal sampling began on 24 February. (D) Temperature and (E) salinity were relatively constant during the bloom.

K_d values in other South Bay studies and with results (Lee and Luoma 1998) that showed high algal biomass increased metal partitioning.

Models describing K_d *values*—As shown by the models in Table 6, no single factor governed the partitioning of all metals. The bloom factor explained variability in K_d values for two metals: Ni and Pb. The sorbent factor, which was partially composed of SPM, was important for only Zn and Ni partitioning. When we used partial residual plots to look at the direction of that relationship, we found a weak positive correlation between the sorbent factor and Ni, but a negative correlation for Zn. The decay factor explained some of the variability in K_d values for Zn, Ni, and Pb. For those metals, partial residual plots showed that K_d values decreased as the bloom decayed. The K_d values for Co, Cu, Ni, and Pb varied by site, with the highest values at site 21. The partitioning of many of the metals (e.g., Ni) was affected by multiple factors, which justified this statistical approach because trends were not readily apparent by looking at the raw data. Clearly, the partitioning of metals was a complex process specific to each metal.

Spring bloom conditions—The spring bloom of 2003 was one of the largest blooms on record (http://sfbay.wr.usgs.gov/access/wqdata); Chl *a* peaked at >150 μg L^{-1} at site 36 in the extreme South Bay (Fig. 3). On 19 February, before dissolved metal measurements began, there was a pulse of SPM (Fig. 3). However, by 24 February, warm, calm conditions prevailed, and SPM and salinity remained relatively constant during our sampling (Fig. 3).

By bloom peak on 04 March, DIN and DSi declined to limiting concentrations (Fig. 4). The bloom consumed 52–56 μmol L^{-1} of DIN and 75–105 μmol L^{-1} of DSi. Phytoplankton composition ratios by Brzezinski (1985) suggested that N and Si should be consumed ~1:1 for a diatom bloom, and the departure from this ratio indicated that N was likely recycled. DRP also declined from 6.99 and 9.91 μmol L^{-1} on 19 February to 2.65 and 3.94 μmol L^{-1} on 04 March (Fig. 4) at sites 32 and 36, respectively. However, DRP was not completely depleted as were DIN and DSi.

By 12 March, Chl *a* began declining (Fig. 3). Ammonium (NH_4^+), one indicator of bloom decay, increased at the end of April (Fig. 4). As the bloom decayed, DOC also

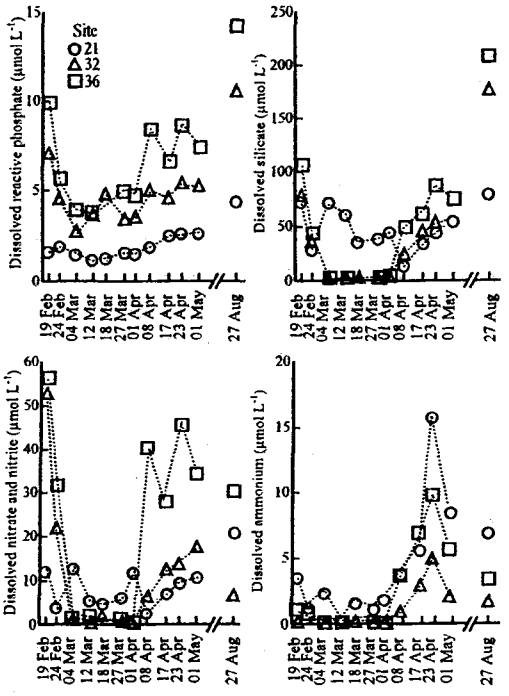

Fig. 4. Dissolved nutrients decreased during the bloom. DSi and DIN were completely depleted by the peak of the bloom on 04 March, and that depletion caused the phytoplankton to crash. Nutrient concentrations from a related USGS cruise on 18 March were added to the graphs for illustrative purposes, although those limited data were not included in the statistical analyses.

increased, beginning 01 April (Fig. 3). Finally, DOC concentrations peaked 01 May (Fig. 3).

Discussion

Role of nutrients in eutrophication—Nutrient inputs from wastewater treatment plants can contribute to the magnitude of South Bay blooms (Hager and Schemel 1996), and the blooms can in turn alter trace metal concentrations (Luoma et al. 1998). Both alterations in bloom magnitude and metal cycling are considered evidence of eutrophication (Cloern 2001). The unusually large bloom in spring 2003 was sustained by high concentrations of DIN and DSi. Figures 3 and 4 show that depletion of those nutrients lead to a crash in Chl *a*. The result was similar to findings from Hager and Schemel (1996) that showed the 1990 and 1993 blooms declined after nutrient depletion. The effect of nutrients on the bloom magnitude was our first piece of evidence for eutrophication during the 2003 bloom.

We sought to determine whether nutrient depletion coincided with trace metal drawdown, which would be further evidence of eutrophication. In contrast to nutrients, which were present at micromole per liter concentrations and depleted by up to 105 μmol L^{-1}, most trace metals measured during this study only were present at nanomole per liter concentrations, and their fractional depletion was likely to be correspondingly small (Table 1). Accordingly, we first quantitatively evaluated the potential for measuring relatively small decreases in dissolved metal concentrations.

Potential to observe changes in metal concentrations—We used known enrichment factors for metals in phytoplankton to calculate potential metal depletion during our bloom (Table 1). We then compared those values to ambient concentrations of dissolved metals to determine whether trace metal depletions could be readily observed by our experimental design. For example, phytoplankton uptake could potentially decrease dissolved Pb by 0.06 nmol L^{-1} (Table 1), a change that was reasonable to measure, given that a deviation of ±0.06 described 95% of the dissolved Pb data from South Bay (0.15 ± 0.06 nmol L^{-1}) in years with intermediate freshwater inputs between 1989 and 1999 (Squire et al. 2002). In contrast, a phytoplankton depletion of dissolved Co on the order of 0.1 nmol L^{-1} (Table 1) would be difficult to detect because of the large range of Co values; only 66% of dissolved Co data for San Francisco Bay fell within 1.12 ± 0.69 nmol L^{-1} (Tovar-Sánchez et al. 2004). Thus, we expected that we would not be able to observe nutrient depletion of dissolved Co and Mn and that any measurable changes in their dissolved concentrations would be the result of other processes, particularly microbial oxidation.

We also used concentration factors (concentration per unit mass of organism/concentration per unit mass of seawater, IAEA 2004) to determine which metals were highly particle reactive and thus likely to be depleted by sorption to phytoplankton. For example, the concentration factor of Pb in phytoplankton is 10^5 (IAEA 2004), indicating that a phytoplankton bloom has the potential to remove Pb. In contrast, Ni, Co, and Zn are less particle reactive than Pb (concentration factors on the order of 10^3 to 10^4, IAEA 2004) and hence were more difficult to observe by this experimental design.

The question of whether Ni and Zn depletions could be theoretically observed was complicated by uncertainly in [metal]:[C] ratios (Table 1). For example, Twining et al. (2004) measured an order of magnitude higher [Zn]:[C] in diatoms under high iron conditions in the Southern Ocean than Bruland et al. (1991) reported for diatoms under bloom conditions in Monterey Bay on the basis of data from Martin and Knauer (1973). As a result of this uncertainty, there was an order of magnitude range in our calculated potential uptake of dissolved Zn (Table 1). For metals for which we observed algal depletion, we calculated our own [metal]:[C] ratios and compared them with previous studies. Those results are presented in the individual discussion of each metal below.

Manganese—The cycling of Mn was affected by the bloom, sorbent, and decay factors (Table 5). The bloom factor accounted for reductions in dissolved Mn concen-

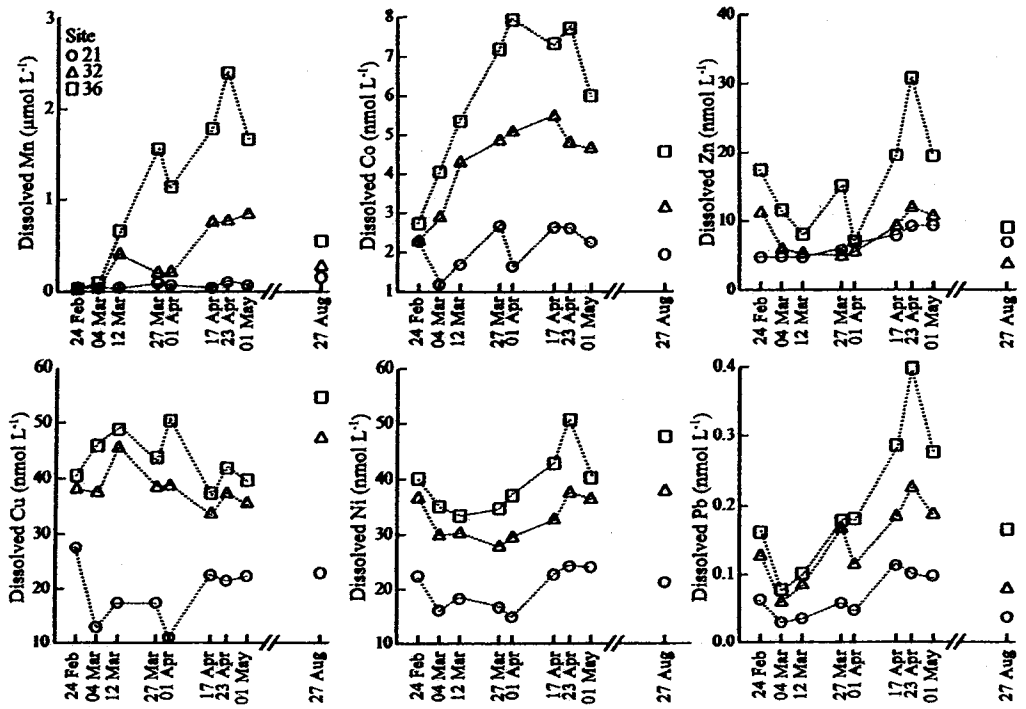

Fig. 5. Descriptive plots of dissolved trace metal concentrations during the spring 2003 bloom at sites 36, 32, and 21. These plots correspond with the plots of ancillary parameters and nutrients. For reference, Chl *a* peaked on 04 March, and DOC began to increase 01 April. To determine whether these fluctuations in dissolved metal concentrations were statistically significant, general linear models were used, and partial residual plots are presented in subsequent figures.

trations (Fig. 7). Around the time of the bloom, the number of Mn-oxidizing bacteria in the water column presumably increased as they consumed carbon generated by the bloom. Those bacteria could have decreased dissolved Mn by oxidizing soluble Mn(II) to much less soluble Mn(III) and Mn(IV).

This bacterial oxidation mechanism was proposed by Beck et al. (2002) to explain the loss of 80% of the dissolved Mn during their microcosm simulations of a South Bay bloom. Those authors investigated the cause of the Mn drawdown by adding Cu to the microcosms at concentrations that were toxic to bacteria, but not to diatoms. The resulting inhibition of Mn oxidation was evidence that Mn oxidation was bacterially mediated.

Research by Sunda and Huntsman (1987) also indicated a microbial role in Mn cycling. Those authors showed that Mn oxidation rates in seawater were too rapid to be explained by abiotic mechanisms. On the basis of these studies, we attributed most of our observed Mn depletion during the bloom to bacterial oxidation and not to nutrient uptake by diatoms, even though Mn is needed as a cofactor in photosynthetic enzymes (Morel et al. 2004).

Although the bloom factor explained a small amount of the variability in Mn concentrations (Table 5), the effect might have been greater had sampling started earlier in the season. When our sampling began in February, dissolved Mn was low: 42 and 11 nmol L^{-1} at sites 21 and 32, respectively (Fig. 5). A month before this study, concentrations of dissolved Mn were higher: 112 and 397 nmol L^{-1} at Yerba Buena Island and Dumbarton Bridge, respectively (Buck and Bruland 2005). Those sites correspond very closely our sites 21 and 32. Thus, it was likely that the sampling scheme in this study did not capture the full extent of Mn drawdown as the bloom grew.

As the bloom decomposed, dissolved Mn significantly ($p < 0.01$, Table 5) increased (Fig. 7). Dissolved Mn concentrations peaked at 2,400 nmol L^{-1} at site 36 on 23 April (Fig. 5). At that time, concentrations of particulate Mn (270 nmol L^{-1}; Fig. 6) and SPM (12 mg L^{-1}; Fig. 3) were low, indicating that the increase was not due to resuspension of sediments with high Mn concentrations. Instead, sinking and decomposition of the bloom likely reduced and released Mn from Fe and Mn (hydr)oxides in surficial sediments. When the bloom material sinks to the bottom, bacteria first use O_2 to decompose the organic material (Schoemann et al. 1998). The resulting increase in O_2 demand has been observed in sediments below South San Francisco Bay channels following a bloom (Caffrey et al.

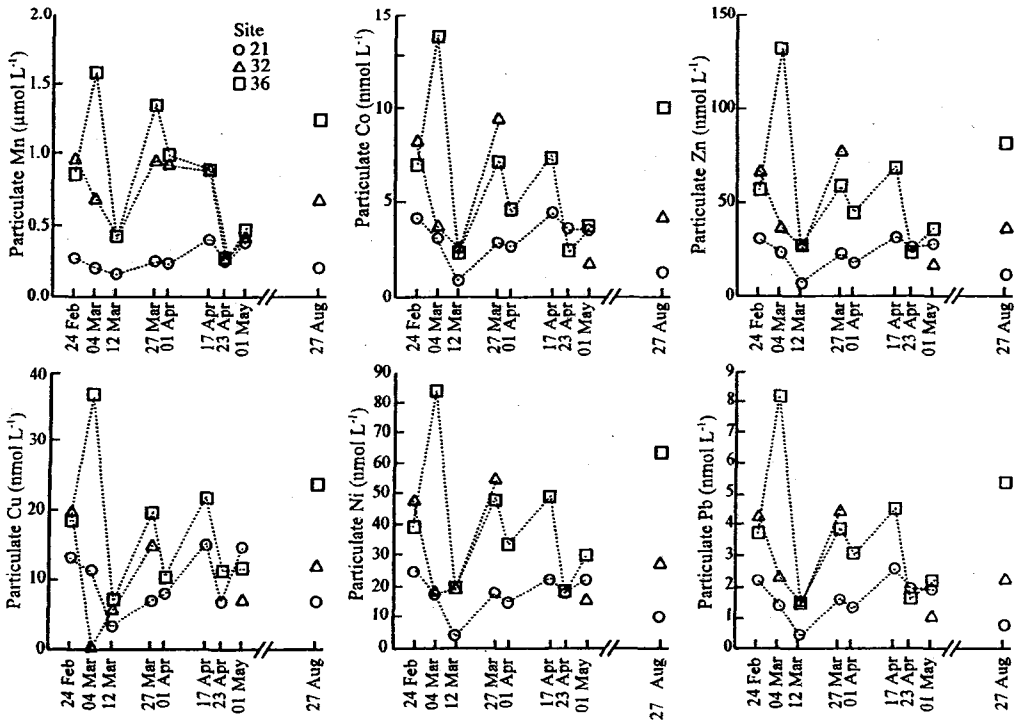

Fig. 6. Descriptive plots of particulate metal concentrations (on a per liter basis) during the spring 2003 bloom. Because most of the metals were associated with particles, minor changes in the concentration or composition of the SPM could alter the concentration of particulate metals and thus make it hard to discern the effects of the bloom. For example, at site 36, the concentration of particulate metals increased from 24 February to the peak of the bloom on 04 March, but at site 32, particulate metals decreased during that same growth period. It was unclear whether the discrepancy between sites was due to the larger magnitude of the bloom at site 36 or the loss of some components of the SPM. At site 36, the total SPM concentration (Fig. 3) did not change as the bloom grew between 24 February and 04 March, which means that the increase in bloom-derived material (Chl *a* plus Phaeo) of 14 mg L^{-1} was balanced by loss of other suspended material. During that period at site 32, bloom-derived material increased by only 2 mg L^{-1}, which did not compensate for the decrease in SPM concentrations (13 mg L^{-1}; Fig. 3). Thus, at both sites, some suspended material was lost between 24 February and 04 March. If the composition of that lost material differed between the sites, it could explain why particulate metals increased at one site but decreased at the other. Because of the difficulty in interpreting the cause of changes in particulate metal concentrations, we focused our analyses on the dissolved fraction.

1998; Grenz et al. 2000). When conditions then become suboxic, bacteria can use other elements as electron receptors, such as Mn(IV) (Beck and Bruland 2000). By reducing particulate Mn(IV) to soluble Mn(II), bacteria in suboxic conditions can increase dissolved Mn concentration (Schoemann et al. 1998; Beck and Bruland 2000).

Reduction and dissolution of Mn(IV) in suboxic sediments was the mechanism proposed by Schoemann et al. (1998) and Roitz et al. (2002) to explain increases in dissolved Mn after a phytoplankton bloom in South San Francisco Bay and in the coastal waters of the North Sea, respectively. Although Roitz et al. (2002) found that a number of different factors, including higher temperature in the summer, could contribute to fluxes of dissolved Mn from the sediments to the water, they found that intense remobilization after a phytoplankton bloom was responsible for the some of the highest concentrations of dissolved Mn. Similarly, we concluded that reduction and dissolution of Mn(IV) during bloom decomposition explained why dissolved Mn was exceptionally high in April (Fig. 5).

The following calculations also indicated that release of Mn from sediments, and not algal remineralization, was the major mechanism for the increase in dissolved Mn during April. By multiplying the increase in [C] or the decrease in [P] during the bloom by [metal]:[C] or [metal]:[P] ratios in phytoplankton, we calculated the potential amount of Mn assimilated by algae during the bloom (Table 1). We determined ΔP for sites 32 and 36 by quantifying the average decrease in DRP from 19 February to 04 March (8.45–3.29 = 5.16 µmol L^{-1}; Fig. 4). We then multiplied ΔP by the average [Mn]:[P] ratio in phytoplankton

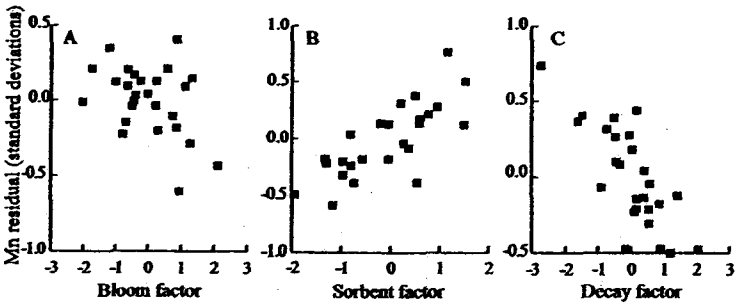

Fig. 7. Partial residual plots showing how the three PCA factors that were significant in the model (Table 5) affected dissolved Mn concentrations. (A) The bloom factor, which characterized growth of the bloom, decreased dissolved Mn concentrations. (B) Dissolved Mn concentrations increased as sorbent increased. (C) During decay, which was indicated by, declining values of that factor, dissolved Mn concentrations increased. These plots display multiple linear regression results by graphing each factor on the *x*-axis versus the residuals when the model was run without that factor. The magnitude of the *y*-axis and the direction of the slope indicate the relative contribution of that factor to Mn concentrations and whether the relationship between the factor and dissolved Mn was positive or negative.

(Table 1). The resulting calculation suggested that the bloom could have at most assimilated 1.7 nmol L^{-1} of Mn:

$$\left(\frac{5.16\ \mu\text{mol P}}{\text{L}}\right)\left(\frac{0.34\ \text{mmol Mn}}{1\ \text{mol P}}\right) = \frac{1.7\ \text{nmol Mn}}{\text{L}}$$

If all 1.7 nmol L^{-1} of Mn was later remineralized from phytoplankton, it would have accounted for only 0.1% of the observed increase in dissolved Mn between 24 February and 23 April (Table 1; Fig. 5). A similar result was obtained with the use of [metal]:[C] ratios (Table 1). We concluded that remobilization from sediments likely accounted for most of the increase in dissolved Mn.

Cobalt—Cobalt cycling during the bloom differed from Mn cycling because the bloom factor did not measurably affect dissolved Co concentrations (Table 5). The difference between the two metals was unexpected. We assumed Co and Mn cycling would be linked because they are both microbially oxidized via the same pathway (Lee and Fisher 1993; Moffett and Ho 1996). According to Moffett and Ho (1996), few studies compare Mn and Co in coastal waters, but because those areas typically have high rates of microbial Mn oxidation, the two elements should have similar biogeochemistries in coastal environments. In their study of the Waquoit Bay estuary, the authors did observe one difference between the two elements: Mn oxidation was ~7× faster than Co oxidation. In our study, it was possible that differing oxidation rates explained why Mn was depleted by the bloom factor, whereas Co was not.

Alternatively, organic complexation might have blocked depletion of dissolved Co by preventing Co from being co-oxidized by Mn-oxidizing bacteria. Complexation of Co and resulting inhibition of Co oxidation was argued to be responsible for higher dissolved Co than Mn, which was not complexed, in deep waters of the Sargasso Sea (Saito and Moffett 2002).

Finally, it was possible that we did not see a decrease in dissolved Co because our sampling began too late. Although Table 1 indicated that a depletion of dissolved Co by phytoplankton was too small to measure, microbial oxidation of Co could have occurred but not been captured by our sampling scheme. Our group's previous studies, conducted as part of the Regional Monitoring Program (RMP; http://www.sfei.org/rmp/2000/2000_Annual_Results.htm and http://www.sfei.org/rmp/2001/2001_Annual_Results.htm), suggested that dissolved Co concentrations were higher when Chl *a* was <10 μg L^{-1} at the beginning of February in 2000 and 2001. During that time, dissolved Co at the Coyote Creek and Dumbarton Bridge sites, which correspond well to USGS sites 36 and 32, averaged 3.8 and 3.1 nmol L^{-1}, respectively. On the basis of the RMP data and this study, we figured that in South Bay, dissolved Co concentrations are relatively high at the beginning of February (~3.4 nmol L^{-1}), decrease before the bloom peaks (~2.5 nmol L^{-1}), exceed baseline concentrations during bloom decomposition (~6.4 nmol L^{-1}), and eventually return to baseline levels in August (~3.8 nmol L^{-1}) or even exceed those levels in some years (e.g., 2000 and 2001). Elevated Co concentrations in summer are consistent with its input from sewage discharges and remobilization from contaminated sediments in South Bay (Tovar-Sánchez et al. 2004).

Unlike the bloom factor, the decay factor significantly ($p < 0.01$; Table 5) affected dissolved Co concentrations. Dissolved Co concentrations increased as the bloom decayed (Fig. 8), largely because of reductive dissolution of Fe and Mn (hydr)oxides. Although the timing of our peak in dissolved Co (well after the Chl *a* peak; Fig. 5) was consistent with observations by Lee and Fisher (1992), showing that decaying diatoms release Co more slowly than carbon, the values in Table 1 indicate that algal remine-

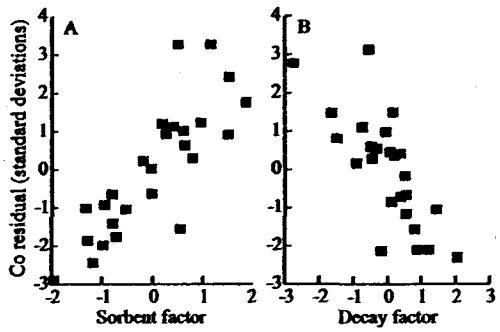

Fig. 8. Partial residual plots showing how the PCA factors that were significant in the model (Table 5) affected dissolved Co concentrations. (A) Dissolved Co concentrations significantly increased as sorbent increased. (B) During decay, which was indicated by declining values of that factor, dissolved Co concentrations increased. These plots display multiple linear regression results by running the model without one of the factors and then plotting the residuals against the omitted factor. Both the sorbent and the decay factors explained the variance in the residuals and were therefore important for determining Co concentrations.

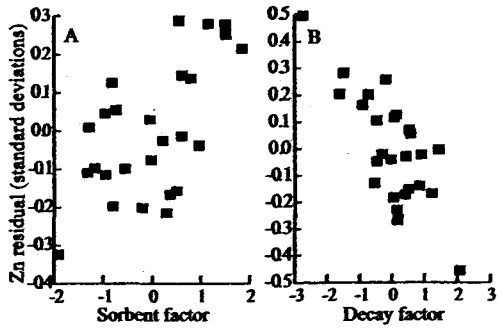

Fig. 9. Partial residual plots showing how the PCA factors that were significant in the model (Table 5) affected dissolved Zn concentrations. (A) Dissolved Zn concentrations significantly increased as sorbent increased. (B) During decay, which was indicated by declining values of that factor, dissolved Zn concentrations increased. The y-axis shows the residuals when the factor on the x-axis was omitted from the model.

alization accounted for <10% of the observed Co increase. The remainder of the increase in dissolved Co from 24 February to 01 April (Fig. 5) was likely caused by reduction and dissolution of Fe and Mn (hydr)oxides in suboxic sediments. Dissolution of Mn (hydr)oxides releases Co because it is incorporated into (hydr)oxides when bacteria co-oxidize both elements (Moffett and Ho 1996). The proposed release of Co from sediments was also consistent with the benthic remobilization observed by Rivera-Duarte and Flegal (1997). Those authors showed that for Co and Zn, concentrations were 10–100 and 1–100 (respectively) times higher in porewater than in surface water in the estuary.

Another possible explanation for the increase in dissolved Co was that high DOC in the decaying bloom caused Co to desorb from the particulate phase, but that explanation was not supported by our K_d values. Tovar-Sánchez et al. (2004) determined that desorption from the particulate phase was a major factor controlling dissolved Co concentrations in San Francisco Bay. They also found that in San Francisco Bay, Co desorbed at salinities >20. Although salinity ranged from 17 to 30 in this study, and dissolved Co as a percentage of the total did not change with salinity. The Co K_d values changed only as a function of site (Table 6). Furthermore, some of our values for dissolved Co were higher than the range of dissolved Co concentrations supported by particle desorption in Tovar-Sánchez et al. (2004). Thus, the peak that we observed in dissolved Co (Fig. 5) was tentatively attributed to diagenetic remobilization from sediments, not from Co desorption.

Zinc—Dissolved Zn was not measurably affected by the bloom factor according to our GLM (Table 5; Fig. 9). One of the advantages of using multivariate statistics to analyze the effects of the PCA factors on dissolved Zn concentrations (Table 5) is that the model measures the variation associated with a particular factor after accounting for the other terms in the model. For example, the model would have accounted for conditions, such as a pulse of SPM, which could have made a dissolved Zn depletion difficult to detect. Therefore, we were confident that the GLM (Table 5) correctly represented the sorbent and decay factors as the only two terms that affected dissolved Zn concentrations.

Furthermore, the distribution of dissolved Zn (Fig. 5) supported our statistical analyses that showed the bloom was not an important factor for describing dissolved Zn concentrations. Although the concentration of dissolved Zn at site 36 declined from the end of February to the beginning of March (Fig. 5), its concentration subsequently increased from 12 March to 27 March and then decreased to 01 April (Fig. 5). In contrast, dissolved Ni, which was significantly ($p < 0.01$; Table 5) depleted by the bloom factor, showed a steady decrease in concentration (Fig. 5).

Consequently, the factors (sorbent and decay) that affected dissolved Zn concentrations were the same as those that affected dissolved Co concentrations (Table 5) and differed from our hypothesis that phytoplankton would deplete dissolved Zn during the bloom. Phytoplankton blooms have the potential to deplete first Zn and then Co because the elements are used in the enzyme carbonic anhydrase (Morel et al. 2004). That enzyme is responsible for converting HCO_3^- to CO_2 to provide inorganic carbon during the dark reactions of the Calvin cycle.

The lack of a measurable decline in dissolved Zn concentrations in this study also differed from observations in previous field (Luoma et al. 1998; Zwolsman and van Eck 1999) and mesocosm studies (Riedel and Sanders 2003; Wang et al. 2005). In a field study of the 1994 South Bay bloom, Luoma et al. (1998) found that dissolved Zn was depleted from the water. Similarly, Zwolsman and van Eck

(1999) observed a decrease in dissolved Zn in the Scheldt estuary during a spring bloom. Mesocosm studies have confirmed those findings by adding nutrients to stimulate a bloom under controlled conditions. For example, Riedel and Sanders (2003) found that dissolved Zn was depleted in mesocosm studies with Patuxent River water, and Wang et al. (2005) showed that phytoplankton accumulated Zn from Hong Kong coastal waters. The contrasting results in our study could be because (1) sampling started too late to capture a Zn drawdown, (2) Zn was rapidly repartitioned from the particulate phase, (3) organic complexation limited Zn bioavailability, or (4) a combination of these factors.

The relationship between when sampling started and whether the metal was depleted might have been influenced by the kinetics of metal repartitioning between dissolved and particulate phases. Gee and Bruland (2002) showed that in South Bay, the Zn equilibrium between particulate and dissolved phases was established rapidly, in about 2 weeks, whereas Ni repartitioned in about 1 month. Thus, it was possible that dissolved Zn was initially depleted, but by the time this study began, Zn desorption from particulates masked any algal drawdown. The possibility that Zn was redistributed between the two phases was supported by our statistical results that showed Zn K_d values decreased with the decay factor (Table 6). A redistribution of Zn would also be consistent with its rapid desorption rates; Gee and Bruland (2002) showed that Zn desorbed more rapidly than it adsorbed (unlike Ni), and its dissolved concentration could increase by roughly 20% in a single day because of particle desorption. Therefore, in this study, Ni could have remained depleted in the water for a longer time because of its slower kinetics. Its decline was more easily observed in our experimental design.

To determine the extent to which organic complexation could have limited uptake of dissolved Zn, studies of Zn complexation in South Bay are needed. On the basis of the limited studies available (e.g., Brand et al. 1983; Sunda et al. 2005), free Zn concentrations govern growth and uptake to phytoplankton, indicating that the Zn complex might not be readily bioavailable to phytoplankton. Site-specific studies of Zn complexation in San Francisco Bay are needed because Zn complexation in estuaries is highly variable. For example, Sunda et al. (2005) showed that the amount of free Zn available for phytoplankton uptake in the Elizabeth River estuary varied by 20,000 between samples. Similarly, Kozelka and Bruland (1998), found that the percentage of complexed Zn in Narragansett Bay, Rhode Island, ranged from 51% to 97%. That complexation could be by ligands released from dying phytoplankton (Muller et al. 2005). Consequently, the sequestration of Zn in unavailable complexes could explain why it was not depleted by the bloom factor.

Both dissolved Zn and Co concentrations significantly ($p < 0.01$; Table 5) increased with the decay factor (Fig. 9). That result was consistent with previous research linking high DOC and elevated Zn in South Bay (Kuwabara et al. 1989). The possible contribution of remineralization of phytoplankton to the observed increase in dissolved Zn varied between 10% and 100%, depending which numbers were used (Table 1). However, the increase was most likely due to reductive dissolution of Fe and Mn (hydr)oxides, which have been shown (Luoma and Bryan 1981) to strongly bind Zn.

Copper—The categorical variable, site, was the most important term explaining dissolved Cu concentrations ($p < 0.01$), as demonstrated by its mean square error (Table 5). Concentrations of dissolved Cu were highest at site 36, intermediate at site 32, and lowest at site 21, which was consistent with previous research (Flegal et al. 1991). Unlike some of the other elements in this study, the decay factor was relatively unimportant for determining Cu concentrations (Table 5), and the bloom factor was not included in the model. We attributed these relatively stable dissolved Cu concentrations (Fig. 5) to complexation of dissolved Cu by organic ligands.

Previous research has demonstrated that between 80% and >99% of dissolved Cu is complexed to organic ligands in South Bay (Donat et al. 1994; Buck and Bruland 2005; Hurst and Bruland 2005). That complexation could be by (1) ligands produced by cyanobacteria (Moffett and Brand 1996), (2) natural humic and fulvic substances (Kogut and Voelker 2001), (3) synthetic chelating agents in surface or wastewater inputs (Sedlak et al. 1997), or (4) a combination of these ligands. Moreover, this complexation of Cu to strong chelating agents has been demonstrated in all seasons in South Bay (Buck and Bruland 2005).

Previous studies have demonstrated that the strong Cu complexation in South Bay limits Cu uptake to phytoplankton. Beck et al. (2002) found that >99.9% of dissolved Cu was bound to strong organic ligands in South Bay water samples collected in April 2000. According to those authors, that complexation explained why Cu was not depleted in their laboratory grow-out experiments of San Francisco Bay water isolated from benthic grazers. Similarly, Luoma et al. (1998) found that dissolved Cu was not depleted during the 1994 South Bay spring bloom. Also in a South Bay field study, Buck and Bruland (2005) found that Cu concentrations and speciation were not affected by the spring 2003 bloom.

Buck and Bruland (2005) sampled in the same year as in this study, and their data also demonstrated that dissolved Cu concentrations in January 2003 were comparable to concentrations measured here. In January, their measured dissolved Cu concentrations at Yerba Buena Island and Dumbarton Bridge were 18.9 and 33.7 nmol L^{-1}, respectively. Those values were within the range of concentrations (11.0–27.5 and 33.7–45.4 nmol L^{-1}, respectively) that we measured at our corresponding USGS sites 21 and 32 between February and May. We therefore concluded that it was unlikely that Cu depletion occurred before our first sampling date.

Copper K_d values were controlled by site-specific processes, as they were for Co. In the final model, the only variable controlling Cu K_d values was the site from which the samples were collected (Table 6). The importance of the variable site indicates that Cu partitioning was controlled by spatial factors that are not explained by the sorbent factor.

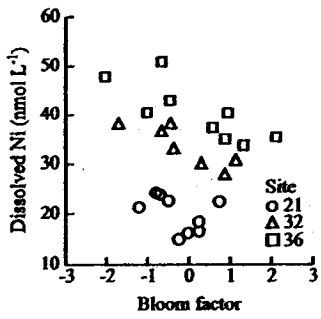

Fig. 10. Dissolved Ni concentrations were affected by both the bloom and site factors, which were significant (Table 5) factors in the Ni model. Within each site, growth of the bloom (increasing values of that factor) decreased dissolved Ni concentrations, indicating uptake by phytoplankton.

Nickel—Dissolved Ni was significantly ($p < 0.01$; Table 5) depleted by the bloom factor (Fig. 10), which followed from its role as a trace nutrient. The categorical variable, site, also significantly ($p < 0.01$; Table 5) affected dissolved Ni concentrations. Those concentrations increased from our most oceanic site to our site in the extreme South Bay (Fig. 10). In the Ni model (Table 5), the decay factor was statistically significant ($p = 0.054$; Table 5), but its comparatively low mean square error (Table 5) indicated that it accounted for only a very small amount of the variability. Thus, the two principal terms controlling Ni cycling were site and the bloom factor (Fig. 10).

The depletion of Ni during this bloom was consistent with a decrease (75% reduction) in dissolved Ni concentrations observed during the 1994 South Bay bloom (Luoma et al. 1998) but contrasted with laboratory simulations of the South Bay bloom that showed no Ni depletion (Beck et al. 2002). This discrepancy could be because of differences in the time of year the studies were conducted; seasonal changes in the relative contribution of wastewater inputs and surface runoff sources might affect the proportion of complexed Ni (Sedlak et al. 1997). About 25% of Ni surface runoff is strongly complexed by ethylenediaminetetraacetic acid (EDTA), whereas 75% of Ni in wastewater is bound to EDTA (Sedlak et al. 1997; Bedsworth and Sedlak 1999). Accordingly, in summer, when wastewater is the dominant source of freshwater to South Bay, a larger percentage of Ni is complexed by EDTA. The Beck et al. (2002) laboratory study could have contained a higher percentage of complexed Ni than in this study or the Louma et al. (1998) study because Beck and colleagues collected water in April, 2 months later than field sampling began in the other studies. Therefore, greater complexation of Ni in the Beck et al. (2002) study than in the field studies could explain why they did not observe Ni depletion.

Alternatively, the difference between the results of the studies could have been caused by UV degradation of the EDTA–Ni complex, which has been observed by Sedlak et al. (1997). UV degradation could have increased the amount of bioavailable Ni in the field relative to the Beck et al. (2002) laboratory study, which used standard fluorescent lights to culture the phytoplankton. Further field sampling and laboratory studies are needed to resolve this disparity.

We used the average increase in Chl *a* at sites 32 and 36 from 24 February to 04 March (65 μg L^{-1}) and the corresponding average decrease in dissolved Ni (5.8 nmol L^{-1}) to calculate the Ni concentration per mass of phytoplankton. We multiplied the increase in Chl *a* by the [C]:[Chl *a*] ratio (Cloern et al. 1995) and then divided by 0.3 to convert [C] to dry weight of phytoplankton (Luoma et al. 1998) as follows:

$$\left(\frac{65\ \mu\text{g Chl } a}{\text{L}}\right)\left(\frac{35\ \mu\text{g C}}{\mu\text{g Chl } a}\right)\Big/\frac{0.3\ \mu\text{g C}}{\mu\text{g phytoplankton}} = \frac{8\ \text{mg phytoplankton}}{\text{L}}$$

We divided the decrease in dissolved Ni concentrations (5.8 nmol L^{-1}; Fig. 5) by the mass of phytoplankton produced (8 mg phytoplankton L^{-1}) to estimate that phytoplankton contained ~0.7 μmol Ni g^{-1} dry weight. This estimate was an order of magnitude higher than concentrations of Ni in phytoplankton reported by Luoma et al. (1998) for South Bay (0.04 μmol g^{-1}) and those cited by Bruland et al. (1991) from Monterey Bay (0.05 ± 0.04 μmol g^{-1}). However, the results were more consistent with Twining et al. (2004), who reported higher [metal]:[C] ratios in phytoplankton than Bruland et al. (1991), as shown in Table 1.

Lead—The bloom factor significantly ($p < 0.01$; Table 5) depleted dissolved Pb. This depletion (Fig. 11) was presumably due to Pb sorption onto phytoplankton surfaces because Pb is highly particle reactive. The K_d values for Pb averaged ~10^6 L kg^{-1} in this study, which was consistent with previously reported K_d values ($10^{5.3}$ L kg^{-1}) for Pb in South Bay (Squire et al. 2002). The affinity of Pb for particles was also demonstrated by the order of magnitude higher Pb concentrations in the particulate phase (Fig. 6) relative to the dissolved phase (Fig. 5).

Our hypothesis that Pb was sorbed to phytoplankton was also consistent with previous calculations showing that surface area determined the Pb concentration of planktonic organisms (Michaels and Flegal 1990). Lead sorption to phytoplankton was also demonstrated in short-term laboratory experiments with Connecticut River water (Mylon et al. 2003). In those experiments, algal uptake rates of Pb spiked into Connecticut River water were not affected by temperature, indicating that most uptake was caused by binding to cell surfaces. Finally, it was unlikely that algae took up dissolved Pb internally because >95% of Pb is organically complexed in San Francisco Bay (Kozelka et al. 1997).

We calculated the Pb concentration per mass of phytoplankton following the same method we used to calculate the Ni concentration in phytoplankton. We

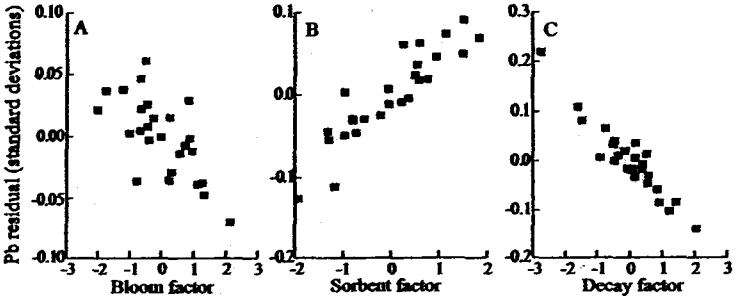

Fig. 11. Partial residual plots showing how the three PCA factors that were significant in the model (Table 5) affected dissolved Pb concentrations. (A) Dissolved Pb concentrations decreased during the bloom. (B) Dissolved Pb concentrations increased as sorbent increased. (C) During decay, which was indicated by declining values of that factor, dissolved Pb concentrations increased. The plots show the residuals when the model was run with two of the three factors versus the remaining factor on the *x*-axis. The residuals on the *y*-axis are shown in terms of standard deviations. Accordingly, decay, which explained large standard deviations in the residuals, was more important to the model than bloom.

divided the decrease in dissolved Pb (0.08 nmol L^{-1}; Fig. 5) from 24 February to 04 March at sites 32 and 36 by the mass of phytoplankton produced (8 mg phytoplankton L^{-1}) during that time to determine that phytoplankton contained 0.01 μmol Pb g^{-1} dry weight. That estimated concentration was consistent with the single detectable value for Pb in phytoplankton (0.01 μmol Pb g^{-1}) with low Al (<100 μg g^{-1}; *see* Bruland et al. 1991) reported by Martin and Knauer (1973). Similarly, in the Seine estuary, Pb concentrations in diatoms were 0.07 μmol Pb g^{-1} (Miramand et al. 1998). Our results were also consistent with culture studies that showed phytoplankton could accumulate up to 1.7×10^4 more Pb per cell volume than in an equivalent amount of ambient water, and that the uptake was associated with the cell walls (Fisher et al. 1983). Finally, by scavenging Pb, the bloom could help retain that metal within the estuary, as has been observed for other metals (Luoma et al. 1998).

Although the bloom factor accounted for depletion of dissolved Pb concentrations, the most important factor affecting dissolved Pb concentrations was the decay factor (Table 5). During decomposition of the bloom, which was indicated by decreasing values of the decay factor, dissolved Pb concentrations increased (Table 5; Fig. 11). The increase in dissolved Pb was consistent with the diagenetic release of Pb from historically contaminated sediments, which are now the major source of Pb to San Francisco Bay waters (Steding et al. 2000; Flegal et al. 2005).

Annual contribution of phytoplankton—We calculated the amount of Ni from wastewater treatment plants that was cycled through phytoplankton annually to determine whether phytoplankton could be an important mechanism for trapping anthropogenically derived metals in the estuary. We focused on the region of the South Bay south of the Dumbarton Bridge (lower South Bay) because our sites 32 and 36 bracketed that area (Fig. 1). Following calculations in Luoma et al. (1998), we calculated the ratio of metal depleted (*Δ*Metal) to DRP depleted (*Δ*DRP) for the period between 24 February and 04 March.

$$\gamma_{\text{Metal}} = \frac{\Delta\text{Metal}}{\Delta\text{DRP}} = \frac{5.8 \text{ nmol L}^{-1}}{1{,}750 \text{ nmol L}^{-1}} = 3.3 \times 10^{-3}$$

We then determined the annual DRP consumption, according to

$$\left(\frac{12.5 \text{ mol C}}{\text{m}^2} \text{ net production}\right)(3.4 \times 10^7 \text{ m}^2 \text{ surface area})\left(\frac{1 \text{ mol P}}{106 \text{ mol C}}\right) = 4.0 \times 10^6 \text{ mol P yr}^{-1}$$

where the product of the annual South Bay net production (Cole and Cloern 1984) and the lower South Bay surface area (Hager and Schemel 1996) gave the South Bay annual primary production, and division by the Redfield ratio converted the annual C production to annual P consumption. Then, we multiplied the annual P consumption by γ_{Metal} and found that algae in lower South Bay have the potential to sorb (adsorb or assimilate) 1.3×10^4 mol of Ni each year.

The 1.3×10^4 mol of Ni cycled by the phytoplankton was about 75% of the Ni discharged into the lower South Bay by wastewater treatment plants in 2003. In that year, the Palo Alto, San Jose and Santa Clara, and Sunnyvale wastewater treatment plants released 1.8×10^4 mol of Ni to the lower South Bay (R. E. Looker pers. comm.). The trapping of discharged Ni by phytoplankton was consistent with results from Luoma et al. (1998), which showed that about 60% of the Ni discharged to the entire South Bay was assimilated by phytoplankton. As those authors discussed, these calculations were rough because [metal]:[P] uptake ratios by phytoplankton vary. Furthermore, our calculation of Ni assimilation was conservative because we used the primary productivity calculated for South Bay, not the

lower South Bay where blooms are more intense. Despite these uncertainties, we concluded that (1) Ni loadings to South Bay from wastewater treatment plants are relatively large, (2) phytoplankton trap enough Ni that changes in phytoplankton biomass will affect metal cycling and retention, and (3) the bloom has the potential to introduce Ni to the food chain because benthic organisms often take advantage of the bloom to grow and reproduce (Thompson and Nichols 1988).

Phytoplankton play an important role in metal cycling in the estuary by trapping metals, making those metals bioavailable to the food chain, and altering metal concentrations during bloom events. Accordingly, changes in phytoplankton biomass (e.g., from nutrient enrichment) are likely to have complex effects on metal cycling that might not be readily anticipated. That conclusion is consistent with models by Cloern (2001) that show eutrophication has unique and subtle manifestations in each estuary, including alterations in metal cycling in the San Francisco Bay.

By exploiting the predictability of the South Bay bloom, we were able to determine which metals were affected by nutrient-enriched blooms. Only 3 of the metals in this study (Mn, Ni, and Pb) were decreased by the bloom factor (Table 5). During the bloom, Ni was likely assimilated by phytoplankton and made bioavailable to the food chain. Contrary to our hypotheses, dissolved Co and Zn were not measurably depleted by the bloom factor, possibly because (1) sampling started too late to capture the drawdown, (2) kinetics of oxidation and repartitioning masked the depletions, (3) organic complexation limited the bioavailability of the metals, or (4) a combination of these factors. Consistent with our hypothesis, dissolved Cu was not affected by either the bloom or decay factors, attesting to its strong organic complexation that limits its bioavailability and toxicity in the estuary. The decay of the bloom material also affected cycling of other metals. Dissolved Mn, Co, Zn, and Pb were remobilized, presumably by reductive dissolution of Fe and Mn (hydr)oxides in surficial sediments during algal decomposition. The effects of the bloom and its decay on metal concentrations in the estuary were consistent with the biogeochemistries of the metals and demonstrated that nutrient-enriched blooms affect metal cycling.

References

Beck, N. G., and K. W. Bruland. 2000. Diel biogeochemical cycling in a hyperventilating shallow estuarine environment. Estuaries **23:** 177–187.

———, ———, and E. L. Rue. 2002. Short-term biogeochemical influence of a diatom bloom on the nutrient and trace metal concentrations in South San Francisco Bay microcosm experiments. Estuaries **25:** 1063–1076.

Bedsworth, W. W., and D. L. Sedlak. 1999. Sources and environmental fate of strongly complexed nickel in estuarine waters: The role of ethylenediaminetetraacetate. Environ. Sci. Technol. **33:** 926–931.

Brand, L. E., W. G. Sunda, and R. R. L. Guillard. 1983. Limitation of marine phytoplankton reproductive rates by zinc, manganese, and iron. Limnol. Oceanogr. **28:** 1182–1198.

Bruland, K. W., J. R. Donat, and D. A. Hutchins. 1991. Interactive influences of bioactive trace metals on biological production in oceanic waters. Limnol. Oceanogr. **36:** 1555–1577.

———, and M. C. Lohan. 2004. Controls of trace metals in seawater. Treatise Geochem. **6:** 23–47.

Brzezinski, M. A. 1985. The Si:C:N ratio of marine diatoms: Interspecific variability and the effect of some environmental variables. J. Phycol. **21:** 347–357.

Buck, K. N., and K. W. Bruland. 2005. Copper speciation in San Francisco Bay: A novel approach using multiple analytical windows. Mar. Chem. **96:** 185–198.

Caffrey, J. M., J. E. Cloern, and C. Grenz. 1998. Changes in production and respiration during a spring phytoplankton bloom in San Francisco Bay, California, USA: Implications for net ecosystem metabolism. Mar. Ecol. Prog. Ser. **172:** 1–12.

Cloern, J. E. 1996. Phytoplankton bloom dynamics in coastal ecosystems: A review with some general lessons from sustained investigation of San Francisco Bay, California. Rev. Geohpys. **34:** 127–168.

———. 2001. Our evolving conceptual model of the coastal eutrophication problem. Mar. Ecol. Prog. Ser. **210:** 223–253.

———, and R. Dufford. 2005. Phytoplankton community ecology: Principles applied in San Francisco Bay. Mar. Ecol. Prog. Ser. **285:** 11–28.

———, C. Grenz, and L. Vidergar-Lucas. 1995. An empirical model of the phytoplankton chlorophyll:carbon ratio—the conversion factor between productivity and growth rate. Limnol. Oceanogr. **40:** 1313–1321.

Cole, B. E., and J. E. Cloern. 1984. Significance of biomass and light availability to phytoplankton productivity in San Francisco Bay. Mar. Ecol. Prog. Ser. **17:** 15–24.

Donat, J. R., K. A. Lao, and K. W. Bruland. 1994. Speciation of dissolved copper and nickel in South San Francisco Bay: A multi-method approach. Anal. Chim. Acta **284:** 547–571.

Fisher, N. S., K. A. Burns, R. D. Cherry, and M. Heyraud. 1983. Accumulation and cellular distribution of ^{241}Am, ^{210}Po, and ^{210}Pb in two marine algae. Mar. Ecol. Prog. Ser. **11:** 233–237.

Flegal, A. R., C. H. Conaway, G. M. Scelfo, S. A. Hibdon, and S. A. Sañudo-Wilhelmy. 2005. A review of factors influencing measurements of decadal variations in metal contamination in San Francisco Bay, California. Ecotoxicology **14:** 645–660.

———, G. J. Smith, G. A. Gill, S. Sañudo-Wilhelmy, and L. C. D. Anderson. 1991. Dissolved trace element cycles in the San Francisco Bay estuary. Mar. Chem. **36:** 329–363.

Gee, A. K., and K. W. Bruland. 2002. Tracing Ni, Cu, and Zn kinetics and equilibrium partitioning between dissolved and particulate phases in South San Francisco Bay, California, using stable isotopes and high-resolution inductively coupled plasma mass spectrometry. Geochim. Cosmochim. Acta **66:** 3063–3083.

Granéli, W., and E. Granéli. 1991. Automatic potentiometric determination of dissolved oxygen. Mar. Biol. **108:** 341–348.

Grenz, C., J. E. Cloern, S. W. Hager, and B. E. Cole. 2000. Dynamics of nutrient cycling and related benthic nutrient and oxygen fluxes during a spring phytoplankton bloom in South San Francisco Bay (USA). Mar. Ecol. Prog. Ser. **197:** 67–80.

Hager, S. W. 1994. Dissolved nutrient and suspended particulate matter data for the San Francisco Bay estuary, California, October 1991 through November 1993. U.S. Geol. Surv. open-file report 94-471.

———, AND L. E. SCHEMEL. 1996. Dissolved inorganic nitrogen, phosphorus and silicon in South San Francisco Bay I. Major factors affecting distributions. *In* J. T. Hollibaugh [ed.], San Francisco Bay, The ecosystem: Further investigations into the natural history of San Francisco Bay and Delta with reference to the influence of man. Pacific Division of the American Association for the Advancement of Science.

HURST, M. P., AND K. W. BRULAND. 2005. The use of Nafion-coated thin mercury film electrodes for the determination of the dissolved copper speciation in estuarine water. Anal. Chim. Acta **546:** 68–78.

[IAEA] INTERNATIONAL ATOMIC ENERGY AGENCY. 2004. Sediment distribution coefficients and concentration factors for biota in the marine environment. Tech. Rep. Ser. 422, IAEA.

INGRI, J., AND OTHERS. 2004. Size distribution of colloidal trace metals and organic carbon during a coastal bloom in the Baltic Sea. Mar. Chem. **91:** 117–130.

KOGUT, M. B., AND B. M. VOELKER. 2001. Strong copper-binding behavior of terrestrial humic substances in seawater. Environ. Sci. Technol. **35:** 1149–1156.

KOZELKA, P. B., AND K. W. BRULAND. 1998. Chemical speciation of dissolved Cu, Zn, Cd, Pb in Narragansett Bay, Rhode Island. Mar. Chem. **60:** 267–282.

———, S. SANUDO-WILHELMY, A. R. FLEGAL, AND K. W. BRULAND. 1997. Physico-chemical speciation of lead in South San Francisco Bay. Estuar. Coast. Shelf Sci. **44:** 649–658.

KUWABARA, J. S., C. C. Y. CHANG, J. E. CLOERN, T. L. FRIES, J. A. DAVIS, AND S. N. LUOMA. 1989. Trace metal associations in the water column of South San Francisco Bay, California. Estuar. Coast. Shelf Sci. **28:** 307–326.

LEE, B.-G., AND N. S. FISHER. 1992. Degradation and elemental release rates from phytoplankton debris and their geochemical implications. Limnol. Oceanogr. **37:** 1345–1360.

———, AND ———. 1993. Microbially mediated cobalt oxidation in seawater revealed by radiotracer experiments. Limnol. Oceanogr. **38:** 1593–1602.

———, AND S. N. LUOMA. 1998. Influence of microalgal biomass on absorption efficiency of Cd, Cr, and Zn by two bivalves from San Francisco Bay. Limnol. Oceanogr. **43:** 1455–1466.

LUOMA, S. N., AND G. W. BRYAN. 1981. A statistical assessment of the form of trace metals in oxidized estuarine sediments employing chemical extractants. Sci. Total Environ. **17:** 165–196.

———, A. VAN GEEN, B.-G. LEE, AND J. E. CLOERN. 1998. Metal uptake by phytoplankton during a bloom in South San Francisco Bay: Implications for metal cycling in estuaries. Limnol. Oceanogr. **43:** 1007–1016.

MARTIN, J. H., AND G. A. KNAUER. 1973. The elemental composition of plankton. Geochim. Cosmochim. Acta **37:** 1639–1653.

MICHAELS, A. F., AND A. R. FLEGAL. 1990. Lead in marine planktonic organisms and pelagic food webs. Limnol. Oceanogr. **35:** 287–295.

MIRAMAND, P., D. FICHET, D. BENTLEY, J.-C. GUARY, AND F. CAURANT. 1998. Heavy metal concentrations (Cd, Cu, Pb, Zn) at different levels of the pelagic trophic web collected along the gradient of salinity in the Seine estuary. Earth Planet. Sci. **327:** 259–264.

MOFFETT, J. W., AND L. E. BRAND. 1996. Production of strong, extracellular Cu chelators by marine cyanobacteria in response to Cu stress. Limnol. Oceanogr. **41:** 388–395.

———, AND J. HO. 1996. Oxidation of cobalt and manganese in seawater via a common microbially catalyzed pathway. Geochim. Cosmochim. Acta **60:** 3415–3424.

MOREL, F. M. M., AND J. G. HERING. 1993. Principles and applications of aquatic chemistry. Wiley.

———, A. J. MILLIGAN, AND M. A. SAITO. 2004. Marine bioinorganic chemistry. The role of trace metals in the oceanic cycles of major nutrients. Treatise Geochem. **6:** 113–143.

MULLER, F. L. L., A. LARSEN, C. A. STEDMON, AND M. SONDERGAARD. 2005. Interactions between algal–bacterial populations and trace metals in fjord surface waters during a nutrient-stimulated summer bloom. Limnol. Oceanogr. **50:** 1855–1871.

MYLON, S. E., B. S. TWINING, N. S. FISHER, AND G. BENOIT. 2003. Relating the speciation of Cd, Cu, and Pb in two Connecticut rivers with their uptake in algae. Environ. Sci. Technol. **37:** 1261–1267.

NDUNG'U, K., R. P. FRANKS, K. W. BRULAND, AND A. R. FLEGAL. 2003. Organic complexation and total dissolved trace metal analysis in estuarine waters: Comparison of solvent-extraction graphite furnace atomic absorption spectrometric and chelating resin flow injection inductively coupled plasma–mass spectrometric analysis. Anal. Chim. Acta **481:** 127–138.

OSENBERG, C. W., R. J. SCHMITT, S. J. HOLBROOK, AND D. CANESTRO. 1992. Spatial scale of ecological effects associated with an open coast discharge of produced water. Environ. Sci. Res. **46:** 387–402.

PARSONS, T. R., Y. MAITA, AND C. M. LALLI. 1984. A manual of chemical and biological methods for seawater analysis, 1st ed. Pergamon.

RIEDEL, G. F., AND J. G. SANDERS. 2003. The interrelationships among trace element cycling, nutrient loading, and system complexity in estuaries: A mesocosm study. Estuaries **26:** 339–351.

RIVERA-DUARTE, I., AND A. R. FLEGAL. 1997. Porewater gradients and diffusive benthic fluxes of Co, Ni, Cu, Zn, and Cd in San Francisco Bay. Croat. Chem. Acta **70:** 389–417.

ROITZ, J. S., A. R. FLEGAL, AND K. W. BRULAND. 2002. The biogeochemical cycling of manganese in San Francisco Bay: Temporal and spatial variations in surface water concentrations. Estuarine, Coastal and Shelf Science **54:** 227–239.

SAITO, M. A., AND J. W. MOFFETT. 2002. Temporal and spatial variability of cobalt in the Atlantic Ocean. Geochim. Cosmochim. Acta **66:** 1943–1953.

SCHOEMANN, V., H. J. W. DE BAAR, J. T. M. DE JONG, AND C. LANCELOT. 1998. Effects of phytoplankton blooms on the cycling of manganese and iron in coastal waters. Limnol. Oceanogr. **43:** 1427–1441.

SEDLAK, D. L., J. T. PHINNEY, AND W. W. BEDSWORTH. 1997. Strongly complexed Cu and Ni in wastewater effluents and surface runoff. Environ. Sci. Technol. **31:** 3010–3016.

SHARP, J. H., R. BENNER, L. BENNETT, C. A. CARLSON, R. DOW, AND S. E. FITZWATER. 1993. Re-evaluation of high temperature combustion and chemical oxidation measurements of dissolved organic carbon in seawater. Limnol. Oceanogr. **38:** 1774–1782.

SQUIRE, S., G. SCELFO, M. J. REVENAUGH, AND A. R. FLEGAL. 2002. Decadal trends of silver and lead contamination in San Francisco Bay surface waters. Environ. Sci. Technol. **36:** 2379–2386.

STEDING, D. J., C. E. DUNLAP, AND A. R. FLEGAL. 2000. New isotopic evidence for chronic lead contamination in the San Francisco Bay estuary system: Implications for the persistence of past industrial lead emissions in the biosphere. Proc. Natl. Acad. Sci. USA **97:** 11181–11186.

SUNDA, W. G., J. R. DONAT, S. A. HUNTSMAN, AND G. CARRASCO. 2005. Control of zinc uptake by estuarine plankton by free zinc ion concentration (abstract). The American Society of Limnology and Oceanography Aquatic Sciences Meeting. Salt Lake City, 20–25 February.

———, AND S. A. HUNTSMAN. 1987. Microbial oxidation of manganese in a North Carolina estuary. Limnol. Oceanogr. **32:** 552–564.

———, AND ———. 1988. Effect of sunlight on redox cycles of manganese in the southwestern Sargasso Sea. Deep-Sea Res. Part 1 Oceanogr. Res. Pap. **35:** 1297–1317.

———, AND ———. 1998. Processes regulating cellular metal accumulation and physiological effects: Phytoplankton as model systems. Sci. Total Environ. **219:** 165–181.

TABACHNICK, B. G., AND L. S. FIDELL. 2001. Using multivariate statistics, 4th ed. Allyn and Bacon.

THAMDRUP, B., H. FOSSING, AND B. B. JØRGENSEN. 1994. Manganese, iron, and sulfur cycling in a coastal marine sediment, Aarhus Bay, Denmark. Geochim. Cosmochim. Acta **58:** 5115–5129.

THOMPSON, J. K., AND F. H. NICHOLS. 1988. Food availability controls seasonal cycle of growth in *Macoma Balthica* (L.) in San Francisco Bay, California. J. Exp. Mar. Biol. Ecol. **116:** 43–62.

TOVAR-SÁNCHEZ, A., S. A. SAÑUDO-WILHELMY, AND A. R. FLEGAL. 2004. Temporal and spatial variations in the biogeochemical cycling of cobalt in two urban estuaries: Hudson River estuary and San Francisco Bay. Estuar. Coast. Shelf Sci. **60:** 717–728.

TWINING, B. S., S. B. BAINES, AND N. S. FISHER. 2004. Element stoichiometries of individual plankton cells collected during the Southern Ocean iron experiment (SOFeX). Limnol. Oceanogr. **49:** 2115–2128.

WANG, W. X., R. C. H. DEI, AND H. S. HONG. 2005. Seasonal study on the Cd, Se, and Zn uptake by natural coastal phytoplankton assemblages. Environ. Toxicol. Chem. **24:** 161–169.

WARNKEN, K. W., D. TANG, G. A. GILL, AND P. H. SANTSCHI. 2000. Performance optimization of a commercially available iminodiacetate resin for the determination of Mn, Ni, Cu, Cd and Pb by on-line preconcentration inductively coupled plasma–mass spectrometry. Anal. Chim. Acta **423:** 265–276.

ZWOLSMAN, J. J. G., AND G. T. M. VAN ECK. 1999. Geochemistry of major elements and trace metals in suspended matter of the Scheldt estuary, southwest Netherlands. Mar. Chem. **66:** 91–111.

Received: 4 January 2006
Accepted: 19 September 2006
Amended: 29 November 2006

CHAPTER 2: DEPLETION OF DISSOLVED METHYL MERCURY BY A PHYTOPLANKTON BLOOM IN SAN FRANCISCO BAY

Abstract

To study the effects of phytoplankton on mercury cycling, we followed the spring 2003 diatom bloom in San Francisco Bay as it grew and decayed. The growth and decay phases were characterized by principal component analyses of the water chemistry data. During growth of the bloom, dissolved (< 0.45 μm) methyl mercury (MeHg) concentrations significantly ($p = 0.03$) decreased in the water column. Then, those concentrations significantly ($p = 0.04$) increased during decay, likely due to mineralization of phytoplankton detritus and/or production in sediments. We used the dissolved MeHg depletion to calculate that the algal MeHg concentration was 3-10 pmol g^{-1} (dry weight), with the lowest values at the bloom's peak. In contrast to dissolved MeHg, dissolved total Hg (Hg_T) concentrations were not measurably altered by bloom growth or decay. That difference corroborated previous culture studies in which phytoplankton accumulated more MeHg than inorganic Hg because MeHg uptake was active. As the bloom decayed, Hg_T K_d values significantly ($p = 0.012$) increased, presumably because (1) more Hg_T associated with particles when dissolved organic carbon concentrations were high and (2) particles (i.e., phytoplankton) with low Hg_T concentrations were lost from the water column. Based on the relationship between Hg_T particulate concentrations and percent phytoplankton, the algal Hg_T concentration was 0.5 nmol g^{-1} (dry weight). An

increase in phytoplankton biomass in the estuary could affect mercury bioavailability by transferring MeHg from water to phytoplankton, increasing MeHg concentrations in water and particles as algae decay, and entraining Hg_T in the estuary through biogenic scavenging.

Introduction

Studies in laboratories (Mason et al. 1996; Moye et al. 2002), mesocosms (Pickhardt et al. 2002), and lakes (Chen and Folt 2005; Watras and Bloom 1992) indicate that phytoplankton play a critical role in mercury uptake and bioavailability. For example, culture studies show that phytoplankton actively accumulate methyl mercury (MeHg) and concentrate it by a factor of 10^4 to 10^5 (Moye et al. 2002; Pickhardt and Fisher 2007). Because phytoplankton store MeHg in the cytoplasm, where it is readily assimilated by zooplankton, phytoplankton are responsible for the preferential accumulation of MeHg over inorganic forms of mercury in food chains (Mason et al. 1995; Mason et al. 1996).

Ultimately, the concentration of MeHg in fish may depend on the abundance of phytoplankton, based on studies with mesocosms and lakes that show an inverse correlation between algal abundance and MeHg concentrations in zooplankton and fish (Chen and Folt 2005; Pickhardt et al. 2002) . We sought to evaluate the role of phytoplankton in the San Francisco Bay estuary, where mercury concentrations are generally lower than in culture studies, and myriad other processes affect mercury cycling. To capture a change in phytoplankton biomass, we sampled during a predictably occurring spring diatom bloom in the southern reach of San Francisco Bay, or South Bay (Figure 2.1).

Sampling during a spring bloom is a strategy that has been previously used in South Bay to study the uptake of other metals (e.g., Cd, Cu, Mn, Ni, Pb, Zn) by

phytoplankton (Luengen et al. 2007; Luoma et al. 1998). The conditions that setup the bloom— calm, stratified water and neap tides (Cloern 1996)— also minimize sediment resuspension and horizontal movement of water. Thus, changes in metal concentrations during a bloom may be attributed to biological activity. Luoma et al. (1998) used the 1994 spring bloom to show that Cd, Ni, and Zn were bioavailable because they were depleted from the water during the bloom, but that dissolved Cu was not depleted and not bioavailable. Additional research on the South Bay bloom in spring 2003 (Luengen et al. 2007) found that some metals (e.g., Mn, Co, Zn, and Pb) increased as the bloom degraded, demonstrating that decay of the bloom also impacted metal cycling. However, neither total Hg (Hg_T), which includes both inorganic and organic forms of mercury, nor MeHg has been previously measured during a South Bay bloom, despite concerns with mercury pollution in the estuary (Thompson et al. 2000).

Concentrations of Hg_T as high as 440 pmol L^{-1} (Conaway et al. 2003) in unfiltered surface waters are primarily the result of both historic gold and mercury mining in the estuary's watersheds (Domagalski 2001; Thomas et al. 2002). Mercury that enters the northern reach of the estuary via the Sacramento and San Joaquin Rivers was transported to the Sierra Nevada during historic gold mining operations (Domagalski 2001; Ganguli et al. 2000; Hornberger et al. 1999). That mercury was originally mined in the Coast Range, and the now abandoned Coast Range mines drain into South Bay through the Guadalupe River and other small tributaries (Alpers et al. 2005; Cargill et al. 1980; Thomas et al. 2002). The combined mercury inputs

from the Sierra Nevada and the Coast Range contribute up to several hundred kilograms of mercury to the estuary every year, far more than contemporary sources (e.g. atmospheric deposition, wastewater treatment plants, and surface water runoff) (Conaway et al. 2003; Domagalski 2001; Thomas et al. 2002). Although the cycling of this mercury in the estuary has been previously studied (Choe and Gill 2003; Choe et al. 2003; Conaway et al. 2003), the role of phytoplankton in mercury cycling needs further investigation (Choe et al. 2003).

Data from the northern reach of San Francisco Bay (Choe and Gill 2003; Choe et al. 2003) along with field data from other studies indicate that phytoplankton can affect mercury cycling. For example, Choe et al. (2003) found a relationship between chlorophyll *a* (Chl *a*) and particulate Hg_T in some seasons in North Bay. Those variables were likewise correlated in a study of the Kara Sea, Siberia (Coquery et al. 1995), and the authors attributed that relationship to uptake of Hg_T by phytoplankton. Field studies have also found evidence of uptake of MeHg by phytoplankton. For example, in Minnesota lakes MeHg concentrations increased in net plankton ($\geq$ 300 μm) while simultaneously decreasing in water (Monson and Brezonik 1998). Finally, phytoplankton may be involved in Hg^0 formation, based on the correlation between phytoplankton pigments and Hg^0 in the Scheldt estuary, Netherlands (Baeyens et al. 1998). Our research expands on these field studies by following a specific bloom event, where inputs of mercury were likely minimal, across a large range of Chl *a* concentrations and by using principal component

analyses (PCA) and general linear models to ascribe changes in mercury concentrations to specific processes.

By closely following the spring bloom, we sought to test in an estuary some of the hypotheses that were developed in mesocosms and lakes. First, we predicted that the bloom would deplete dissolved (< 0.45 μm) MeHg but not dissolved Hg_T. That finding would corroborate previous culture studies that showed phytoplankton accumulate more MeHg than inorganic Hg, likely because only the former is actively (i.e., energy expended) taken up by phytoplankton (Moye et al. 2002; Pickhardt and Fisher 2007).

Second, we looked for evidence that MeHg concentrations in phytoplankton decreased when Chl *a* concentrations were high, which would be evidence of bloom dilution. According to the bloom dilution hypothesis, which has been tested in mesocosms (Pickhardt et al. 2002) and lakes (Chen and Folt 2005), an increase in algal biomass decreases the amount of MeHg per individual phytoplankter and thus the amount of MeHg accumulated in higher trophic levels. If bloom dilution occurs in South Bay, we would expect that the recently observed increase in algal biomass in San Francisco Bay (Cloern et al. 2006) would decrease MeHg availability to the food chain.

Third, we calculated the concentration of MeHg and Hg_T in South Bay phytoplankton to provide regulators with site-specific bioaccumulation factors that can be used to model mercury transport in the estuary. Finally, we wanted to determine if the decay of the bloom affected MeHg and Hg_T concentrations or

partitioning, as has been observed for other metals during that period (Luengen et al. 2007). Based on these studies, we expected that the growth and decay of the bloom would alter mercury cycling in San Francisco Bay and that processes affecting phytoplankton biomass (e.g., eutrophication) could impact mercury bioavailability in estuaries.

Methods

Sampling— Samples were collected at three sites in the channel of South Bay (Figure 2.1) as part of a previously described study focused on the 2003 phytoplankton bloom (Luengen et al. 2007). Sampling began 19 February 2003 and continued at approximately weekly intervals until 01 May 2003, well after the peak of the bloom. A subsequent cruise on 27 August 2003 provided a non-bloom contrast to the spring data at those sties. All samples were taken aboard the United States Geological Survey (USGS) *R/V Polaris.*

Using trace metal clean techniques previously employed in San Francisco Bay (Flegal et al. 1991), surface water for mercury analyses was collected via two peristaltic pumps equipped with acid-cleaned Teflon tubing. One pump was equipped with an acid-cleaned Osmonics polypropylene filter (Calyx Capsule) to collect dissolved (< 0.45 μm) samples. The second pump was used to collect total (unfiltered) samples. Samples were immediately frozen on dry ice and stored frozen

until analysis. Particulate MeHg and Hg_T concentrations were later calculated as the difference between total (unfiltered) and dissolved concentrations.

In addition to the mercury samples, we measured 15 water chemistry variables: Chl *a*, phaeophytin (Phaeo), Chl *a* /(Chl *a* + Phaeo), suspended particulate matter (SPM), salinity, dissolved oxygen, temperature, water density (σ_t), dissolved organic carbon (DOC), dissolved reactive phosphate, dissolved silicate, dissolved inorganic nitrogen, tidal amplitude, and total (unfiltered) Fe and Mn. The techniques for collecting and analyzing those samples, including the use of a Sea-Bird Electronics underwater unit (SBE-9 plus) to take vertical profiles, are described elsewhere (Caffrey et al. 1998; Luengen et al. 2007)

PCA factors—As described previously (Luengen et al. 2007), principal component analysis (PCA) was used to reduce the 15 water chemistry variables to three composite factors. The purpose of this step was to create new factors that were, by definition, independent (i.e. non-collinear) and could be used in subsequent analyses in place of the original variables, many of which were collinear and would therefore violate the assumptions of multivariate analysis. The contribution of the original water chemistry variables to the derived PCA factors was given by the component loadings in Luengen et al. (2007).

The first derived factor was a bloom factor. Increasing values of the bloom factor described declining temperature and salinity, decreasing concentrations of dissolved inorganic nitrogen and silicate, rising dissolved oxygen values, and growth

of Chl *a*. Thus, the bloom factor characterized both the environmental conditions that set the stage for that phytoplankton bloom and the resultant increase in Chl *a*.

The second composite factor represented the amount of material available for mercury sorption. Increasing values of the sorbent factor were characterized by increasing concentrations of the following: SPM, unfiltered Fe and Mn, and dissolved reactive phosphate, which is particle reactive. Increasing values of the sorbent factor were also characterized by declines in σ_t, which was likely the result of fluvial inputs with high SPM concentrations.

The third factor was a decay factor, with deceasing values of that factor associated with decomposition of the bloom. Decreasing values of the decay factor represented declining values of Phaeo and increasing values of DOC, as organic matter decomposed from the particulate to the dissolved phase.

Analyses of MeHg and Hg_T—Dissolved and total (unfiltered) water samples for MeHg analyses were preserved by addition of 0.02% sulfuric acid (Parker and Bloom 2005). Samples were then analyzed by distillation, aqueous phase ethylation, volatile organic trapping, and quantification by CVAFS (Bloom 1989; Bloom and Von Der Geest 1995; Horvat et al. 1993). The detection limit was 0.041 pmol L^{-1}. Because no certified reference material for MeHg in water existed, we analyzed a diluted digestion of a dogfish reference material (DORM-2) from the National Research Council, Canada. Recovery was 86%. Our matrix spike recoveries averaged 94%.

Dissolved and total (unfiltered) water samples for Hg_T analyses were thawed and oxidized by addition of 0.5% bromine monochloride for at least 2 hours. Samples were then pre-reduced with hydroxylamine hydrochloride, reduced with tin chloride, and then analyzed by cold vapor atomic fluorescence spectrophotometry (CVAFS) and two-stage gold amalgamation trapping (Bloom and Fitzgerald 1988; Gill and Fitzgerald 1987).

At the University of California, Santa Cruz (UCSC), Hg_T samples were analyzed with a Tekran 2600, as described in Conaway et al. (2003). The instrument was calibrated using a five point curve with an $r^2 > 0.99$. We checked accuracy by running ORMS-3, a certified reference material from the National Research Council, Canada that consisted of river water spiked with inorganic Hg. The certified value ($\bar{x} \pm 2\sigma$) was 62.8 ± 5.5 pmol L^{-1}, and our measured value was 59.6 ± 4.5 pmol L^{-1}. We also ran matrix spikes with quantitative (82 - 100%) recoveries. Sample concentrations were above detection limits (3σ of the blanks), which were 0.43 pmol L^{-1} for dissolved samples and 3.7 pmol L^{-1} for total (unfiltered) samples. For dissolved samples, the relative standard deviation (RSD) of laboratory duplicates was 15%, and the RSD of duplicate field samples was 17%. For total (unfiltered) samples, the RSD of laboratory replicates was 4%, and the RSD of duplicate field samples was 6.5%.

Development of multivariate models—The first goal of our statistical analysis was to determine if the composite factors developed by PCA were associated with MeHg

concentrations or partitioning. Because most of our MeHg samples were from site 36, our statistical analysis focused only on that site. We began by examining the dissolved MeHg and MeHg K_d data for normality, and we log transformed the MeHg K_d values to achieve a normal distribution. We then used a general linear model routine (GLM) in Systat (Version 10.2.05) to run multi-linear regression analyses with the dependent variable as either dissolved MeHg concentrations or MeHg K_d values. The composite factors were by definition independent, and we therefore initially included all of them in the analysis. Composite factors with $p > 0.15$ were then successively dropped from the model to develop models that described the dependent variables with the fewest number of variables, an approach that we used previously (Luengen et al. 2007) for other metals.

We also a used model-building approach to look at the effects of the three PCA factors and the categorical variable, site, on dissolved Hg_T concentrations and Hg_T K_d values. Both of those dependent variables were normally distributed. Because this model included a categorical variable (site), we used the GLM routine to run an analysis of covariance (ANCOVA). We first ran a "full" model that included that four way interaction (factor 1*factor 2*factor 3*site) to test the assumption of homogeneity of complex shapes. If the p value was > 0.15, we dropped the interaction term and ran the "reduced" model (Quinn and Keough 2002). As in our approach to the MeHg data, we then dropped factors with $p > 0.15$ to build models that best described dissolved Hg_T concentrations and Hg_T K_d values.

By developing these multivariate models, we were able to account for co-occurring processes, such as decay of phytoplankton and a simultaneous pulse of SPM. Thus, this approach was critical to allowing us to work in an estuary where processes cannot be isolated, as they are in culture studies. To graphically depict these multiple processes, we used partial residual plots, which showed the contribution of a single term by removing it from the model and plotting the residuals against the omitted factor. The contribution of the omitted term was then judged by the extent to which it accounted for variability in residuals.

Results

MeHg concentrations—Concentrations of dissolved MeHg ranged from below the detection limit (0.041 pmol L^{-1}) to 0.13 pmol L^{-1} and averaged 0.060 pmol L^{-1} (Figure 2.2). Those concentrations were consistent with the range of dissolved MeHg concentrations (0.05 - 0.4 pmol L^{-1}) measured in South San Francisco Bay between 1999 and 2001 (Choe and Gill 2003; Conaway et al. 2003). Concentrations of total (unfiltered) MeHg in this study ranged from 0.12 to 1.3 pmol L^{-1} and averaged 0.45 pmol L^{-1} (Figure 2.2). Those values were also consistent with concentrations (0.10 to 1.2 pmol L^{-1}) recently measured in South Bay (Choe and Gill 2003; Conaway et al. 2003).

Most of the MeHg measured in this study was bound to particles, as evidenced by our MeHg distribution coefficients (K_d values) shown in Table 2.1. As indicated

by the high K_d values, MeHg associated with particles comprised 63-96% of the total (unfiltered) MeHg. That result was consistent with those of Choe and Gill (2003), who found that 85% of total (unfiltered) MeHg was associated with particles at their site in the extreme South Bay. Our highest value of total (unfiltered) MeHg, of 1.3 pmol L^{-1} on 19 February at site 32 (Figure 2.2), was associated with a pulse of SPM (Table 2.1), attesting to the importance of MeHg associated with resuspended particles in this system.

Statistical models for MeHg—Dissolved MeHg concentrations were significantly ($p < 0.05$) affected by both the bloom and decay factors (Table 2.2). The contribution of those two factors to dissolved MeHg concentrations was roughly equal, based on the comparable t values, which can be used to assess the relative contribution of the terms in the model. To determine the direction and magnitude of the relationship between the PCA factors and dissolved MeHg concentrations, we used partial residual plots. Those plots (Figure 2.3) showed that increasing values of the bloom factor (growth of the bloom) explained decreases in dissolved MeHg concentrations. Similarly, decreasing values of the decay factor (decay of the bloom) explained increases in dissolved MeHg concentrations (Figure 2.3).

The K_d values for MeHg at site 36 were significantly ($p = 0.021$) affected by the bloom factor (Table 2.3). As the bloom grew (increasing values of the bloom factor), the MeHg K_d values increased (Figure 2.4). That increase was likely due to

phytoplankton uptake of MeHg, which would have increased MeHg concentrations in the particulate phase.

Hg_T concentrations—Concentrations of dissolved Hg_T in this study ranged from 1.5 - 6.6 pmol L^{-1} and averaged 3.9 pmol L^{-1} (Figure 2.2), which was consistent with concentrations (2.8 - 53 pmol L^{-1}) observed in two previous studies in that reach of the estuary (Choe et al. 2003; Conaway et al. 2003). Concentrations of unfiltered Hg_T in this study ranged from 8.1 - 150 pmol L^{-1} and averaged 40 pmol L^{-1} (Figure 2.2), which also agreed with previous measurements (1.8 - 210 pmol L^{-1}). Our highest value, 150 pmol L^{-1} was measured at site 32, near the Dumbarton Bridge. Choe et al. (2003) found that their highest concentration of unfiltered Hg_T was in South Bay; they measured 163 pmol L^{-1} in the extreme South Bay in March 2001. Concentrations at their other two South Bay sites were considerably lower (~20 and ~40 pmol L^{-1}), and consistent with average values reported by Conaway et al. (2003) for the southern and central reaches of the estuary.

Our K_d values for Hg_T ranged from 1 x 10^5 to 7 x 10^5 L kg^{-1} (Table 2.2). Those relatively high values demonstrated that most Hg_T was associated with SPM. Strong particle association was also shown by Conaway et al. (2003), who reported K_d values ranging from 10^4 to 10^7 L kg^{-1} for Hg_T throughout the estuary. Similarly, Choe et al. (2003) found that 88 ± 7% of the unfiltered Hg_T from their sites throughout the estuary was associated with particulates.

Statistical models for Hg_T—In our GLM for dissolved Hg_T, concentrations of Hg_T were significantly ($p < 0.01$) affected only by location (Table 2.2). Concentrations of dissolved Hg_T were highest at site 36, intermediate at site 32, and lowest at site 21 (Figure 2.2). In contrast to dissolved MeHg concentrations, dissolved Hg_T concentrations were not measurably affected by the bloom or decay factors.

In addition to looking at the effects of bloom processes on dissolved Hg_T concentrations, we developed a GLM to determine what processes affected Hg_T partitioning. Table 2.3 shows that the decay factor significantly ($p = 0.012$) affected Hg_T K_d values. As the bloom decayed (decreasing values of the decay factor), Hg_T K_d values increased (Figure 2.5), indicating that more Hg_T became associated with SPM over that period. This result differed from MeHg K_d values, which were not measurably altered by the decay of the bloom, perhaps because Hg(II) reacts with cellular debris much more rapidly than MeHg (Mason et al. 1996).

The categorical variable, site, and the sorbent factor also had significant ($p = 0.048$) and marginally significant ($p = 0.068$) effects, respectively, on Hg_T K_d values (Table 2.3). However, site and the sorbent factor were less important than the decay factor for describing Hg_T K_d values, based on their comparatively lower p values and mean-square values (Table 2.3). The mean-square values provide an estimate of the variance associated with each of the terms and can therefore be used to assess the relative contribution of each of the terms to the model fit. Accordingly, we concluded that the most important term explaining Hg_T partitioning in the model was the decay factor.

Discussion

Bloom affects dissolved MeHg concentrations—Dissolved MeHg was depleted during the bloom (Figure 2.3), consistent with uptake of MeHg by phytoplankton. Depletion of dissolved Mn, Ni, and Pb (Luengen et al. 2007) has been previously observed during the 2003 bloom and depletion of dissolved Cd, Ni, and Zn occurred during the 1994 spring bloom (Luoma et al. 1998). Depletion of some metals during phytoplankton blooms has also been observed in other bays, including dissolved Cd and Zn in the Scheldt estuary, Netherlands (Zwolsman and Van Eck 1999) and truly dissolved (< 1 kD) Al, Co, Cu, Mn, and Ni in Ekhagen Bay, Baltic Sea (Ingri et al. 2004).

MeHg in phytoplankton—We calculated the concentration of MeHg in phytoplankton based on our observed depletion of dissolved MeHg. Because of the limited data from the other sites, we focused our calculations on site 36. At that site, Chl *a* concentrations were already at 62 μg L^{-1} (Table 2.1) by the time we made our first measurement of dissolved MeHg on 24 February. We accordingly looked for values in the literature to establish a winter pre-bloom value for our site. In February 2000, when Chl *a* concentrations were 4.9 μg L^{-1}, Conaway et al. (2003) measured a dissolved MeHg concentration of 0.085 pmol L^{-1} at their corresponding site (37.470° N, 122.063° W) which was located less than 300 m from our site 36 (37.472°N, 122.065°W). That value was in excellent agreement with our non-bloom (Chl *a* 6.3

$\mu g\ L^{-1}$) summer concentration of dissolved MeHg of 0.083 pmol L^{-1} at site 36. A slightly higher concentration of 0.11 pmol L^{-1} of dissolved MeHg was measured by Choe and Gill (2003) under low Chl *a* (4.09 $\mu g\ L^{-1}$) conditions in March 2001 at their site (37.467°N, 122.062°W) in South Bay. Therefore, we used the average of those three values, which was 0.093 pmol L^{-1}, as our best estimate of the pre-bloom concentration of dissolved MeHg at that site.

We then calculated that the algal bloom assimilated 0.067 pmol L^{-1} of dissolved MeHg, which was the difference between the pre-bloom concentration (0.093 pmol L^{-1}) and the bloom concentration (0.026 pmol L^{-1}). The bloom concentration was the value measured on both 24 February and 04 March (Figure 2.2) when Chl *a* concentrations were 62 $\mu g\ L^{-1}$ and 169 $\mu g\ L^{-1}$, respectively (Table 2.1). Under those rapid growth conditions, dissolved MeHg concentrations were depleted below our analytical detection limit of 0.041 pmol L^{-1}. Accordingly, a value of half the detection limit (0.020 pmol L^{-1}) would also have been a reasonable value for our calculation, but would have resulted in an assimilation of the same magnitude.

Although our calculated assimilation of 0.067 pmol L^{-1} of MeHg was small, it was above the background noise, based our detection limit and our precision from duplicate field samples. If we used the detection limit of 0.041 pmol L^{-1} as an indicator of the amount of change that we could measure, 0.067 pmol L^{-1} was above that threshold. Our precision from duplicate field samples was even lower; our dissolved field duplicates at site 32 on 04 March differed by only 0.006 pmol L^{-1} (Figure 2.2).

Accordingly, we calculated the MeHg concentration in phytoplankton by dividing the MeHg assimilation (0.067 pmol L^{-1}) by the corresponding increase in bloom-derived material from pre-bloom conditions to 24 February. Then, we converted the increase in bloom derived material (58 μg L^{-1} of Chl *a* and Phaeo), to grams dry weight of phytoplankton, following ratios previously used for South Bay (Cloern et al. 1995; Luengen et al. 2007; Luoma et al. 1998):

$$\left(\frac{58\ \mu g\ Chl\ a}{L}\right)\left(\frac{35\ \mu g\ C}{\mu g\ Chl\ a}\right)\Big/\frac{0.3\ \mu g\ C}{\mu g\ phytoplankton}=\frac{6.8\ mg\ phytoplankton}{L}$$

Division of 0.067 pmol L^{-1} of MeHg by 6.8 mg phytoplankton/L yielded a MeHg concentration in phytoplankton on 24 February of 10 pmol g^{-1} (dry weight). That result was consistent with previously reported concentrations in the estuary and elsewhere (Table 2.4).

We repeated the process to calculate the concentration of MeHg in phytoplankton from pre-bloom conditions to 04 March. We converted the algal increase in Chl *a* plus Phaeo concentrations (177 μg L^{-1}) to 21 mg (dry weight) phytoplankton. Division of 0.067 pmol L^{-1} of MeHg by 21 mg of phytoplankton yielded a concentration of 3.2 pmol per g^{-1} phytoplankton. That 04 March algal value was lower than the 24 February value because Chl *a* concentrations nearly tripled between 24 February and 04 March while dissolved MeHg concentrations remained the same (Table 2.1, Figure 2.2). Thus, our calculated ~30% decrease in phytoplankton MeHg concentrations was a result of an initial depletion of MeHg

from the water column at the beginning of February, which subsequently limited the amount of MeHg available as the bloom continued growing.

Even if dissolved MeHg concentrations had been depleted to 0 pmol L^{-1} on 04 March, the depletion of 0.093 pmol L^{-1} would have resulted in a MeHg concentration of 4.4 pmol g^{-1} (dry weight) of phytoplankton, a value still below that of 24 February. These results are consistent with bloom dilution. Bloom dilution has been previously observed in experiments where researchers varied nutrient concentrations in different mesocosms to create a range of bloom intensities (Pickhardt et al. 2002). The researchers then added different stable isotopes ($CH_3{}^{200}Hg^+$ and $^{201}Hg^{2+}$) of MeHg and inorganic Hg to the water and found that when Chl *a* concentrations were high, concentrations of MeHg in phytoplankton and zooplankton decreased.

One limitation to this study is that it was not possible to MeHg or Hg_T concentrations directly in phytoplankton. Although our calculations indicated that algal MeHg concentrations decreased during the bloom, if phytoplankton rapidly assimilated MeHg from another source (e.g., production in sediments or desorption from the particulate phase), the algal MeHg concentration could have remained constant during the bloom. However, we think that desorption from the particulate phase was unlikely, based on mesocosm experiments on tidal resuspension that showed that dissolved MeHg and Hg_T concentrations did not increase as a result of sediment resuspension (Kim et al. 2004a). Furthermore, stratification of the water column would have limited the flux of dissolved MeHg to the surface water that we sampled. During the unusually warm, calm conditions of the bloom, the South Bay

would have resembled the mesocosm conditions in previous bloom dilution experiments (Pickhardt et al. 2002) more closely than it would have at any other time of year. Accordingly, our results are consistent with bloom dilution, and demonstrate for the first time that bloom dilution could be an important process in an estuary. However, bloom dilution was a transient event, and as we will discuss in the next section, decay may have a larger impact on mercury cycling within the estuary because of the potential for MeHg production during bloom decay.

Decay increases dissolved MeHg concentrations—During decay of the bloom, which was indicated by decreasing values of the decay factor, dissolved MeHg increased (Figure 2.3). We attributed that increase to a combination of remineralization of phytoplankton and production of MeHg in anoxic sediments. Previous research has demonstrated that MeHg is produced in San Francisco Bay sediments (Marvin-Dipasquale and Agee 2003; Olson and Cooper 1974), presumably due to methylation of inorganic Hg by bacteria that reduce sulfate and/or Fe (Benoit et al. 2003; Gilmour et al. 1998; Kerin et al. 2006). As the bloom decayed, conditions would have been favorable for mercury methylation because the decomposing algae likely depleted dissolved oxygen in sediments, as was seen following the South Bay bloom in 1996 (Grenz et al. 2000). Those low oxygen conditions would have facilitated the transfer of MeHg to the water column, based on a study that showed MeHg fluxes to the water column increased when dissolved oxygen concentrations decreased at night in Lavaca Bay, Texas (Gill et al. 1999). A flux of MeHg from sediments to water under

hypoxic conditions was also demonstrated in laboratory incubations of sediments from Baltimore Harbor (Mason et al. 2006). In that study, MeHg and sulfide co-occurred in the overlying water, indicating that sulfate reduction was producing MeHg. Our results support the conclusions of Mason et al. (2006) that production of MeHg at the sediment-water interface could be an important, yet overlooked, source of MeHg to the water column.

Our proposed production of MeHg in sediments following a bloom was also consistent with past studies showing that concentrations of other dissolved metals could be measurably increased by release from sediments following a bloom. For example, dissolved Mn increased following the spring 1996 bloom in South Bay (Roitz et al. 2002), and dissolved Co, Mn, Zn, and Pb increased after the spring 2003 bloom (Luengen et al. 2007). In both cases, the increase was attributed to reductive dissolution of Fe and Mn hydr(oxides) in suboxic sediments. The release of Mn from surface sediments in hypoxic conditions has been demonstrated in laboratory experiments with sediment cores (Riedel et al. 1999). Furthermore, in South Bay, diagenetic remobilization from surface sediments is a known source of other trace metals (e.g., Cd, Zn, Co, Fe, Pb, and Zn) to the water column (Flegal et al. 1991; Rivera-Duarte and Flegal 1997). The remobilization of other metals during the decay of the spring 2003 bloom indicates that there were low oxygen conditions in surface sediments, which could have lead to the production and release of MeHg.

Factors affecting dissolved Hg_T concentrations—Concentrations of dissolved Hg_T increased from our most oceanic site (21) to our site in the extreme South Bay (36), as shown in Figure 2.2. We attributed that distribution to diagenetic remobilization of mercury from historically contaminated sediments within the estuary and ongoing mercury inputs to the extreme South Bay from abandoned mercury mines in the watershed (Conaway et al. 2003; Thomas et al. 2002). The extreme South Bay also has proportionately long residence times and seasonally high concentrations of many metals due to its limited hydraulic flushing (Flegal et al. 1991). These results further indicate that the concentrations of dissolved Hg_T in the estuary are primarily controlled by physical processes, such as inputs and mixing.

Unlike dissolved MeHg, dissolved Hg_T was not significantly ($p = 0.16$, Table 2.2) depleted by the phytoplankton bloom, consistent with active uptake and internalization of MeHg versus passive sorption of Hg_T onto cell surfaces. Because most (90%) inorganic Hg sorbs onto cell surfaces (Mason et al. 1995; Pickhardt and Fisher 2007), the phytoplankton bloom may have had a limited capacity to deplete inorganic Hg. In contrast, phytoplankton actively uptake MeHg, although the mechanism is not understood (Moye et al. 2002; Pickhardt and Fisher 2007). That active uptake of MeHg could have explained why it was depleted from the water, similar to dissolved nutrients (Luengen et al. 2007). Furthermore, the phytoplankton presumably provided a new sink for MeHg because a large fraction (~60%) of MeHg is accumulated in the algal cytoplasm (Mason et al. 1995; Pickhardt and Fisher 2007). Because of these differences in uptake, volume concentration factors for MeHg in

phytoplankton can be roughly an order of magnitude higher than those of inorganic Hg (Pickhardt and Fisher 2007). Accordingly, our observed depletion of dissolved MeHg, but not dissolved Hg_T, may due to active uptake of dissolved MeHg into the algal cytoplasm.

The magnitude of any Hg_T depletion should have been large enough for us to detect, based on Hg: C ratios. A bloom of 65 μg L^{-1} Chl *a* (average Chl *a* increase at sites 32 and 36 between 24 February and 04 March) would have produced 0.19 mmol C L^{-1}, given Chl *a*: C ratios used previously (Cloern et al. 1995; Luengen et al. 2007; Luoma et al. 1998):

$$\left(\frac{65\ \mu g\ Chl\ a}{L}\right)\left(\frac{35\ \mu g\ C}{\mu g\ Chl\ a}\right)\left(\frac{1\ mol\ C}{12\ g\ C}\right)=\frac{0.19\ mmol\ C}{L}$$

Multiplying 0.19 mmol C L^{-1} by a Hg: C ratio of 0.037 μmol mol^{-1} (Martin and Knauer 1973) gave a potential depletion of 7 pmol Hg L^{-1}, which was well within the precision of our samples (Figure 2.2). Accordingly, the lack of a measurable depletion was not an analytical artifact.

We had expected that because Hg_T is surface-reactive (see K_d values in Table 2.1), it would be depleted by sorption onto phytoplankton during growth of the bloom, as we previously observed for dissolved Pb during this bloom (Luengen et al. 2007). However, dissolved Hg_T behaved similarly to dissolved Cu, which was not measurably affected by the growth or decay of the bloom (Luengen et al. 2007). While dissolved Cu was presumably bound to strong organic ligands (Buck and Bruland 2005), dissolved Hg_T may have preferentially sorbed to non-bloom particles.

As we will discuss later, non-bloom particles have higher Hg_T concentrations than phytoplankton, and Hg_T partitioning has been shown to be controlled by its association with sediments, not with biotic particles like MeHg (Kim et al. 2004a). This study suggests that growth of a phytoplankton bloom does not measurably alter dissolved Hg_T concentrations, unlike dissolved MeHg concentrations.

Cycling of dissolved Hg_T also differed from that of MeHg because dissolved Hg_T concentrations did not increase as the bloom decomposed (Table 2.2). Previous studied attributed increases in dissolved trace metal concentrations during decay to release of metals associated with Fe and Mn (hydr)oxides, which were presumably reduced during the suboxic conditions created by decomposing organic matter (Flegal et al. 1991; Luengen et al. 2007; Roitz et al. 2002). In those studies, algal remineralization accounted for only a small amount (e.g., < 1% for Mn) of the increase in dissolved trace metals, indicating that release from sediments was the main source of the metals during decay. Thus, the increase in other trace metals, but not Hg_T, suggested that Hg_T was not strongly associated with Fe and Mn (hydr)oxides. Lack of association between Hg_T and Fe and Mn (hyrd)oxides was previously demonstrated in laboratory incubations that quantified flux of metals from Baltimore Harbor sediments to overlying waters (Mason et al. 2006). In the Baltimore Harbor sediment incubations, fluxes of Fe and Mn to the overlying waters were not related to Hg_T fluxes, suggesting that dissolution of Fe and Mn hydr(oxides) did not release Hg_T.

Hg_T partitioning—Hg_T K_d values were only marginally (Table 2.3) impacted by the sorbent factor, which was a factor partially derived from concentrations of SPM and unfiltered Fe and Mn. That result indicated that SPM was not a driving predictor of Hg_T K_d values, unlike previous studies (Choe et al. 2003; Stordal et al. 1996) that found a negative correlation between SPM and Hg_T K_d values (the particle concentration effect). The particle concentration effect occurs when proportional increases in both SPM and colloidal material are associated with additional metals in both phases, but the colloidally bound metals pass through a 0.45 μm filter and are thus counted in the dissolved fraction (Benoit 1995). One of the assumptions of the particle concentration effect is that changes SPM concentrations are proportional to changes in colloidal material (Benoit and Rozan 1999), an assumption that may not have been true during a bloom when growing algae rapidly increase the amount of particulates. In our study, the composition of the SPM changed whereas previous studies on the particle concentration effect focused on a change in SPM concentrations (Benoit 1995; Benoit and Rozan 1999). As a result, our study was not well-suited for observing the particle concentration effect, and different processes likely governed Hg_T partitioning in our study.

Consistent with past studies demonstrating that organic matter controlled Hg_T partitioning (Hammerschmidt and Fitzgerald 2004; 2006; Turner et al. 2004), Hg_T K_d values in our study were explained primarily by the decay factor (Table 2.3), which was a composite factor that characterized DOC and Phaeo concentrations. As the bloom decayed and DOC increased, Hg_T partitioning onto particles increased (Figure

2.5). Similarly, Hg_T K_d values were positively correlated with the amount of organic matter in sediments (Hammerschmidt and Fitzgerald 2004; 2006; Sunderland et al. 2006). Enhanced partitioning in the presence of organic matter could decrease the amount of inorganic Hg available for uptake by methylating bacteria (Hammerschmidt and Fitzgerald 2004; Hammerschmidt and Fitzgerald 2006). However, in this study, that effect could be counteracted if partitioning on particles helped entrain Hg_T within the estuary where it could undergo further chemical transformation and eventual methylation. To explore the potential consequences of the enhanced partitioning, we considered four potential causes of the increase in Hg_T K_d values during decay: (1) an increase in the surface area available for metal sorption as a result of increased particulate surface area during the decay of the bloom, (2) sorption of Hg_T to organically coated clay particles, (3) loss of colloidal organic matter containing Hg_T, and (4) change in composition of the SPM, as summarized in the following paragraphs.

First, Hg_T K_d values could have increased during the decay as a result of increased surface area from the growth of bacteria. As the cells degraded, the release of organic matter presumably stimulated microbial activity, as has been observed following the addition of glucose or arginine during phytoplankton growth and decay experiments with Chesapeake Bay waters (Miller et al. 1997). That additional surface area could have accounted for the increase in Hg_T K_d values observed in this experiment.

Second, K_d values could have increased if DOC generated from decomposing algae sorbed onto clay surfaces, creating an organic coating that favored Hg_T binding. DOC created during decomposition would have tended to sorb onto clays because clays have a net negative surface charge that attracts organic matter (Stumm and Morgan 1996). In studies where fulvic acid was added to inorganic particles, creation of an organic coating enhanced Hg(II) sorption (Gagnon and Fisher 1997; Xu and Allard 1991). Studies that studies removed organic matter, instead of adding it, found that less (up to 2 orders of magnitude) Hg(II) sorbed to sediments and calcite after digestion with H_2O_2 and UV-irradiation, respectively (Bilinski et al. 1991; Turner et al. 2001).

Third, K_d values could have increased during decay if the addition of DOC facilitated removal of colloidal organic matter and associated Hg_T. Because a substantial (38 – 57%) amount of the dissolved Hg_T is San Francisco Bay is associated with colloids (Choe et al. 2003), flocculation of colloidal material could affect Hg_T K_d values. Previous research found that colloidal humic acids and associated trace metals flocculated along a salinity gradient, either because the seawater ions (principally Ca^{2+} and Mn^{2+}) bound to the colloids and caused coagulation (Sholkovitz and Copland 1981) or because addition of seawater ions decreased the number of water molecules available to solvate the organic matter, causing salting out of mercury-organic complexes (Turner et al. 2001).

Although we did not have a large change in salinity during the decay of the bloom (Table 2.1), it was possible that our observed increase in DOC during decay

functioned similarly. For example, Turner et al. (2001) found a positive relationship between the amount of Hg(II) sorbed to estuarine particles and DOC concentrations in laboratory mixing experiments with river water of varying DOC concentrations from three U.K. estuaries. They mixed river water and seawater in various portions, spiked the waters with radioactive ^{203}Hg(II), added sediments, and then followed the concentrations of Hg(II) in the dissolved and particulate phases. In our study, the increase in DOC could have facilitated flocculation of colloidal material and thus contributed to the increase in Hg_T K_d values during decay.

Fourth, Hg_T K_d values could have increased during decay if the phytoplankton that were lost from the water column had lower Hg_T concentrations than the remaining particles. Figure 2.6 supports that hypothesis by indicating that Hg_T particulate concentrations were highest when most of the material in suspension was not bloom derived. There was a significant ($p = 0.011$, $F = 7.5$, linear regression) negative relationship when we excluded the outlier (the datum with > 50% bloom material) and log transformed the percent bloom derived material to normalize the data. Dilution of SPM by phytoplankton has been previously observed for other metals (e.g., Al, Co, Cr) in the Scheldt estuary, Netherlands (Zwolsman and Van Eck 1999).

Although there are not many studies on Hg_T partitioning to different types of particles, two field studies from estuaries in France (Laurier et al. 2003; Schäfer et al. 2006) suggest that phytoplankton could dilute Hg_T K_d values. In the Lot–Garonne Estuary, France, Hg_T particulate concentrations (1.0 – 2.4 nmol g^{-1}) were lower

during an intense algal bloom than concentrations (> 2.5 nmol g^{-1}) during non-bloom conditions (Schäfer et al. 2006). In another study of a French estuary (Laurier et al. 2003), Hg_T in particles leaving the high turbidity zone of the Seine estuary were diluted in summer by phytoplankton with low mercury concentrations (0.2 – 0.8 nmol g^{-1} dry weight in net-collected plankton, Table 2.4). Laurier et al. (2003) suggested that living phytoplankton had fewer functional groups available to bind Hg_T than degraded organic material. In our study, a decrease in phytoplankton biomass and a change to degraded material during the decay of our bloom could have accounted for the increase in Hg_T K_d values.

Hg_T in phytoplankton—Results from our study suggested that Hg_T concentrations in non-bloom particles in the estuary were ~1.8 nmol g^{-1} (dry weight), higher than concentrations in phytoplankton of 0.47 nmol g^{-1} (dry weight). The value for Hg_T in non-bloom particles in this study, from the Y-intercept of the linear regression (Figure 2.6), was 1.8 nmol g^{-1}. That value agreed with previous results (Conaway et al. 2003) that showed the average concentration of Hg_T in suspended particles collected throughout the estuary under generally low Chl *a* conditions (median Chl *a* of 3 µg L^{-1}) was 1.8 ± 0.6 nmol g^{-1}. Phytoplankton would dilute that suspended material, based on our linear regression, which showed that when there was ~100% phytoplankton (i.e., a log-transformed X value of 2.0), the concentration of Hg_T in suspended material would be 0.47 nmol g^{-1} (dry weight).

Our calculated concentration of 0.47 nmol g^{-1} Hg_T in pure phytoplankton agreed with previous values shown in Table 2.4. Kim et al. (2004a) calculated a concentration of Hg_T in phytoplankton of 0.3 to 0.5 nmol g^{-1} (dry weight), using equations derived from culture studies by Mason et al. (1996). Two field studies in California bays also indicated that Hg_T concentrations in phytoplankton were in that range, although both had contamination from suspended sediments. Martin and Knauer (1973) measured concentrations of Hg_T in phytoplankton collected under bloom conditions in Monterey Bay. To minimize contamination by suspended sediments, we selected data from that study with low Al concentrations (as per Bruland et al. 1991). Accordingly, the best estimate of Hg_T concentrations in phytoplankton from that study was 0.98 ± 0.4 nmol g^{-1} (dry weight). Finally, Flegal (1977) calculated that phytoplankton from San Francisco Bay contained 0.5 to 1.5 nmol Hg_T g^{-1} (dry weight) by performing regression analyses and simultaneous equations on seston samples from the estuary. These analyses indicated that Hg_T concentrations in phytoplankton from the estuary were 0.3 to 1.5 nmol g^{-1} (dry weight), which agreed with our calculated value of 0.47 nmol g^{-1}.

Implications of an increase in phytoplankton biomass—Recent research in San Francisco Bay (Cloern et al. 2006) indicates that within the last decade, phytoplankton biomass, as measured by Chl *a*, has increased within all reaches of the estuary (i.e., North, Central and South Bays). That increase has manifested as (1) higher baseline Chl *a* concentrations, (2) greater magnitude of the annual spring

bloom, and (3) addition of a new fall bloom (Cloern and Dufford 2005; Cloern et al. 2006). Although the estuary has relatively high nutrient concentrations, primarily from wastewater treatment plant inputs (Smith and Hollibaugh 2006), the additional phytoplankton biomass is not related to nutrient concentrations, which have remained constant or slightly decreased (Cloern et al. 2006). The exact cause of the phytoplankton increase is uncertain, but may be due to a variety of factors including greater water clarity (Cloern et al. 2006).

That increase in algal abundance is a concern because of the potential for algae to transfer MeHg to the food chain, thus exacerbating the existing mercury impairment in the estuary. Currently, high mercury concentrations (> 1.1 nmol g^{-1} wet weight) in fish are responsible for consumption advisories in the estuary (Thompson et al. 2000). Mercury pollution also threatens wildlife, particularly the reproductive success of the endangered California Clapper Rail, *Rallus longirostris obsoletus* (Schwarzbach et al. 2006). To protect fish and wildlife from mercury exposure, we need to understand the relationship between Chl *a* concentrations and MeHg concentrations in phytoplankton and subsequent trophic levels.

In this study, our calculated algal MeHg concentrations were lowest during the peak of a phytoplankton bloom. That result suggests that bloom dilution can occur in the estuary, as has been previously demonstrated for freshwater mesocosms (Pickhardt et al. 2002; Pickhardt et al. 2005). In contrast to the mesocosm experiments, bloom dilution in this study was the result of depletion of dissolved MeHg from the water column, indicating that the concentration of MeHg is an

important variable in this system. Bloom dilution has also been observed in lakes in the northeastern United States, where high zooplankton concentrations were correlated with low Hg_T concentrations in fish (Chen and Folt 2005). However, in San Francisco Bay, benthic organisms consume extra food during blooms (Thompson and Nichols 1988), potentially counteracting any beneficial effects of bloom dilution. The effect on higher trophic levels may also be limited because bloom dilution is transient. Thus, additional studies are needed to determine how MeHg concentrations in higher trophic levels respond to the growth of a phytoplankton bloom.

Mercury bioavailability in the estuary may also be altered by the decay of the bloom, which is a component of high algal biomass that has received relatively little attention. Our maximum concentrations of dissolved and particulate MeHg occurred when the bloom was almost completely decayed, on 23 April (Table 2.1, Figure 2.2). The MeHg associated with that decayed material is bioavailable to at least some organisms, based on experiments showing that amphipods can assimilate MeHg from phytoplankton cells that are highly decayed (Lawson and Mason 1998). Moreover, if decaying algal material causes production of MeHg in sediments (Figure 2.3), an increase in algal abundance could boost MeHg production in the estuary. Finally, we observed an increase in Hg_T partitioning onto particles during the decay of the bloom, which could serve to entrain Hg_T in the estuary, where it may be eventually methylated. In conclusion, although both the growth and decay of the bloom have the potential to alter mercury cycling, the most readily observable and long-lasting effects of an increase in algal abundance may occur when that material decays.

Table 2.1. Water chemistry variables and distribution coefficients (K_d values) for MeHg and Hg_T at three locations in South San Francisco Bay during a spring bloom in 2003.

Date	Site	Particulate MeHg (pmol g^{-1} SPM)	Particulate Hg_T (nmol g^{-1} SPM)	Log Hg_T K_d (L kg^{-1})	Log MeHg K_d (L kg^{-1})	SPM (mg L^{-1})	Chl *a* (µg L^{-1})	Phaeo (µg L^{-1})	% of bloom-dervied material in SPM	DOC (µmol L^{-1} C)	Salinity
19 Feb	21		1.9	5.8		6	5.9	2.1	16		25.8
24 Feb	21		1.0	5.4		24	28	4.1	16	310	24.3
04 Mar	21	2.9	0.45	5.4	4.8	25	14	3.1	8	108	24.9
12 Mar	21		1.1	5.6		5	7.9	0.8	20	179	23.7
27 Mar	21		0.88	5.6		18	17	1.7	12	164	25.9
01 Apr	21		0.85	5.8		14	12	3.6	13	285	27.4
17 Apr	21		1.4	5.7		19	7.2	2.2	6	170	26.8
23 Apr	21	7.2	1.6	5.7	5.5	13	3.5	1.1	4	843	27.1
01 May	21		1.4	5.6		14	7.0	2.8	8	393	26.0
27 Aug	21		0.40	5.0		13	8.0	4.1	11	107	29.8
19 Feb	32		1.5			103	35	7.4	5		19.9
24 Feb	32		1.1	5.3		46	59	8.7	17		21.2
04 Mar	32	7.9	1.0	5.4	5.4	33	84	1.8	30	277	21.6
12 Mar	32		0.8			25	45	3.1	23	238	21.2
27 Mar	32		1.5	5.7		42	28	3.4	9	354	23.0
01 Apr	32		1.2	5.5		40	16	3.1	6	604	23.4
17 Apr	32		1.5	5.6		30	7.8	2.8	4	428	22.7
23 Apr	32		1.2	5.4		10	4.3	0.9	6	609	22.6
01 May	32		2.1			15	7.7	2.6	8	577	23.8
27 Aug	32	7.6	0.83	5.1	5.1	37	10	11	7	217	28.5
19 Feb	36					245	32	19	2		17.2
24 Feb	36		0.93	5.3	5.4	42	62	5.0	19	262	20.7
04 Mar	36	14	1.8	5.4	5.7	42	169	17	52	283	19.2
12 Mar	36		0.38	4.8		32	75	4.9	29	275	19.8
27 Mar	36	7.7	1.4	5.6	5.1	65	48	4.7	9	225	21.1
01 Apr	36	9.4	1.0	5.3	5.1	30	16	2.4	7	383	21.6
17 Apr	36	15	1.7	5.7	5.2	37	6.1	3.4	3	289	19.6
23 Apr	36	21	1.6	5.5	5.2	12	3.8	1.0	5	520	18.8
01 May	36		1.5	5.5		15	3.7	1.8	4	686	21.2
27 Aug	36	5.5	1.2	5.3	4.8	65	6.3	5.2	2	266	27.2

Table 2.2. Best fit models relating the factors that best describe concentrations of dissolved MeHg and Hg_T in our study of the 2003 spring diatom bloom in San Francisco Bay. The bloom and decay factors are composite variables, formed by principal component analysis of the water chemistry data, which describe the conditions surrounding the growth and decomposition of the bloom. The categorical variable, site, is the location where the samples were collected.

Best fit model for dissolved MeHg, adjusted r^2=0.77						
Effect	Coefficient	SE	Std Coef	Tolerance	t	p (2-tail)
Constant	0.0708	0.00708	0	.	10.0	<0.01
Decay factor	-0.0170	0.00570	-0.587	0.97	-2.99	0.040
Bloom factor	-0.0174	0.00549	-0.624	0.97	-3.18	0.034

Best fit model for dissolved Hg_T, r^2=0.51					
Source	Sum-of-Squares	df	Mean-Square	F-ratio	p
Site	20.7	2	10.4	12.2	<0.01
Error	19.6	23	0.852		

Table 2.3. Best fit models relating the factors that best describe MeHg K_d values and Hg_T K_d values in our study of the 2003 spring diatom bloom. The K_d values, or distribution coefficients, are calculated as: (concentration of particulate metal per gram of SPM)/(concentration of dissolved metal).

Best fit model for MeHg K_d, adjusted r^2=0.63						
Effect	Coefficient	Std Error	Std Coef	Tolerance	*t*	*p* (2 Tail)
Constant	5.17	0.0645	0	.	80.2	<0.01
Bloom factor	0.170	0.0509	0.830	1	3.33	0.021

Best fit model for Hg_T K_d, r^2=0.37					
Source	Sum-of-Squares	*df*	Mean-Square	*F*-ratio	*p*
Site	1.09×10^{11}	2	5.46×10^{10}	3.57	0.048
Sorbent factor	5.73×10^{10}	1	5.73×10^{10}	3.75	0.068
Decay factor	1.18×10^{11}	1	1.18×10^{11}	7.73	0.012
Error	2.90×10^{11}	19	1.53×10^{10}		

Table 2.4. Mercury concentrations in phytoplankton (dry weight) from various water bodies. We selected studies that minimized non-phytoplankton particulates. For example, Kuwabara et al. (2005) found no detritus when they examined their samples microscopically. Laurier et al. (2003) used nets to collect a size fraction (150μm – 1 mm fraction) that favored large biological material. Other studies focused on lakes with low SPM (Kainz and Mazumder; Watras and Bloom 1992). Results from Back et al. (2003) are shown as the average of four size fractions of seston (<35, 35–63, 63–112, and >112 μm) sieved from Lake Superior in spring and summer.

System	MeHg (pmol g^{-1})	Hg_T (nmol g^{-1})	Reference
Culture studies of coastal diatom	5 - 30	0.3 - 0.5	Mason et al. (1996); Kim et al. (2004)
Wisconsin lake	200	1.5	Watras and Bloom (1992)
Lake Superior	10 - 80	—	Back et al. (2003)
Vancouver Island, Canada lakes	35 ± 15	—	Kainz and Mazumder (2005)
Vancouver Island, Canada reservoirs	95 ± 100	—	Kainz and Mazumder (2005)
Guadalupe Reservoir	<7.5	0.86	Kuwabara et al. (2005)
Seine estuary, France	23 ± 17	0.2 - 0.8	Laurier et al. (2003)
Monterey Bay diatom bloom	—	0.98 ± 0.4	Martin and Knauer (1973)
San Francisco Bay, CA	—	0.5 - 1.5	Flegal (1977)
South San Francisco Bay, CA	3 -10	0.47	Present study

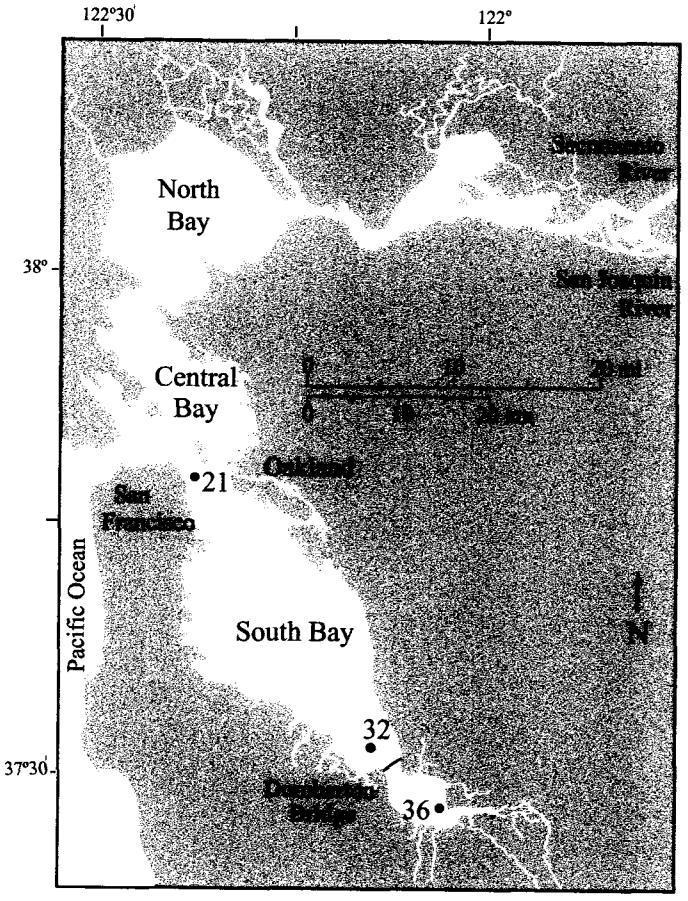

Figure 2.1. Samples were collected in the southern reach of San Francisco Bay (South Bay) at sites 21 (Bay Bridge), 32 (Ravenswood Point), and 36 (Calaveras Point).

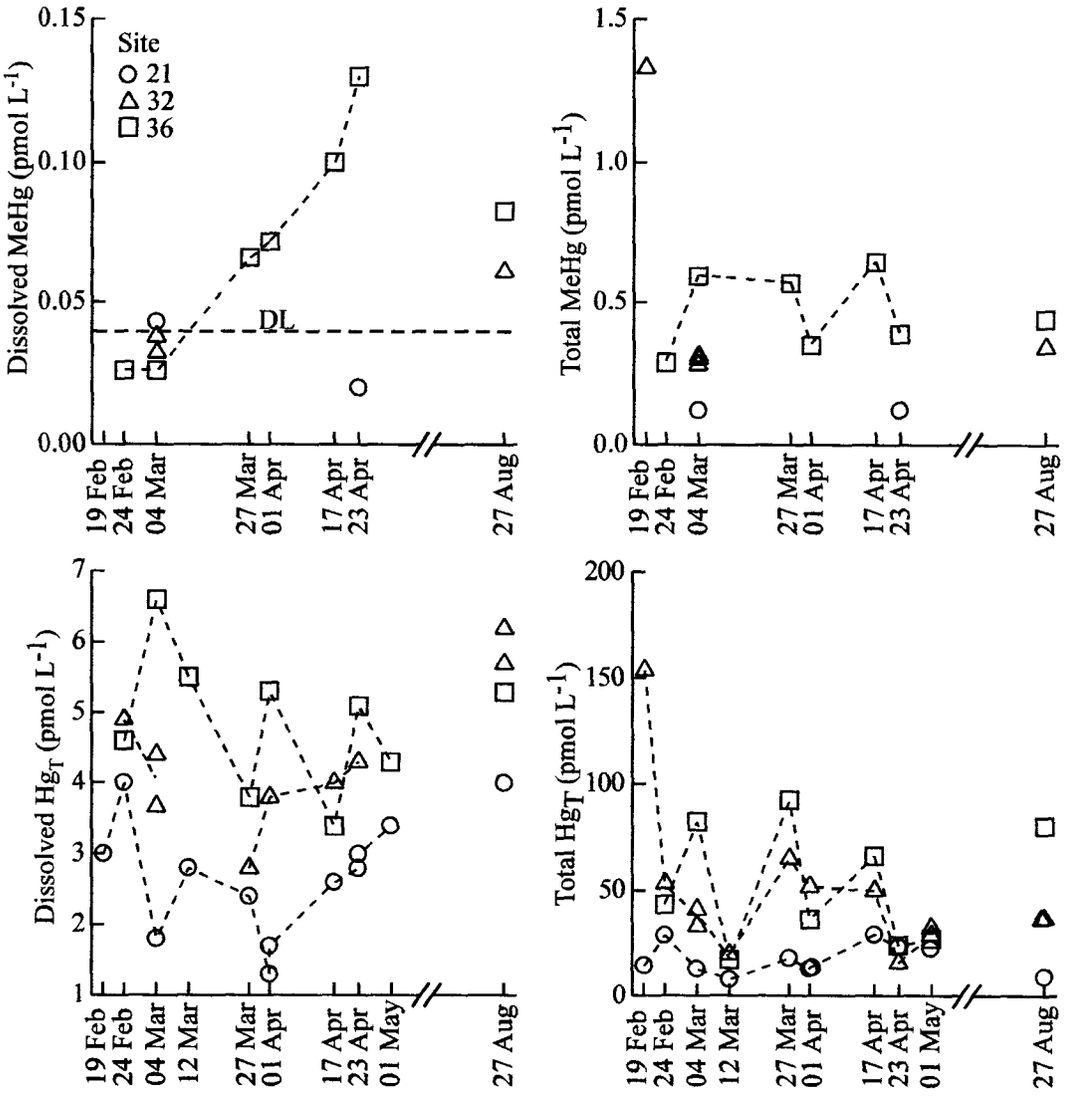

Figure 2.2. Descriptive plots of dissolved (< 0.45 μm) and total (unfiltered) MeHg and Hg_T concentrations. DL = detection limit. Dissolved MeHg duplicate field samples are shown on 04 March at site 32. Total MeHg duplicate field samples and a distillation replicate are shown for that same site and date. Dissolved Hg_T duplicate field samples are shown on 04 March and 27 August for site 32 and on 01 April and 23 April for site 21. Total Hg_T duplicate field samples are shown on 04 March, 01 May, and 27 August for site 32, and on 01 April for site 21.

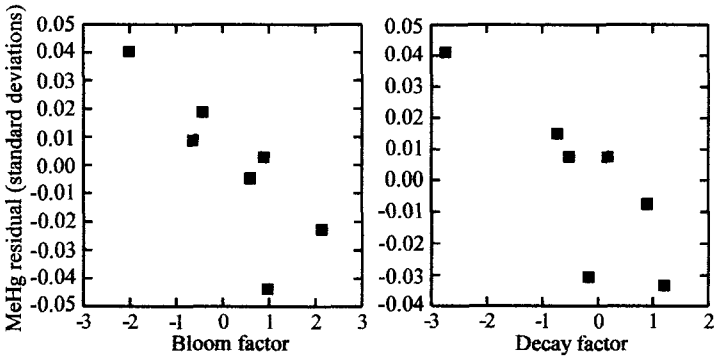

Figure 2.3. Partial (studentized) residual plots showing the effects of the bloom and decay factors on dissolved MeHg concentrations. Values are the residuals (standardized by dividing by the standard deviation), when the model was run without the factor on the x-axis, plotted against the omitted factor.

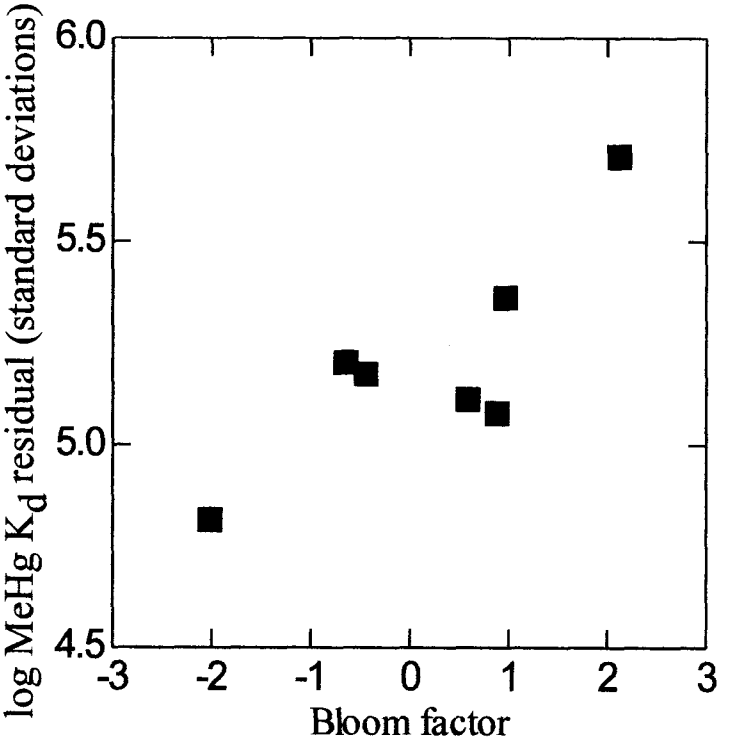

Figure 2.4. Partial (studentized) residual plot showing that as the bloom grew (increasing values of the bloom factor), MeHg K_d values increased, indicating that more MeHg was associated with particles.

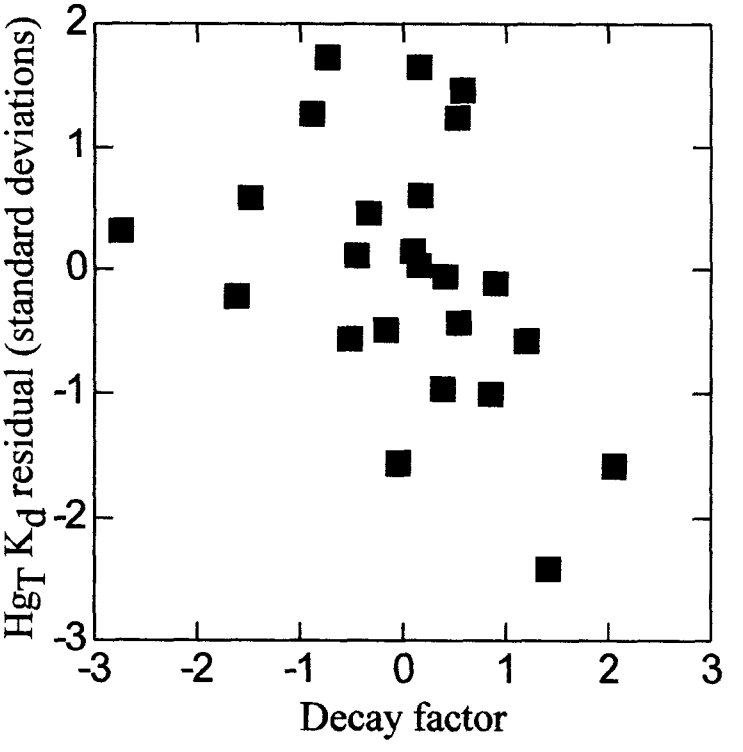

Figure 2.5. Partial (studentized) residual plot showing that during decay, which was indicated by decreasing values of that factor, $Hg_T K_d$ increased.

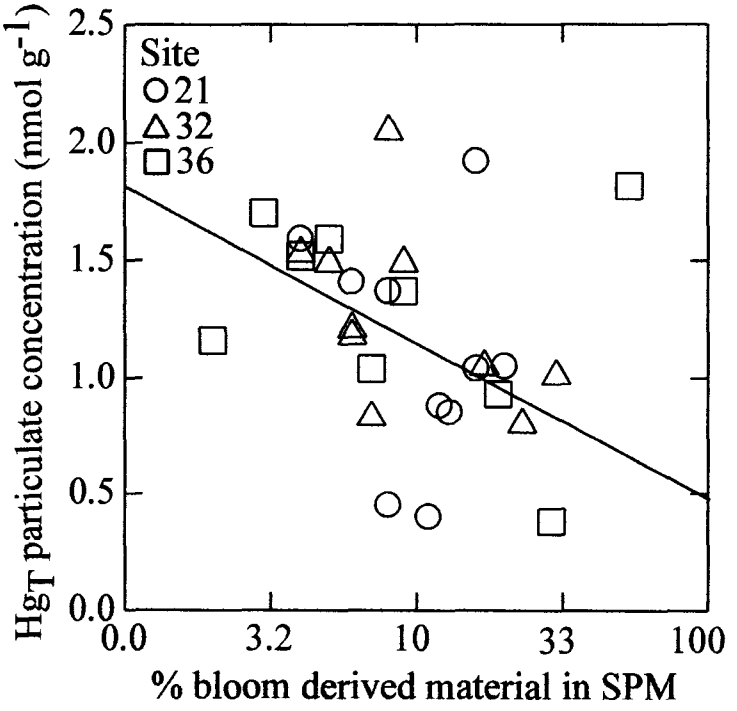

Figure 2.6. Particulate Hg_T concentrations (normalized to SPM) were significantly ($p = 0.011$, $F = 7.5$, linear regression) correlated with amount of bloom derived material in the SPM when the datum with > 50% phytoplankton at site 36 was excluded from the data set. The relationship suggests that phytoplankton have relatively low Hg_T concentrations compared to other types of suspended particles.

CHAPTER 3: FINE SCALE CHANGES IN PHYTOPLANKTON COMMUNITY COMPOSITION AND WATER CHEMISTRY DURING A SPRING BLOOM IN SAN FRANCISCO BAY

Abstract

Phytoplankton community composition in South San Francisco Bay changed significantly over small spatial and temporal scales during the spring 2003 phytoplankton bloom. Phytoplankton communities, which included all species present on a given day and site combination, were assessed along with water quality over ten cruises and three sites. Analysis of algal abundance data by multi-dimensional scaling demonstrated that small species contributed to broad-based differences in communities. Although the large, centric diatom *Thalassiosira punctigera* dominated the bloom by biomass, small phytoplankton (e.g., the euglenophyte, *Eutreptia lanowii,* and cyanobacteria, *Cyanobium sp.*) bloomed along with the diatoms, indicating the bloom was a diverse assemblage. As the bloom decayed, algal community composition changed weekly. Those changes were attributed to a combination of community succession, physical exchange (e.g., movement of the benthic species *Nizschia closterium* into the water column), and alterations in water chemistry. Water chemistry variables that best matched patterns in algal community composition were water temperature (primarily) and dissolved ammonium concentrations (secondarily), based on BIO-ENV analysis. Dissolved ammonium concentrations increased as the diatoms decayed and corresponded with growth of *Synechocystis sp.*, indicating those cyanobacteria disproportionately

responded to that nutrient. BIO-ENV analysis also showed that algal community composition was not linked to trace metal concentrations, despite the known toxicity of some metals (e.g., Cu) to phytoplankton. The absence of a relationship between metals and algal communities was consistent with previous studies demonstrating that organic complexation limits the bioavailability of toxic metals to phytoplankton.

Introduction

In the southern reach of San Francisco Bay (South Bay), phytoplankton bloom predictably every spring when the water column stratifies (Cloern 1996). Past studies have investigated the factors (e.g., nutrient enrichment and turbidity) that control the magnitude of the bloom and the amount of primary production within the estuary (Cloern 1996; Jassby et al. 2002; May et al. 2003). In this study, we analyzed abundance data for 83 species of phytoplankton collected during the spring 2003 bloom. We looked for changes in algal community composition over weekly time scales as the bloom grew and then decayed. Then, we sought to relate those changes to measurements of water quality, including dissolved (< 0.45 μm) metal concentrations, to evaluate the impact of anthropogenic modifications of the estuary.

Previous studies on algal biomass in the estuary have shown that the amount of algal biomass is shaped by environmental perturbations as well as physical and biological processes. Environmental disturbances that have altered primary productivity include introduction of the clam *Potamocorbula amurensis* in the northern reach of the estuary (Jassby et al. 2002; Kimmerer 2005) as well as climate variation and water diversion (Lehman 2000). The most extensive effort to evaluate environmental impacts on phytoplankton biomass in San Francisco Bay has focused on the effects of nutrient enrichment (Cloern 2001; Cloern et al. 2006; Hager and Schemel 1996). That research has demonstrated that the response of phytoplankton to nutrient enrichment in the estuary is modulated by biological and physical factors,

such as turbidity (Cloern 2001; Cloern et al. 2006). For example, since the late 1990s, phytoplankton biomass has increased throughout the estuary in spite of reduced nutrient loadings, presumably due to decreased turbidity and predation (Cloern et al. 2006). Such changes in the amount algal biomass are important because phytoplankton are a critical food source to the planktonic food web in the estuary due to their high bioavailability compared to detrital carbon (Sobczak et al. 2002).

To complement these past studies on biomass, we used multidimensional scaling (MDS) to analyze the composition of algal communities, where a community includes all of the species present in any sample (Clarke 1993). MDS is a community-level approach that is designed to look for spatial and temporal patterns in biological surveys with large numbers of organisms (Field et al. 1982). Patterns in the biological community data can then be matched with environmental data, allowing assessment of the effect of anthropogenic disturbances (Clarke and Ainsworth 1993).

We focused our MDS analysis on algal abundance data because changes in community composition can occur without a measurable change in algal biomass. For example, we hypothesized that small cyanobacteria were most likely to be affected by elevated concentrations of some trace metals (e.g., Cu); an analysis based on biovolume would be weighted towards large diatoms and would likely miss changes in cyanobacterial populations. Similarly, high silicate concentrations could alter algal communities by favoring diatoms over flagellates (Egge and Aksnes 1992),

and high ammonium concentrations could favor cyanobacteria (Paerl 1999). We compared the species that discriminated between algal communities in our MDS analysis with those that dominated by the bloom by biovolume. In that comparison, we explored the role that large species play in driving biogeochemical changes versus the role that all species play in contributing to community diversity and community succession. The goal was to investigate the links and feedbacks between algal community composition, water quality data, and anthropogenic modifications of the estuary.

South Bay (Figure 3.1) is heavily modified by anthropogenic activities, including water diversions (Nichols et al. 1986), discharges of nutrients from wastewater treatment plants (Hager and Schemel 1996; Smith and Hollibaugh 2006), and historic and current inputs of trace metals (Flegal et al. 1991). Metals such as Co, Zn, Cu, Ni, Pb, and Hg have relatively high concentrations in South Bay sediments as a result of historic contamination and can be released to the water column by benthic remobilization (Conaway et al. 2003; Rivera-Duarte and Flegal 1997; Tovar-Sánchez et al. 2004) and desorption from resuspended sediments (Gee and Bruland 2002). Some of these metals (e.g., Co, Zn, Cu, and Ni) have additional on-going industrial inputs from wastewater treatment plant discharges (Bedsworth and Sedlak 1999; Flegal et al. 1996; Tovar-Sánchez et al. 2004). Aqueous concentrations of these metals are then affected by biogeochemical scavenging and hydraulic flushing; concentrations are generally highest at the most southerly sites where digenetic

remobilization may be highest and hydraulic residence time is longest (Flegal et al. 1991).

Anthropogenically enriched metal concentrations in South Bay are of concern because of their potential toxicity to phytoplankton, especially cyanobacteria (Palenik and Flegal 1999). In laboratory experiments, cyanobacteria were the most sensitive to Cd and Cu toxicity, followed by dinoflagellates and then diatoms (Brand et al. 1986). High concentrations of Cd and Cu inhibit cellular growth by interfering with uptake of dissolved Mn, which is an essential nutrient (Sunda and Huntsman 1996; Sunda and Huntsman 1998a). Such competition between metals for cellular uptake is a relatively common mechanism of toxicity (Sunda and Huntsman 1998b; Sunda and Huntsman 1998c). Accordingly, it is appropriate to evaluate algal toxicity in the estuary as a combination of multiple metals.

The toxicity of those metals could be limited if they are strongly complexed to organic ligands in the estuary. For example, > 99% of dissolved Cu in the estuary is strongly bound to organic ligands and thus not readily bioavailable for algal uptake or algal inhibition (Beck et al. 2002; Buck and Bruland 2005; Hurst and Bruland 2005). Instead, the pool of Cu that is in equilibrium with cellular uptake receptors is a much smaller pool that consists of Cu bound to inorganic complexes and Cu^{2+}, as described in the free ion model (Sunda and Huntsman 1998c). Although there are some measurements of Ni and Pb complexation in South Bay (Kozelka et al. 1997; Sedlak et al. 1997), the complexation of many of other metals has not been characterized in the estuary, making it impossible to predict the toxicity of those metals to algal

communities. A primary goal of this project was, therefore, to indirectly assess the role of metals (Co, Cu, Hg, Mn, Ni, Pb, and Zn) on phytoplankton community structure to determine if these metals exhibit inhibitory effects on different types of phytoplankton (e.g., cyanobacteria vs. diatoms).

Methods

Collection and measurement—Surface (~ 1m) water samples from three sites were collected for phytoplankton species composition, trace metal concentrations, and water chemistry during our studies of the 2003 spring bloom (Luengen et al. submitted; Luengen et al. 2007). The three sampling sites were located in the channel of South Bay (Figure 3.1). Sampling began on 19 February 2003, when we collected water from sites 21 and 32 only. Thereafter, sampling continued (ca. weekly) at all three sites until 01 May 2003. Another sampling of the three sites was conducted on 27 August 2003 to provide a non-bloom contrast to the spring data. All samples were collected aboard the *R/V Polaris* in conjunction with a United States Geological Survey (USGS) research program that has monitored phytoplankton dynamics in the estuary since 1968 (Cloern 1996).

Phytoplankton samples were analyzed as described by Cloern and Dufford (2005). Briefly, samples were preserved with acid Lugol's solution and then counted with a phase-contrast inverted microscope. Relatively large cells (> 30 μm) were counted at 125x magnification whereas smaller cells (< 30 μm) were counted at

1250x magnification. Identification of diatoms and dinoflagellates occurred after removal of cellular contents by digestion with 30% hydrogen peroxide. Mean cellular volumes for each algal species were calculated by applying biovolume factors based on geometric formulas (Wetzel and Likens 1991) using length (size) estimates obtained from 50 – 100 cells.

We previously reported dissolved (< 0.45 μm) and total (unfiltered) trace metal concentrations during this bloom (Luengen et al. submitted; Luengen et al. 2007). Samples for both dissolved and total Mn, Co, Zn, Cu, Ni, Pb, and Fe (total only) were acidified (pH < 1) in the laboratory prior to analyses. Then, dissolved Co, Zn, Cu, Ni, and Pb were measured by high resolution inductively coupled plasma magnetic sector mass spectrometry (Luengen et al. 2007). Dissolved and total Mn and total Fe were measured by inductively coupled plasma optical emission spectrometry (Luengen et al. 2007). Samples for total Hg (Hg_T), which included both organic and inorganic species, were oxidized with 0.5% bromine monochloride, pre-reduced with hydroxylamine hydrochloride, reduced with tin chloride, and then analyzed by cold vapor atomic fluorescence spectrophotometry (Luengen et al. submitted).

We also quantified 13 environmental variables: Chl *a*, phaeophytin (Phaeo), Chl *a* /(Chl *a* + Phaeo), suspended particulate matter (SPM), salinity, dissolved oxygen, temperature, water density (σ_t), dissolved organic carbon (DOC), dissolved reactive phosphate, dissolved silicate, dissolved inorganic nitrogen, and tidal amplitude. Analyses techniques were described in our earlier work (Luengen et al.

2007). Water quality data were collected by both discrete samples and vertical profiles of the water column taken with a Sea-Bird Electronics underwater unit (Cloern and Dufford 2005; Luengen et al. 2007).

PCA factors—We (Luengen et al. 2007) previously reported the results of principal component analysis (PCA) on the 13 environmental variables as well as total (unfiltered) Mn and Fe concentrations. The goal of PCA analysis was to develop three independent factors which, unlike the original variables, did not covary with each other. PCA produced three independent factors: 1) a bloom factor that described the growth of the bloom, 2) a sorbent factor that characterized the amount of sorbent, including SPM and Mn and Fe hydr(oxides), 3) a decay factor that characterized the decomposition of the bloom material. The contribution of original environmental variables to each of the PCA factors was previously given by the component loadings. We utilized these 3 PCA factors for analysis of environmental variables versus phytoplankton community composition for this study.

Statistical analyses—The goals of our statistical analyses were to 1) determine if phytoplankton communities changed over space and time and, if so, to identify species responsible for those differences and 2) relate patterns in community composition to our environmental variables (i.e., water quality data and trace metal concentrations). These analyses were conducted with the statistical package from

Plymouth Routines in Multivariate Ecological Research (PRIMER 5, Clarke and Warwick 1994).

For our statistical analyses, we used fourth root transformed abundance data. Fourth root transformed abundance data are frequently used in MDS and were previously used in an MDS analysis of diatom communities in Greece (Clarke and Ainsworth 1993). In our study, the use of abundance data was consistent with our interest in the role of small phytoplankton (e.g., cyanobacteria) in algal communities. The fourth root transformation allowed us to minimize the impact of common species because it would be both difficult and undesirable to distinguish communities by using only common species (Clarke and Warwick 1994).

In the first phase of our statistical analyses, we tested the hypothesis that the phytoplankton species composition varied temporally and spatially by using non-metric MDS. MDS uses similarities between samples to graphically represent the relationship of samples to each other (Clarke and Warwick 1994). We began by establishing the similarities by creating a Bray-Curtis similarity matrix. This method of looking at relative similarities was particularly well-suited for our biological data, which contained numerous zero values, because it did not make any assumptions about the distribution of the data (Clarke and Warwick 1994). Then, we ran MDS on our Bray-Curtis matrix to visualize the relationship of sites and dates to each other.

To decide if the groups were statistically different from each other, we ran an analysis of similarities, ANOSIM (Clarke and Warwick 1994) on our Bray-Curtis matrix. The ANOSIM analysis compared the similarity of the data within groups

(i.e., sites and dates) to the similarity between groups to determine if the groups differed statistically. Because ANOSIM evaluated the distances between samples given in Bray-Curtis matrix, the ANSOIM output reflected the true differences between samples, unlike MDS. We ran ANOSIM for a 2-way crossed case with no replication, where each date and site combination was treated as a separate sample. We chose that layout because we expected that the phytoplankton composition would change both spatially and temporally, meaning that the dates would not be replicates of each site. Because the results then showed that site was significant, we decomposed the site effect by running a 1-way ANOSIM with dates as replicates. By sequentially removing one site and evaluating the significance of the remaining pairing, we determined which sites were most different from each other.

To evaluate the contribution of individual phytoplankton species to differences in site and date, we used a procedure called SIMPER (Clarke and Warwick 1994). SIMPER, or similarity percentages, sequentially removed species and quantified the degree to which that removal made the sites or dates more similar to each other (as defined by Bray-Curtis). Species that consistently contributed to the differentiation in groups for all pairings within that group (e.g., for every date within the sites) were discriminating species (Clarke and Warwick 1994). When multiple species contributed a small amount to the differences between dates or sites, the overall communities were found to have broad-based differences.

In the second phase of our statistical analyses, we tested the hypothesis that changes in environmental variables (water chemistry data and trace metal

concentrations) explained patterns in the phytoplankton communities using the BIO-ENV procedure. That procedure matched biotic data to environmental data by generating a series of environmental matrices based on all combinations of environmental variables, comparing those matrices to the single biological similarity matrix, and then ordering the environmental data to achieve the best correlation with the biological matrix (Clarke and Ainsworth 1993). We ran BIO-ENV using normalized Euclidean distances to identify any correlations between the phytoplankton similarity matrix and our PCA factors. Based on those results, we decomposed the PCA factor that was best correlated with the phytoplankton data back into its original environmental variables to assess the contribution of each of those original variables. We then ran BIO-ENV with those original variables and the trace metal concentrations to look for any correspondence between the phytoplankton similarity matrix and the environmental variables.

Results

Algal abundance and biomass—The spring 2003 phytoplankton bloom was a month-long period of high Chl *a* concentrations (Figure 3.2). By biovolume, diatoms were the dominant group; 24 of the 25 greatest biovolumes measured for each species on each date and site were diatoms. The diatoms were dominated by *Thalassiosira punctigera,* which alone accounted for 17 of the top 25 biomass measurements, because it bloomed for an extended time at the 3 sites. When the maximum

biovolume reached by each species was used to derive a list of the top bloom species by biovolume (Table 3.1), *T. punctigera*, topped the list with a maximum biovolume of 82,500,000 μm^3 mL^{-1}. *Thalassiosira punctigera* accounted for 99% of the algal biovolume on 04 March at site 36, when the bloom peaked (Table 3.1).

Concurrent abundance data showed that *Nannochloropsis sp.* was the most numerous species; 23 of the 25 greatest measurements of abundance for each species on each date and site were *Nannochloropsis sp.*. Because of its small size (< 5 μm), *Nannochloropsis sp.* was never among the top 10 species by biovolume. However, those picoeukaryotic phytoplankton topped the list of species with maximum abundances (Table 3.2).

Spatial and temporal effects on phytoplankton communities—Phytoplankton community composition differed significantly between sites (rho = 0.472, $p = 0.007$) and between dates (rho = 0.531, $p = 0.001$) in the ANOSIM analysis. By sequentially removing each site from the analysis, we decomposed the site effect and determined that sites 21 and 36 were the most distinct from each other, then sites 21 and 32, and then sites 32 and 36. That progression was consistent with the geographic locations of the sites; site 21 was our most northerly site with the greatest oceanic influence whereas site 36 was our most southerly (estuarine) site (Figure 3.1).

SIMPER analysis was subsequently used to identify the role of species composition in temporal and spatial variability. No single species contributed more than 7.6% to the dissimilarity between sites, and the top ten species contributed

similar amounts to the variation between the sites (Table 3.3). Similarly, no single species contributed more than 12% to the dissimilarities between dates (Table 3.4), when we compared the beginning of the bloom (19 February), the peak of the bloom (04 March), the early decay of the bloom (01 April), advanced decay (01 May), and non-bloom conditions (27 August). Differences between both dates and sites were caused by multiple species each contributing a small amount, which indicated that there were broad-based differences between the communities.

Relating algal communities to environmental data—By running the BIO-ENV procedure in PRIMER with the three PCA factors, we found that the PCA factor that best matched patterns in algal community composition was the bloom factor (correlation = 0.445). The bloom factor was originally composed of dissolved oxygen (+), temperature (-), salinity (-), dissolved inorganic nitrogen (-), dissolved silicate (-), and log transformed Chl *a* concentrations (+), where the sign in parentheses indicates the direction of the correlation between the bloom factor and the original variables. Of the original variables, we selected temperature, salinity, and nutrients for further analysis because we assumed that they were forcing community response, while the remaining variables were responses to those environmental drivers. We also divided the inorganic nitrogen pool into 1) nitrate plus nitrite and 2) ammonium. Subsequently, we ran a second BIO-ENV procedure with these selected variables and the trace metal concentrations.

We evaluated the results of the BIO-ENV procedure according to how the addition of environmental variables improved the correlation between the biological and environmental data (Table 3.5). Based on the differences between the one-variable and the two-variable models (and between the two-variable and three- and four-variable models), dissolved ammonium concentrations matched some of the variation in algal communities, and temperature data best matched the algal community patterns. The contribution of metals was negligible, and the choice of metal was not statistically important, based on the improvements in model fit.

Discussion

Algal abundance and biomass—By biovolume, diatoms dominated the phytoplankton and were presumably responsible for the depletion of dissolved nutrients and trace metals from the water column. The dominance of diatoms by biovolume (Table 3.1) was consistent with a decadal study (1992 - 2001) that found diatoms accounted for 81% of the total biomass in samples collected throughout the estuary (Cloern and Dufford 2005). Those large cells likely depleted the nitrate, based on research in the northern estuary showing that high rates of nitrate uptake were primarily associated with cells > 5 μm (Wilkerson et al. 2006). We also attributed the drawdown of dissolved silicate (Figure 3), inorganic nitrogen (Figure 3), phosphate (not shown), Ni (Luengen et al. 2007), Pb (Luengen et al. 2007), and MeHg (Luengen et al.

submitted) during the bloom primarily to large diatoms, particularly *Thalassiosira punctigera.*

Past South Bay blooms have been composed of other diatom species, including *Thalassiosira rotula, T. hendeyi, Chaetoceros socialis, C. debilis, Skeletonema costatum, Ditylum brightwellii, Coscinodiscus oculus-iridis, C. curvatulus, C. radiatus, and Eucampia zodiacus* (Cloern and Dufford 2005). The prevalence of *T. punctigera* during this bloom was an example of the stochastic nature of which species was present when conditions were ideal for a bloom. This high variability among bloom species was not surprising, given that even within a single species, populations of differing genetic makeup bloom at different times (Rynearson et al. 2006).

Although diatoms clearly dominated algal biomass, we focus the remainder our discussion on fourth root transformed abundance data to include both small and rare species. This focus addresses current interest in the effects of species diversity on pelagic ecosystem function (Duffy and Stachowicz 2006). A community with high species diversity may function differently than a monoculture, even if primary productivity is dominated by a single organism (Duffy and Stachowicz 2006). By taking an organismal approach, it is also possible to evaluate the trophic consequences of blooms (Smayda 1997). For example, highly abundant *Nannochloropsis sp.* are too small to be included in analyses of biomass, but they are an important part of a community analysis because they are highly nutritious (Mourente et al. 1990; Wacker and Von Elert 2004). Another reason for focusing at a

species level is that factors driving the biomass may not be the same as those driving community succession.

Community succession during the bloom—The SIMPER analysis (Table 3.4) identified species that distinguished the algal community on 19 February, when the bloom was beginning, from the community on 04 March when the bloom peaked (Figure 3.2). Differences between communities were shaped partially by an early bloom (> 25 cells mL^{-1} on 19 February at site 32) of *Chaetoceros didymus*. That early bloom of a small (10-40 μm) chain-forming diatom was consistent with classical succession theory (Margalef 1958), which says the spring bloom begins with small diatoms, such as *Chaetoceros socialis* and *Skeletonema costatum*, and then transitions to larger diatoms. The subsequent community on 04 March was distinguished partially by a bloom of the large (40-190 μm), centric *Thalassiosira punctigera* (Table 3.4), which is common in the Pacific Ocean and regularly blooms in the bay (Cloern et al. 2006). That diatom peaked at > 400 cells mL^{-1}, and its abundance remained high for over a month, mirroring Chl *a* concentrations at site 36.

In addition to diatoms, the SIMPER analysis identified several other groups of phytoplankton that contributed to differences in communities as the bloom grew between 19 February and 04 March (Table 3.4). Those groups included euglenophytes (*Eutreptia lanowii*) and cyanobacteria [*Cyanobium sp.*, which are closely related to *Synechococcus* (Komárek et al. 1999)]. Both *E. lanowii* and *Cyanobium sp.* are very small (11 and < 6 μm, respectively) species that reached peak

abundance on 04 March, like *Thalassiosira punctigera*. In contrast to *T. punctigera*, their blooms were transient. Specifically, *Cyanobium sp.* reached a peak abundance of 500 cells mL^{-1} on 04 March at site 36 but was not otherwise found at that site. Similarly, *E. lanowii* reached an abundance of 120 cells mL^{-1} on 04 March at site 36, whereas at all other times during the study it was present at < 10 cells mL^{-1}. Because *E. lanowii* is mixotrophic and often found in waters contaminated with organic matter (Nikolaides and Moustaka-Gouni 1990), its presence during the peak of the bloom suggested that it capitalized on organic matter produced by other species. The contribution of *E. lanowii and Cyanobium sp.* to temporal differences in communities demonstrated that this spring bloom was a diverse assemblage.

As the bloom decayed in April, the SIMPER analysis identified *Synechocystis sp.* as a species that distinguished the decay community from the bloom community (Table 3.4). *Synechocystis sp.* are picoplanktonic (< 5 μm) cyanobacteria that rely on their large surface area to volume ratio to uptake nutrients because they do not fix N_2 (Paerl 1999). *Synechocystis sp.* reached peak abundances (1250 cells mL^{-1}) on 01 and 17 April at site 36 (Figure 3.4), well after peak Chl *a* concentrations (Figure 3.2).

Growth of *Synechocystis sp.* during decay of the diatom bloom could have been a response to high DOC concentrations during decay, low dissolved silicate concentrations, or the increase in dissolved ammonium. DOC generated by the decaying bloom (Figure 3.2) could have enhanced the growth of *Synechocystis sp.*, which would be consistent with the possibility that DOC supports cyanobacterial growth (Paerl 1999). Alternatively, the depletion of dissolved silicate by 04 March

(Figure 3.3) could have favored cyanobacteria or other non-siliceous phytoplankton over diatoms. *Synechocystis sp.* may have also responded to the increase in dissolved ammonium (Figure 3.3) as the diatoms decayed, as we will discuss later.

Between 01 April and 01 May, the bloom continued to decay, and differences in the communities were partially due to changes in the abundance of *Synechocystis sp.*, *Dolichomastix sp.*, *Cyclotella sp.*, and *Teleaulax amphioxeia* (Table 3.4). At the beginning of May, the abundance of *Synechocystis sp.* was lower than in April (Figure 3.4). In contrast, the small cryptophyte *T. amphioxeia* reached its greatest abundance on 01 May (Figure 3.4). Because the cryptophyte is a mixotrophic species (Cloern and Dufford 2005), we hypothesized that it could have grazed upon the cyanobacteria.

This community analysis indicated that the bloom was not monolithic, but was composed of multiple species that changed on weekly time scales. Even at the peak of a massive bloom of *Thalassiosira punctigera,* other algal groups were thriving, including cyanobacteria (*Cyanobium sp.)* and euglenophytes *(Eutreptia lanowii).* The question of how multiple phytoplankton species can co-exist, competing for the same resources was first raised by the classic Hutchinson (1961) paper "the paradox of the plankton." Since that time, researchers have shown that external forces (e.g., habitat variability, predation, mixing, and exchange with other compartments) contribute to the diversity of phytoplankton (Cloern and Dufford 2005; Scheffer et al. 2003). As previously reported, the variable physical and chemical conditions during the bloom (Luengen et al. 2007) undoubtedly contributed to the diversity of algal species.

The diverse algal communities also could have been sustained by interactions between the species, even in a homogenous environment (Scheffer et al. 2003). Mathematical models have shown that if three different species compete for three separate resources, their abundance can oscillate and those oscillations can sustain other species (Huisman and Weissing 1999). With five or more resources, chaos can occur, making community composition unpredictable and highly dependent on the initial conditions (Huisman and Weissing 1999). Based on these mathematic models, in our study of the spring bloom, the diversity of plankton could be sustained by competition for a handful of resources. Because species that are not dominant by biomass (e.g., *Cyanobium sp.* and *Eutreptia lanowii)* are presumably still competing for resources, those species could play an important functional role in the community by creating interactions that keep the community diverse.

Temporal changes in algal communities related to physical exchange—Some of the diatoms identified in this study contributed to temporal differences in algal communities (Table 3.4), but were not responding to the diatom bloom. For example, we attributed the peak in abundance of *Nizschia closterium* (Figure 3.4), which is a highly mobile benthic diatom (Cloern and Dufford 2005; Smithsonian Environmental Research Center 2007), to the shallow depth of the estuary and movement of that pennate diatom into the water column. These results were consistent with previous research demonstrating the importance of physical transport within the estuary and

interconnectivity of habitats on primary production and species composition (Cloern 2007; Cloern and Dufford 2005).

Spatial and temporal differences between algal communities were also shaped by *Cyclotella striata* (Tables 3.3 and 3.4). The abundance of that centric diatom was similar in August and February at site 36 (Figure 3.4), indicating that conditions other than the bloom favored the species. Marshall and Alden (1990) described *C. striata* as a freshwater species that gradually declines during the transition to from freshwater to estuarine waters in the Chesapeake Bay. Therefore, the high abundance of *C. striata* at sites 36 and 21 and its low abundance at site 32 in South Bay (Figure 3.4) could have been caused by freshwater inputs from the Guadalupe River at site 36 and exchange of freshwater from the Sacramento and San Joaquin Rivers at site 21. However, freshwater inputs did not explain the high abundance of *C. striata* in August (Figure 3.4), a time when the primary source of freshwater to South Bay is wastewater treatment plants (Smith and Hollibaugh 2006). Its abundance may have been shaped by factors other than freshwater exchange; Prasad and Nienow (2006) described *C. striata* as a marine, rather than a freshwater species, and Cloern and Dufford (2005) describe it as a meroplanktonic species that is common in surface sediments. Regardless of its origin (i.e., sediments or freshwater), its distribution was likely not a response to the bloom, demonstrating that physical exchange processes shape algal distributions.

Algal communities and temperature—The BIO-ENV procedure showed that temperature was the environmental variable that best matched patterns in algal communities (Table 3.5). As shown in Figure 3.3, temperature was warmest (e.g., 23.1 °C at site 32) in August, intermediate (14.99 – 16.69 °C at site 32) from mid-March to May, cooler on 04 March (14.15 °C at site 32) and coolest on 19 and 24 February (e.g., 12.94 and 12.97 °C, respectively at site 32). The coolest temperatures occurred during the peak of the bloom.

Algal communities and ammonium—The BIO-ENV procedure showed that dissolved ammonium concentrations were also related to patterns in algal community composition, although they did not contribute as much to the model as did temperature (Table 3.5). Dissolved ammonium concentrations (Figure 3.3) were low (< 1.1 μmol L^{-1}) at sites 32 and 36 when Chl *a* concentrations (Figure 3.2) were high. Then, in April, dissolved ammonium concentrations increased as the bloom decayed, as observed elsewhere (e.g., Nova Scotia, Kim et al. 2004b).

In northern and central San Francisco Bay, ammonium has been suggested to limit primary productivity by inhibiting algal uptake of nitrate (Wilkerson et al. 2006). However, in the field, it is difficult to distinguish whether limited nitrate uptake is caused by ammonium inhibition or by algal preference for ammonium (Dortch 1990). The question of inhibition versus preference was beyond the scope of this study. However, we did observe that the increase in dissolved ammonium

coincided with growth of cyanobacteria, *Synechocystis sp.* (Figure 3.4), which was consistent with a preference of small cells for ammonium (Dortch 1990).

High ammonium concentrations could have benefited *Synechocystis sp.* more than other algal groups, based on mesocosm experiments with water from the Neuse River Estuary, North Carolina (Paerl 1999). In those experiments, equimolar concentrations of nitrate and ammonium were added to an assemblage of cyanobacteria, diatoms, and cryptomonads. Of those groups, cyanobacteria increased the most in response to the ammonium additions. Moreover, during field studies in that estuary, dissolved ammonium reached high concentrations as a result of anoxic conditions following a hurricane, and blooms of cyanobacteria were subsequently observed (Paerl 1999).

We proposed that in South San Francisco Bay, suboxic conditions created by decay of the *Thalassiosira punctigera* bloom caused the increase in dissolved ammonium (Figure 3.3) and enhanced growth of *Synechocystis sp.*. *Synechocystis sp.* consistently contributed to differences between both sites and dates (Tables 3.3 and 3.4), indicating that it was a discriminating species (Clarke and Warwick 1994). Thus, if *Synechocystis sp.* responded to changes in ammonium concentrations, it could have contributed to the community relationship with ammonium.

The complex linkages between nutrient concentrations and algal community composition in the estuary were evidence of eutrophication in San Francisco Bay. High nutrient concentrations initially set the stage for the large diatom bloom, which then depleted the nutrients. The decay of the bloom subsequently increased dissolved

ammonium concentrations, favoring non-diatom species. Although it was difficult to determine if the bloom drove the water chemistry, or vice-versa, nutrient concentrations helped shape algal community composition in the estuary. Changes in algal community composition as a result of nutrient enrichment are considered evidence of eutrophication (Cloern 2001; Pinckney et al. 1997).

Algal communities and dissolved metal concentrations—The BIO-ENV result showing that dissolved metal concentrations were not linked to phytoplankton community composition (Table 3.5) was consistent with previous studies demonstrating that the toxicity of metals to phytoplankton in the estuary was limited by organic complexation. In previous studies, > 99% of dissolved Cu in the estuary was strongly complexed to organic ligands (Buck and Bruland 2005; Hurst and Bruland 2005) and not readily available for algal uptake (Beck et al. 2002; Luengen et al. 2007; Luoma et al. 1998). As a result, diverse populations of cyanobacteria have been observed in the estuary, indicating that plankton were not impaired by the relatively high concentrations of dissolved Cu (Palenik and Flegal 1999).

Similar to dissolved Cu, > 95% of dissolved Pb in the estuary is complexed, primarily to strong ligands (Kozelka et al. 1997). Although the spring 2003 phytoplankton bloom depleted dissolved Pb from the water column, that depletion was likely the result of sorption of Pb to algal surfaces, as opposed to internalization in the cellular cytoplasm (Luengen et al. 2007; Michaels and Flegal 1990). Accordingly, that metal was unlikely to impair phytoplankton growth.

In contrast to Cu and Pb, Ni may be bioavailable at some times of year because of seasonal variations in the amount of its complexation. For example, strong Ni complexation in South Bay in 1997 varied from 0 - 91% seasonally in response to the amount of wastewater treatment plant discharge (Bedsworth and Sedlak 1999). That variation was consistent with contrasting results from previous investigations of Ni uptake by phytoplankton in South Bay. In that previous work, Luengen et al. (2007) and Luoma et al. (1998) found that Ni was bioavailable to phytoplankton in field studies whereas Beck et al. (2002) showed that Ni was not taken up by phytoplankton in laboratory microcosm studies.

Although there are have been no studies on Zn complexation in this estuary, its bioavailability is also likely dictated by organic complexation, based on laboratory studies elsewhere (Brand et al. 1983). The amount of organic complexation in South Bay may vary considerably, given that there is wide range (51 - 87%) in the amount of complexed Zn in Narragansett Bay, Rhode Island (Kozelka and Bruland 1998). Similar variation in complexation in San Francisco Bay may explain why Zn was depleted during the 1994 spring bloom (Luoma et al. 1998), but not during the spring 2003 spring bloom (Luengen et al. 2007).

In summary, this statistical approach allowed us to look for a relationship between metal enrichment and algal community composition without measuring metal speciation. To chemically characterize the complexation of all metals in this study would have been extremely difficult because complexing ligands have various binding strengths (Bedsworth and Sedlak 1999; Buck and Bruland 2005), originate

from myriad sources (Bedsworth and Sedlak 1999; Buck et al. in press), and some (e.g., dithiocarbamate fungicides) could even enhance algal uptake of metals if they were present in the estuary's waters (Phinney and Bruland 1997a; 1997b). This statistical approach also allowed us to simultaneously consider the multiple metals that are enriched in the estuary to potentially toxic levels. We concluded, however, that the patterns of metal enrichment in South Bay were not measurably linked to algal community composition.

Conclusions

This study highlights the complexity and diversity of the spring bloom over relatively short temporal scales (order of weeks) and spatial scales (kilometers). Functional consequences of high algal diversity is currently an area where more research is needed (Duffy and Stachowicz 2006), but our results suggest that one consequence is the presence of species that are poised to take advantage of changes in environmental conditions (such as the increase in dissolved ammonium). Dissolved ammonium concentrations are linked to algal community composition, indicating that the high nutrient concentrations in the estuary have measurable biological effects (i.e., eutrophication). Algal community composition is also linked to temperature, suggesting that changes in water temperature from global warming could affect algal community composition in the estuary. In contrast, anthropogenically enriched metal concentrations in South Bay do not measurably shape algal community composition.

Despite the sensitivity of cyanobacteria to high metal (e.g., Cu) concentrations, cyanobacteria are present in the estuary and help distinguish algal communities over space and time. Accordingly, these results were consistent with previous studies showing that organic complexation of dissolved Cu limits its bioavailability and toxicity in the estuary.

Table 3.1. Top ten bloom species by biovolume, calculated as the maximum biovolume attained by each algal species at any given site and date in 2003. Blooms of species such as *Thalassiosira nodulolineata* were small (e.g., only 3 percent of the biovolume in that sample) relative that of *T. punctigera* (which accounted for the remaining 97% of the biovolume in that sample).

Taxon	Group	Date	Site	Abundance (cells mL^{-1})	Maxiumum biovolume (μm^3 mL^{-1})	Percent of total biovolume in that sample (%)
Thalassiosira punctigera (Castracane) Hasle	Diatoms	04 Mar	36	408	82,500,000	99
Thalassiosira gravida Cleve	Diatoms	01 Apr	36	52	12,000,000	97
Thalassiosira hendeyi Hasle & Fryxell	Diatoms	17 Apr	21	24	3,500,000	46
Coscinodiscus curvatulus Grunow	Diatoms	17 Apr	21	6	3,000,000	44
Alexandrium fundyense Balech	Dinoflagellates	27 Aug	32	290	1,620,000	74
Thalassiosira nodulolineata	Diatoms	12 Mar	36	6	1,000,000	3
Corethron hystrix Hensen	Diatoms	12 Mar	21	1	1,000,000	29
Ditylum brightwellii (T. West) Grunow	Diatoms	19 Feb	21	2	900,000	32
Coscinodiscus concinnus W. Smith	Diatoms	27 Aug	21	4	900,000	33
Dactyliosolen fragilissimus (Bergon) Hasle	Diatoms	04 Mar	21	5	600,000	5

Table 3.2. Top ten bloom species by abundance, calculated as the maximum abundance attained by each algal species at any given site and date in 2003.

Taxon	Group	Date	Site	Maximum abundance (cells mL^{-1})	Biovolume ($\mu m^3 mL^{-1}$)	Percent of total biovolume in that sample (%)
Nannochloropsis sp.	Eustigmatophyta	24 Feb	21	72,750	109,000	0.33
Plagioselmis prolonga var. nordica Novarino	Cryptomonads	27 Aug	21	7,680	474,000	18
Dolichomastix sp.	Prasinomonads	01 Apr	36	1,500	3,200	0.03
Skeletonema costatum (Greville) Cleve	Diatoms	27 Aug	32	1,480	261,000	12
Synechocystis salina Wislouch	Cyanobacteria	01 Apr	36	1,250	1,440	0.01
Teleaulax amphioxeia (Conrad) Hill	Cryptomonads	01 May	32	1,040	430,000	33
Cyclotella sp.	Diatoms	24 Feb	32	800	270,000	0.40
Pyramimonas orientalis Butcher	Prasinomonads	12 Mar	21	720	28,000	0.65
Cyanobium sp.	Cyanobacteria	04 Mar	36	500	350	0.0004
Thalassiosira punctigera (Castracane) Hasle	Diatoms	04 Mar	36	408	82,500,000	99

Table 3.3. Results from the SIMPER analysis showing the phytoplankton species that contributed most to the observed differences in community composition between the three sites in South Bay in 2003. Species names given in bold face indicate greater abundance at the first site listed than the second site (e.g., *Nannochloropsis sp.* were more abundant at site 21 than site 32).

Species	Group	Contrib%	Cum.%
Average dissimilarity between site 21 & 32 = 44.93			
Nannochloropsis sp.	Eustigmatophyta	5.5	5.5
Synechocystis sp.	Cyanobacteria	5.5	11
Skeletonema costatum (Greville) Cleve	Diatoms	4.8	16
***Pyramimonas orientalis* Butcher**	Prasinomonads	4.7	21
Cyclotella sp.	Diatoms	4.5	25
***Teleaulax amphioxeia* (Conrad) Hill**	Cryptomonads	4.0	29
Plagioselmis prolonga var. *nordica* Novarino Lucas & Morrall	Cryptomonads	3.9	33
Thalassiosira punctigera (Castracane) Hasle	Diatoms	3.8	37
Cyclotella atomus Hustedt	Diatoms	3.3	40
***Nitzschia closterium* (Ehrenberg) W. Smith**	Diatoms	2.8	43
***Thalassiosira pacifica* Gran & Angst**	Diatoms	2.6	45
***Biddulphia alternans* Bailey**	Diatoms	2.5	48
***Cyclotella striata* (Kuetzing) Grunow**	Diatoms	2.3	50
Average dissimilarity between site 21 & 36 = 45.52			
Synechocystis sp.	Cyanobacteria	6.2	6.2
***Pyramimonas orientalis* Butcher**	Prasinomonads	5.1	11
Nannochloropsis sp.	Eustigmatophyta	5.0	16
***Skeletonema costatum* (Greville) Cleve**	Diatoms	5.0	21
Cyclotella sp.	Diatoms	4.4	26
Thalassiosira punctigera (Castracane) Hasle	Diatoms	4.4	30
Plagioselmis prolonga var. *nordica* Novarino Lucas & Morrall	Cryptomonads	3.7	34
Cyclotella striata (Kuetzing) Grunow	Diatoms	3.7	37
***Teleaulax amphioxeia* (Conrad) Hill**	Cryptomonads	3.1	41
***Nitzschia closterium* (Ehrenberg) W. Smith**	Diatoms	3.0	44
***Thalassiosira nordenskioeldii* Cleve**	Diatoms	2.7	46
***Chaetoceros subtilis* Cleve**	Diatoms	2.4	49
***Thalassiosira visurgis* Hustedt**	Diatoms	2.3	51
Average dissimilarity between sites 32 and 36= 41.54			
Synechocystis sp.	Cyanobacteria	7.6	7.6
Pyramimonas orientalis Butcher	Prasinomonads	5.6	13
Teleaulax amphioxeia (Conrad) Hill	Cryptomonads	5.5	19
***Thalassiosira punctigera* (Castracane) Hasle**	Diatoms	5.5	24
Nannochloropsis sp.	Eustigmatophyta	5.4	29
Cyclotella sp.	Diatoms	5.3	35
Cyclotella striata (Kuetzing) Grunow	Diatoms	4.5	39
***Skeletonema costatum* (Greville) Cleve**	Diatoms	4.0	43
***Nitzschia closterium* (Ehrenberg) W. Smith**	Diatoms	3.6	47
Dolichomastix sp.	Prasinomonads	3.4	50

Table 3.4. Results from the SIMPER analyses showing the phytoplankton species that contributed most to temporal changes in algal community composition between the beginning of the bloom (19 Feb), the peak of the bloom (04 Mar), the onset of decay (01 Apr), advanced decay (01 May), and non-bloom conditions (27 Aug). Species names given in bold face indicate greater abundance on the first date listed than the second date (e.g., *Synechocystis sp.* were more abundant on 19 Feb than 04 Mar).

Species	Group	Contrib (%)	Cum (%)
Average dissimilarity between 19 Feb and 04 Mar = 39.07			
Synechocystis sp.	Cyanobacteria	7.0	7.0
Cyclotella striata (Kuetzing) Grunow	Diatoms	5.7	13
Nannochloropsis sp.	Eustigmatophyta	5.4	18
***Skeletonema costatum* (Greville) Cleve**	Diatoms	5.3	23
Teleaulax amphioxeia (Conrad) Hill	Cryptomonads	4.6	28
Cyanobium sp.	Cyanobacteria	4.1	32
Eutreptia lanowii Steur	Euglenoids	3.9	36
***Nitzschia fontifuga* Cholnoky**	Diatoms	3.8	40
Plagioselmis prolonga var. *nordica* Novarino, Lucas & Morrall	Cryptomonads	3.8	44
Thalassiosira punctigera (Castracane) Hasle	Diatoms	3.7	47
***Chaetoceros didymus* Ehrenberg**	Diatoms	3.5	51
Average dissimlarity between 04 Mar and 01 Apr = 42.73			
Synechocystis sp.	Cyanobacteria	9.7	10
Dolichomastix sp.	Prasinomonads	8.0	18
Pyramimonas orientalis Butcher	Prasinomonads	5.1	23
Nannochloropsis sp.	Eustigmatophyta	4.7	27
***Cyclotella striata* (Kuetzing) Grunow**	Diatoms	4.7	32
Teleaulax amphioxeia (Conrad) Hill	Cryptomonads	4.5	37
Pyramimonas disomata Butcher	Prasinomonads	4.4	41
Skeletonema costatum (Greville) Cleve	Diatoms	4.0	45
***Thalassiosira punctigera* (Castracane) Hasle**	Diatoms	3.7	49
Nitzschia closterium (Ehrenberg) W. Smith	Diatoms	3.4	52
Average dissimilarity between 01 Apr and 01 May = 47.15			
Synechocystis sp.	Cyanobacteria	12	12
Dolichomastix sp.	Prasinomonads	7.3	19
Cyclotella sp.	Diatoms	7.0	26
Teleaulax amphioxeia (Conrad) Hill	Cryptomonads	5.9	32
Cyclotella atomus Hustedt	Diatoms	4.9	37
Thalassiosira punctigera (Castracane) Hasle	Diatoms	4.2	41
Nitzschia closterium (Ehrenberg) W. Smith	Diatoms	3.9	45
Pyramimonas orientalis Butcher	Prasinomonads	3.8	49
Skeletonema costatum (Greville) Cleve	Diatoms	3.6	52
Average dissimilarity between 04 Mar and 27 Aug = 53.01			
Cyclotella sp.	Diatoms	8.0	8.0
Skeletonema costatum (Greville) Cleve	Diatoms	6.2	14
Alexandrium fundyense Balech	Dinoflagellates	5.5	20
***Thalassiosira punctigera* (Castracane) Hasle**	Diatoms	5.1	25
Nannochloropsis sp.	Eustigmatophyta	5.1	30
Plagioselmis prolonga var. *nordica* Novarino, Lucas & Morrall	Cryptomonads	4.7	35
***Teleaulax amphioxeia* (Conrad) Hill**	Cryptomonads	4.4	39
Cymatosira belgica Grunow in Van Heurck	Diatoms	4.0	43
Rhodomonas marina (Dangeard) Lemmermann	Cryptomonads	3.8	47
Synechocystis sp.	Cyanobacteria	3.7	50

Table 3.5. Results from the BIO-ENV procedure showing the correlation between algal community composition and models with various numbers of environmental variables. The increase in fit is the amount by which the correlation improved when an additional variable was added to the model. The best one-variable model was temperature (correlation = 0.395). The addition of dissolved ammonium to the model increased the fit by 0.086, indicating that dissolved ammonium contributed to community response, but that temperature explained most of the variability. The best three-variable model (temperature, ammonium, and silicate) increased the fit relative to the two-variable model by only 0.016, signifying that dissolved silicate did not contribute much to the model. Similarly, the contribution of dissolved metals to the model was negligible (≤ 0.020).

Model	Correlation	Increase in fit
Pb, temperature, ammonium, silicate	0.517	0.020
Co, temperature, ammonium, silicate	0.500	0.003
Temperature, ammonium, silicate	0.497	0.016
Temperature and ammonium	0.481	0.086
Temperature	0.395	—

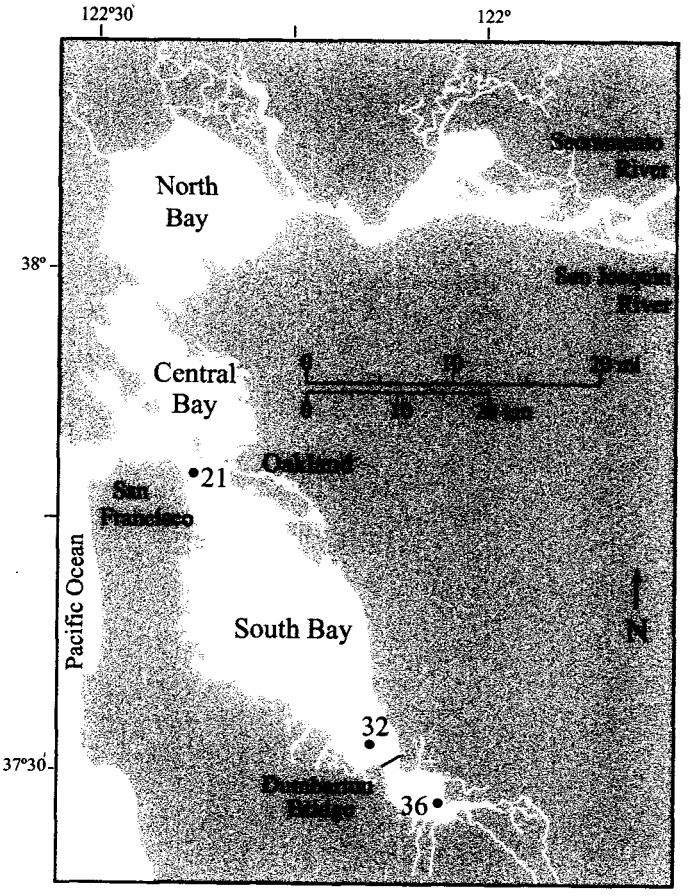

Figure 3.1. Surface water samples for phytoplankton species composition were collected from the southern reach of San Francisco Bay (South Bay) at sites 21 (Bay Bridge), 32 (Ravenswood Point), and 36 (Calaveras Point).

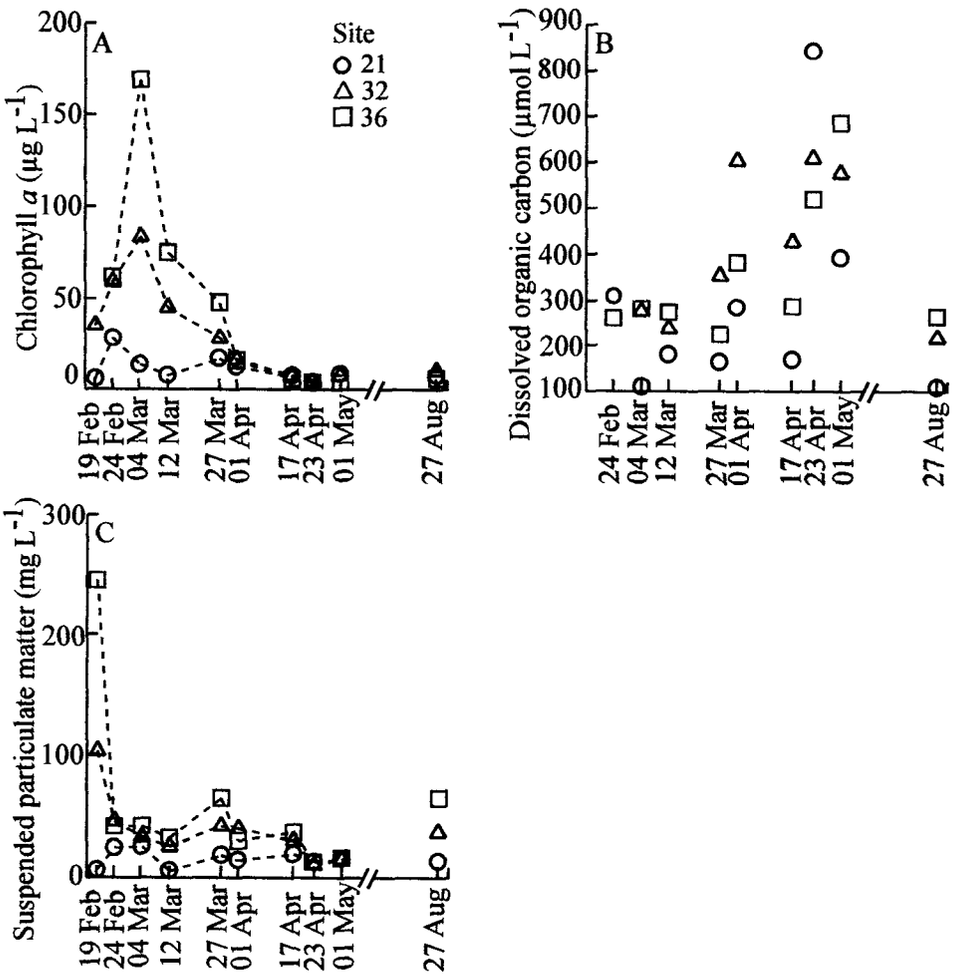

Figure 3-2. (A-C) Concentrations of A) chlorophyll *a*, B) dissolved organic carbon, and C) suspended particulate matter at three sites in San Francisco Bay in 2003.

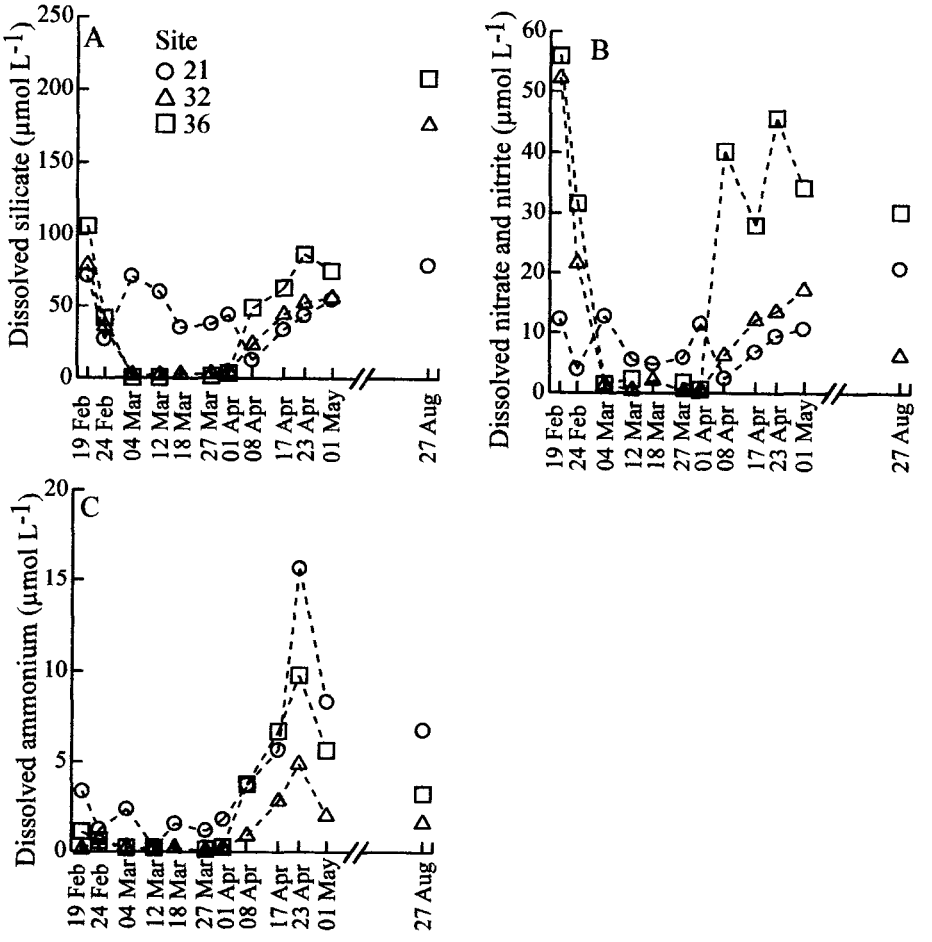

Figure 3.4. (A-C) Concentrations of A) dissolved silicate, B) dissolved nitrate and nitrite, and C) dissolved ammonium during this study.

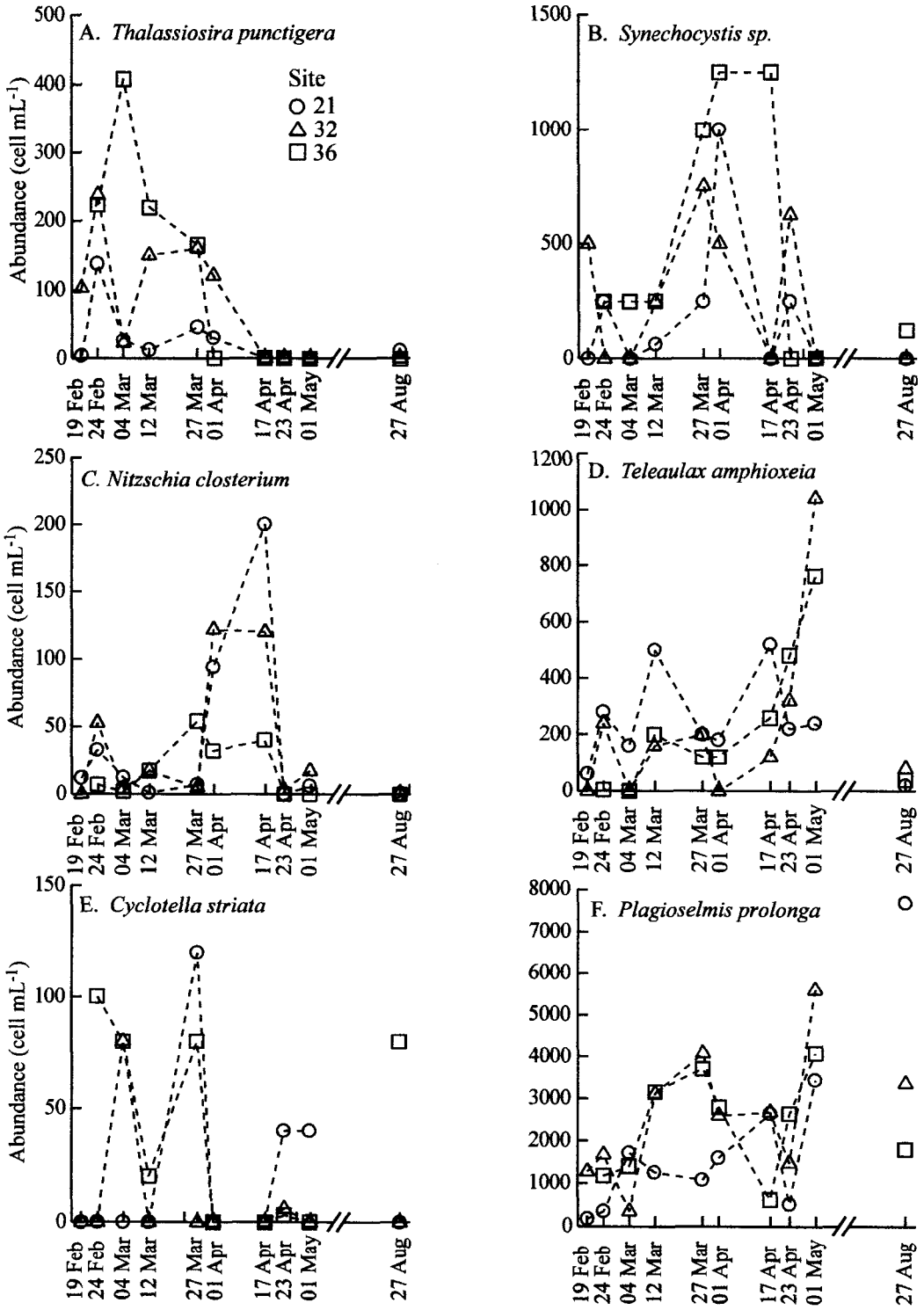

Figure 3.4. (A-F) Abundance of 6 phytoplankton species, representative of A) centric diatoms that compose the spring bloom, B) cyanobacteria that increase during early decay, C) pennate diatoms that are mobilized from benthic sediments, D) cryptophytes that are present during late decay, E) centric diatoms that are most abundant at sites 21 and 36, possibly due to freshwater inputs, and F) cryptophytes that are persistent and variable.

CONCLUSIONS AND FUTURE DIRECTIONS

This work addresses the combined environmental impacts of nutrient enrichment, phytoplankton blooms, and metal contamination in the southern reach of San Francisco Bay (South Bay). The bloom in this study, in spring 2003, was one of the largest blooms on record and crashed following depletion of dissolved nutrients. Thus, the magnitude of blooms can be limited by the amount of nutrients, which are elevated in the estuary as a result of inputs from wastewater treatment plants (Hager and Schemel 1996; Smith and Hollibaugh 2006).

Like nutrients, dissolved metals are enriched in the estuary as a result of anthropogenic inputs (Flegal et al. 2005). The potential of phytoplankton to uptake dissolved methyl mercury is a particular concern because that metal currently reaches concentrations in fish that require consumption advisories in the estuary (Thompson et al. 2000). This work demonstrates that although phytoplankton take up methyl mercury during a bloom, a potentially more important effect is production of methyl mercury in sediments as bloom material decays. Thus, there were unanticipated, yet consequential, links between algal concentrations and metal cycling.

Although the bloom affects metal concentrations, the metal concentrations do not directly shape algal community composition. That result was consistent with previous research demonstrating that organic complexation limits the bioavailability of metals such as copper in the estuary (Buck and Bruland 2005; Sedlak et al. 1997). However, there are spatial and temporal changes in phytoplankton communities

during the bloom, which demonstrate the dynamic nature of algal blooms in the estuary.

The complex and dynamic nature of metal-algal interactions is a fascinating subject, where geochemistry interfaces with biology, and complex statistical models are often needed to analyze data. The study of single celled phytoplankton provides a perfect opportunity to understand metal accumulation in terms of process oriented studies. Of the metals in the estuary, process oriented studies are most needed for mercury. Despite potentially high concentrations of mercury in fish, the exact mechanisms of methyl mercury uptake by phytoplankton at the base of the food chain are still not understood (Pickhardt and Fisher 2007).

One method that has been successfully used to evaluate uptake of metals by phytoplankton is the use of radioisotope tracers (Pickhardt and Fisher 2007). In my future postdoctoral position with Professor Nicholas Fisher, Stony Brook University, I will use mercury radioisotopes to evaluate how mercury uptake by phytoplankton is affected by its association with dissolved organic matter. Previous research has demonstrated that dissolved organic matter may alter processes that occur on phytoplankton surfaces (such as uptake of metals) by binding to cell surfaces (Campbell et al. 1997). Furthermore, the concentration of dissolved organic matter has been shown to increase methyl mercury uptake by phytoplankton in experiments with water from different sites in the San Francisco Bay Delta (Pickhardt and Fisher 2007).

The San Francisco Bay and Delta is an ideal place to conduct future studies on mercury uptake to phytoplankton. Not only is there a pressing need to understand mercury bioavailability there, it is also one of the most well-studied estuaries (Sañudo-Wilhelmy et al. 2004). Those previous studies, including this dissertation, make it possible to frame metal contamination in terms of complex estuarine processes. For example, my postdoctoral work in the estuary will leverage existing knowledge and samples of dissolved organic matter composition through collaboration with Dr. Brian Bergamaschi, United States Geological Survey (USGS).

The research presented here has benefited enormously from previous studies in the estuary, especially those on phytoplankton ecology (led by Dr. Jim Cloern, USGS) and metal speciation (conducted by Professor Ken Bruland, University of California at Santa Cruz, and his students). The San Francisco Bay estuary is an ideal place to conduct interdisciplinary research and evaluate the impacts of multiple anthropogenic stressors. Moreover, as a highly disturbed estuary, which is home to more than 7 million people (Smith and Hollibaugh 2006), San Francisco Bay is in need of our research efforts.

REFERENCES

ALPERS, C. N., M. P. HUNERLACH, J. T. MAY, and R. L. HOTHEM. 2005. Mercury contamination from historical gold mining in California, U.S. Geological Survey Fact Sheet 2005-3014 Version 1.1.

BAEYENS, W., C. MEULEMAN, B. MUHAYA, and M. LEERMAKERS. 1998. Behaviour and speciation of mercury in the Scheldt estuary (water, sediments, and benthic organisms). Hydrobiologia **366:** 63-79.

BECK, N. G., K. W. BRULAND, and E. L. RUE. 2002. Short-term biogeochemical influence of a diatom bloom on the nutrient and trace metal concentrations in South San Francisco Bay microcosm experiments. Estuaries **25:** 1063-1076.

BEDSWORTH, W. W., and D. L. SEDLAK. 1999. Sources and environmental fate of strongly complexed nickel in estuarine waters: The role of ethylenediaminetetraacetate. Environmental Science and Technology **33:** 926-931.

BENOIT, G. 1995. Evidence of the particle concentration effect for lead and other metals in fresh waters based on ultraclean technique analyses. Geochimica et Cosmochimica Acta **59:** 2677-2687.

BENOIT, G., and T. F. ROZAN. 1999. The influence of size distribution on the particle concentration effect and trace metal partitioning in rivers. Geochimica et Cosmochimica Acta **63:** 113-127.

BENOIT, J. M., C. C. GILMOUR, A. HEYES, R. P. MASON, and C. L. MILLER. 2003. Geochemical and biological controls over methylmercury production and degradation in aquatic ecosystems, p. 262-297, Biogeochemistry of environmentally important trace elements. American Chemical Society Symposium Series.

BILINSKI, H., S. KOZAR, M. PLAVSIC, Z. KWOKAL, and M. BRANICA. 1991. Trace metal adsorption on inorganic solid phases under estuarine conditions. Marine Chemistry **32:** 225-233.

BLOOM, N. 1989. Determination of picogram levels of methylmercury by aqueous phase ethylation followed by cryogenic gas chromatography with cold vapor atomic fluorescence detection. Canadian Journal of Fisheries and Aquatic Sciences **46:** 1131-1140.

BLOOM, N., and W. F. FITZGERALD. 1988. Determination of volatile mercury species at the picogram level by low temperature gas chromatography with cold vapor atomic fluorescence detection. Analytica Chimica Acta **208:** 151-161.

BLOOM, N. S., and E. J. VON DER GEEST. 1995. Matrix modification to improve the recovery of MMHg from clear water using distillation, p. 1319-1323. *In* D. B. Porcella, J. W. Huckabee and B. Wheatley [eds.], Mercury as a global pollutant. Kluwer Academic Publishers.

BRAND, L. E., W. G. SUNDA, and R. R. L. GUILLARD. 1983. Limitation of marine phytoplankton reproductive rates by zinc, manganese, and iron. Limnology and Oceanography **28:** 1182-1198.

---. 1986. Reduction of marine phytoplankton reproduction rates by copper and cadmium. Journal of Experimental Marine Biology and Ecology **96:** 225-250.

BRULAND, K. W., J. R. DONAT, and D. A. HUTCHINS. 1991. Interactive influences of bioactive trace metals on biological production in oceanic waters. Limnology and Oceanography **36:** 1555-1577.

BUCK, K. N., and K. W. BRULAND. 2005. Copper speciation in San Francisco Bay: A novel approach using multiple analytical windows. Marine Chemistry **96:** 185-198.

BUCK, K. N., J. R. M. ROSS, A. RUSSELL FLEGAL, and K. W. BRULAND. in press. A review of total dissolved copper and its chemical speciation in San Francisco Bay, California. Environmental Research.

CAFFREY, J. M., J. E. CLOERN, and C. GRENZ. 1998. Changes in production and respiration during a spring phytoplankton bloom in San Francisco Bay, California, USA: Implications for net ecosystem metabolism. Marine Ecology Progress Series **172:** 1-12.

CAMPBELL, P. G. C., M. R. TWISS, and K. J. WILKINSON. 1997. Accumulation of natural organic matter on the surfaces of living cells: implications for the interaction of toxic solutes with aquatic biota. Canadian Journal of Fisheries and Aquatic Sciences **54:** 2543-2554.

CARGILL, S. M., D. H. ROOT, and E. H. BAILEY. 1980. Resource estimation from historical data: Mercury, a test case. Journal of the International Association for Mathematical Geology **12:** 489-522.

CHEN, C. Y., and C. L. FOLT. 2005. High plankton densities reduce mercury biomagnification. Environmental Science and Technology **39:** 115-121.

CHOE, K.-Y., and G. A. GILL. 2003. Distribution of particulate, colloidal, and dissolved mercury in San Francisco Bay estuary. 2. Monomethyl mercury. Limnology and Oceanography **48:** 1547-1556.

CHOE, K.-Y., G. A. GILL, and R. LEHMAN. 2003. Distribution of particulate, colloidal, and dissolved mercury in San Francisco Bay estuary. 1. Total mercury. Limnology and Oceanography **48:** 1535-1546.

CLARKE, K. R. 1993. Non-parametric multivariate analyses of changes in community structure. Australian Journal of Ecology **18:** 117-143.

CLARKE, K. R., and M. AINSWORTH. 1993. A method of linking multivariate community structure to environmental variables. Marine Ecology Progress Series **92:** 205-219.

CLARKE, K. R., and R. M. WARWICK. 1994. Change in marine communities: An approach to statistical analysis and interpretation, p. 144. Plymouth Marine Laboratory.

CLOERN, J. E. 1996. Phytoplankton bloom dynamics in coastal ecosystems: A review with some general lessons from sustained investigation of San Francisco Bay, California. Reviews of Geophysics **34:** 127-168.

---. 2001. Our evolving conceptual model of the coastal eutrophication problem. Marine Ecology Progress Series **210:** 223-253.

---. 2007. Habitat connectivity and ecosystem productivity: Implications from a simple model. American Naturalist **169:** E21-E33.

CLOERN, J. E., and R. DUFFORD. 2005. Phytoplankton community ecology: Principles applied in San Francisco Bay. Marine Ecology Progress Series **285:** 11-28.

CLOERN, J. E., C. GRENZ, and L. VIDERGAR-LUCAS. 1995. An empirical model of the phytoplankton chlorophyll: carbon ratio– The conversion factor between productivity and growth rate. Limnology and Oceanography **40:** 1313-1321.

CLOERN, J. E., A. D. JASSBY, T. S. SCHRAGA, and K. L. DALLAS. 2006. What is causing the phytoplankton increase in San Francisco Bay, p. 62-70, The pulse of the estuary: Monitoring and managing water quality in the San Francisco Estuary. SFEI contribution 517. San Francisco Estuary Institute.

CONAWAY, C. H., S. SQUIRE, R. P. MASON, and A. R. FLEGAL. 2003. Mercury speciation in the San Francisco Bay estuary. Marine Chemistry **80:** 199-225.

COQUERY, M., D. COSSA, and J. M. MARTIN. 1995. The distribution of dissolved and particulate mercury in three Siberian estuaries and adjacent Arctic coastal waters. Water, Air, and Soil Pollution **80:** 653-664.

DOMAGALSKI, J. 2001. Mercury and methylmercury in water and sediment of the Sacramento River Basin, California. Applied Geochemistry **16:** 1677-1691.

DORTCH, Q. 1990. The interaction between ammonium and nitrate uptake in phytoplankton. Marine Ecology Progress Series **61:** 183-201.

DUFFY, J. E., and J. J. STACHOWICZ. 2006. Why biodiversity is important to oceanography: Potential roles of genetic, species, and trophic diversity in pelagic ecosystem processes. Marine Ecology Progress Series **311:** 179-189.

EGGE, J. K., and D. L. AKSNES. 1992. Silicate as regulating nutrient in phytoplankton competition. Marine Ecology Progress Series **83:** 281-289.

FIELD, J. G., K. R. CLARKE, and R. M. WARWICK. 1982. A practical strategy for analyzing multispecies distribution patterns. Marine Ecology Progress Series **8:** 37-52.

FLEGAL, A. R. 1977. Mercury in the seston of the San Francisco Bay Estuary. Bulletin of Environmental Contamination and Toxicology **17:** 733-738.

FLEGAL, A. R., C. H. CONAWAY, G. M. SCELFO, S. A. HIBDON, and S. A. SAÑUDO-WILHELMY. 2005. A review of factors influencing measurements of decadal variations in metal contamination in San Francisco Bay, California. Ecotoxicology **14:** 645-660.

FLEGAL, A. R., I. RIVERA-DUARTE, P. I. RITSON, G. M. SCELFO, G. J. SMITH, M. R. GORDON, and S. A. SANUDO-WILHELMY. 1996. Metal contamination in San Francisco Bay waters: Historic perturbations, contemporary concentrations, and future considerations, p. 173-188. *In* J. T. Hollibaugh [ed.], San Francisco Bay, The ecosystem: Further investigations into the natural history of San Francisco Bay and Delta with reference to the influence of man. Pacific Division of the American Association for the Advancement of Science.

FLEGAL, A. R., G. J. SMITH, G. A. GILL, S. SAÑUDO-WILHELMY, and L. C. D. ANDERSON. 1991. Dissolved trace element cycles in the San Francisco Bay Estuary. Marine Chemistry **36:** 329-363.

GAGNON, C., and N. S. FISHER. 1997. Bioavailability of sediment-bound methyl and inorganic mercury to a marine bivalve. Environmental Science and Technology **31:** 993-998.

GANGULI, P. M., R. P. MASON, K. E. ABU-SABA, R. S. ANDERSON, and A. R. FLEGAL. 2000. Mercury speciation in drainage from the New Idria mercury mine, California. Environmental Science and Technology **34:** 4773-4779.

GEE, A. K., and K. W. BRULAND. 2002. Tracing Ni, Cu, and Zn kinetics and equilibrium partitioning between dissolved and particulate phases in South San Francisco Bay, California, using stable isotopes and high-resolution inductively coupled plasma mass spectrometry. Geochimica et Cosmochimica Acta **66:** 3063-3083.

GILL, G. A., N. S. BLOOM, S. CAPPELLINO, C. T. DRISCOLL, C. DOBBS, L. MCSHEA, R. MASON, and J. W. M. RUDD. 1999. Sediment-water fluxes of mercury in Lavaca Bay, Texas. Environmental Science and Technology **33:** 663-669.

GILL, G. A., and W. F. FITZGERALD. 1987. Picomolar mercury measurements in seawater and other materials using stannous chloride reduction and 2-stage gold amalgamation with gas phase detection. Marine Chemistry **20:** 227-243.

GILMOUR, C. C., G. S. RIEDEL, M. C. EDERINGTON, J. T. BELL, J. M. BENOIT, G. A. GILL, and M. C. STORDAL. 1998. Methylmercury concentrations and production rates across a trophic gradient in the northern Everglades. Biogeochemistry **40:** 327-345.

GRENZ, C., J. E. CLOERN, S. W. HAGER, and B. E. COLE. 2000. Dynamics of nutrient cycling and related benthic nutrient and oxygen fluxes during a spring phytoplankton bloom in South San Francisco Bay (USA). Marine Ecology Progress Series **197:** 67-80.

HAGER, S. W., and L. E. SCHEMEL. 1996. Dissolved inorganic nitrogen, phosphorus and silicon in South San Francisco Bay I. Major factors affecting distributions, p. 189-216. *In* J. T. Hollibaugh [ed.], San Francisco Bay, The ecosystem: Further investigations into the natural history of San Francisco Bay and Delta with reference to the influence of man. Pacific Division of the American Association for the Advancement of Science.

HAMMERSCHMIDT, C. R., and W. F. FITZGERALD. 2004. Geochemical controls on the production and distribution of methylmercury in near-shore marine sediments. Environmental Science and Technology **38:** 1487-1495.

---. 2006. Methylmercury cycling in sediments on the continental shelf of southern New England. Geochimica et Cosmochimica Acta **70:** 918-930.

HORNBERGER, M. I., S. N. LUOMA, A. VAN GEEN, C. FULLER, and R. ANIMA. 1999. Historical trends of metals in the sediments of San Francisco Bay, California. Marine Chemistry **64:** 39-55.

HORVAT, M., L. LIANG, and N. S. BLOOM. 1993. Comparison of distillation with other current isolation methods for the determination of methyl mercury compounds in low level environmental samples: Part II. Water. Analytica Chimica Acta **282:** 153-168.

HUISMAN, J., and F. J. WEISSING. 1999. Biodiversity of plankton by species oscillations and chaos. Nature **402:** 407-410.

HURST, M. P., and K. W. BRULAND. 2005. The use of Nafion-coated thin mercury film electrodes for the determination of the dissolved copper speciation in estuarine water. Analytica Chimica Acta **546:** 68-78.

HUTCHINSON, G. E. 1961. The paradox of the plankton. American Naturalist **95:** 137-145.

INGRI, J., S. NORDLING, J. LARSSON, J. RONNEGARD, N. NILSSON, I. RODUSHKIN, R. DAHLQVIST, P. ANDERSSON, and O. GUSTAFSSON. 2004. Size distribution of colloidal trace metals and organic carbon during a coastal bloom in the Baltic Sea. Marine Chemistry **91:** 117-130.

JASSBY, A. D., J. E. CLOERN, and B. E. COLE. 2002. Annual primary production: Patterns and mechanisms of change in a nutrient-rich tidal ecosystem. Limnology and Oceanography **47:** 698-712.

KERIN, E. J., C. C. GILMOUR, E. RODEN, M. T. SUZUKI, J. D. COATES, and R. P. MASON. 2006. Mercury methylation by dissimilatory iron-reducing bacteria. Applied and Environmental Microbiology **72:** 7919-7921.

KIM, E.-H., R. P. MASON, E. T. PORTER, and H. L. SOULEN. 2004a. The effect of resuspension on the fate of total mercury and methyl mercury in a shallow estuarine ecosystem: A mesocosm study. Marine Chemistry **86:** 121-137.

KIM, K. Y., D. J. GARBARY, and J. L. MCLACHLAN. 2004b. Phytoplankton dynamics in Pomquet Harbour, Nova Scotia: A lagoon in the southern Gulf of St Lawrence. Phycologia **43:** 311-328.

KIMMERER, W. 2005. Long-term changes in apparent uptake of silica in the San Francisco estuary. Limnology and Oceanography **50:** 793-798.

KOMÁREK, J., J. KOPECKY, and V. CEPÁK. 1999. Generic characters of the simplest cyanoprokaryotes *Cyanobium*, *Cyanobacterium* and *Synechococcus*. Cryptogamie Algologie **20:** 209-222.

KOZELKA, P. B., and K. W. BRULAND. 1998. Chemical speciation of dissolved Cu, Zn, Cd, Pb in Narragansett Bay, Rhode Island. Marine Chemistry **60:** 267-282.

KOZELKA, P. B., S. SANUDO-WILHELMY, A. R. FLEGAL, and K. W. BRULAND. 1997. Physico-chemical speciation of lead in South San Francisco Bay. Estuarine Coastal and Shelf Science **44:** 649-658.

LAURIER, F. J. G., D. COSSA, J. L. GONZALEZ, E. BREVIERE, and G. SARAZIN. 2003. Mercury transformations and exchanges in a high turbidity estuary: The role of organic matter and amorphous oxyhydroxides. Geochimica et Cosmochimica Acta **67:** 3329-3345.

LAWSON, N. M., and R. P. MASON. 1998. Accumulation of mercury in estuarine food chains. Biogeochemistry **40:** 235-247.

LEHMAN, P. W. 2000. The influence of climate on phytoplankton community biomass in San Francisco Bay Estuary. Limnology and Oceanography **45:** 580-590.

LUENGEN, A. C., N. S. BLOOM, and A. R. FLEGAL. submitted. Depletion of dissolved methyl mercury by a phytoplankton bloom in San Francisco Bay.

LUENGEN, A. C., P. T. RAIMONDI, and A. R. FLEGAL. 2007. Contrasting biogeochemistry of six trace metals during the rise and decay of a spring phytoplankton bloom in San Francisco Bay. Limnology and Oceanography **52:** 1112-1130.

LUOMA, S. N., A. VAN GEEN, B.-G. LEE, and J. E. CLOERN. 1998. Metal uptake by phytoplankton during a bloom in South San Francisco Bay: Implications for metal cycling in estuaries. Limnology and Oceanography **43:** 1007-1016.

MAHAFFEY, K. R. 2000. Recent advances in recognition of low-level methylmercury poisoning. Current Opinion in Neurology **13:** 699-707.

MARGALEF, R. 1958. Temporal succession and spatial heterogeneity in phytoplankton. *In* A. A. Buzzati-Traverso [ed.], Perspectives in marine biology. University of California Press.

MARSHALL, H. G., and R. W. ALDEN. 1990. A comparison of phytoplankton assemblages and environmental relationships in three estuarine rivers of the Lower Chesapeake Bay. Estuaries **13:** 287-300.

MARTIN, J. H., and G. A. KNAUER. 1973. The elemental composition of plankton. Geochimica et Cosmochimica Acta **37:** 1639-1653.

MARVIN-DIPASQUALE, M., and J. L. AGEE. 2003. Microbial mercury cycling in sediments of the San Francisco Bay Delta. Estuaries **26:** 1517-1528.

MASON, R. P., E.-H. KIM, J. CORNWELL, and D. HEYES. 2006. An examination of the factors influencing the flux of mercury, methylmercury and other constituents from estuarine sediment. Marine Chemistry **102:** 96-110.

MASON, R. P., J. R. REINFELDER, and F. M. M. MOREL. 1995. Bioaccumulation of mercury and methylmercury. Water, Air, and Soil Pollution **80:** 915-921.

---. 1996. Uptake, toxicity, and trophic transfer of mercury in a coastal diatom. Environmental Science and Technology **30:** 1835-1845.

MAY, C. L., J. R. KOSEFF, L. V. LUCAS, J. E. CLOERN, and D. H. SCHOELLHAMER. 2003. Effects of spatial and temporal variability of turbidity on phytoplankton blooms. Marine Ecology Progress Series: 111-128.

MICHAELS, A. F., and A. R. FLEGAL. 1990. Lead in marine planktonic organisms and pelagic food webs. Limnology and Oceanography **35:** 287-295.

MILLER, C. A., P. M. GLIBERT, G. M. BERG, and M. R. MULHOLLAND. 1997. Effects of grazer and substrate amendments on nutrient and plankton dynamics in estuarine enclosures. Aquatic Microbial Ecology **12:** 251-261.

MILLS, E. L. 1989. Biological oceanography: An early history, 1870-1960. Cornell University Press.

MONSON, B. A., and P. L. BREZONIK. 1998. Seasonal patterns of mercury species in water and plankton from softwater lakes in Northeastern Minnesota. Biogeochemistry **40:** 147-162.

MOREL, F. M. M., A. J. MILLIGAN, and M. A. SAITO. 2004. Marine bioinorganic chemistry. The role of trace metals in the oceanic cycles of major nutrients. Treatise on Geochemistry **6:** 113-143.

MOURENTE, G., L. M. LUBIAN, and J. M. ODRIOZOLA. 1990. Total fatty acid composition as a taxonomic index of some marine microalgae used as food in marine aquaculture. Hydrobiologia **203:** 147-154.

MOYE, H. A., J. MILES CARL, J. PHLIPS EDWARD, B. SARGENT, and K. MERRITT KRISTEN. 2002. Kinetics and uptake mechanisms for monomethylmercury between freshwater algae and water. Environmental Science and Technology **36:** 3550-3555.

NICHOLS, F. H., J. E. CLOERN, S. N. LUOMA, and D. H. PETERSON. 1986. The modification of an estuary. Science **231:** 567-573.

NIKOLAIDES, G., and M. MOUSTAKA-GOUNI. 1990. The structure and dynamics of phytoplankton assemblages from the inner part of the Thermaikos Gulf, Greece. I. Phytoplankton composition and biomass from May 1988 to April 1989. Helgoland Marine Research **V44:** 487-501.

OLSON, B. H., and R. C. COOPER. 1974. *In situ* methylation of mercury in estuarine sediment. Nature **252:** 682-683.

PAERL, H. W. 1999. Physical-chemical constraints on cyanobacterial growth in the oceans. Bulletin de l'Institut océanographique, Monaco **19:** 319-349.

PALENIK, B., and A. R. FLEGAL. 1999. Cyanobacterial populations in San Francisco Bay, p. 1-3. San Francisco Estuary Institute, RMP Contribution #42.

PARKER, J. L., and N. S. BLOOM. 2005. Preservation and storage techniques for low-level aqueous mercury speciation. Science of the Total Environment **337:** 253-263.

PHINNEY, J. T., and K. W. BRULAND. 1997a. Effects of dithiocarbamate and 8-hydroxyquinoline additions on algal uptake of ambient copper and nickel in South San Francisco Bay water. Estuaries **20:** 66-76.

---. 1997b. Trace metal exchange in solution by the fungicides Ziram and Maneb (Dithiocarbamates) and subsequent uptake of lipophilic organic zinc, copper and lead complexes into phytoplankton cells. Environmental Toxicology and Chemistry **16:** 2046-2053.

PICKHARDT, P. C., and N. S. FISHER. 2007. Accumulation of inorganic and monomethylmercury by freshwater phytoplankton in two contrasting water bodies. Environmental Science and Technology **41:** 125-131.

PICKHARDT, P. C., C. L. FOLT, C. Y. CHEN, B. KLAUE, and J. D. BLUM. 2002. Algal blooms reduce the uptake of toxic methylmercury in freshwater food webs. Proceedings of the National Academy of Sciences of the United States of America **99:** 4419-4423.

---. 2005. Impacts of zooplankton composition and algal enrichment on the accumulation of mercury in an experimental freshwater food web. Science of the Total Environment **339:** 89-101.

PINCKNEY, J. L., D. F. MILLIE, B. T. VINYARD, and H. W. PAERL. 1997. Environmental controls of phytoplankton bloom dynamics in the Neuse River Estuary, North Carolina, U.S.A. Canadian Journal of Fisheries and Aquatic Sciences **54:** 2491-2501.

PRASAD, A. K. S. K., and J. A. NIENOW. 2006. The centric diatom genus *Cyclotella*, (Stephanodiscaceae: Bacillariophyta) from Florida Bay, USA, with special reference to *Cyclotella choctawhatcheeana* and *Cyclotella desikacharyi*, a new marine species related to the *Cyclotella striata* complex. Phycologia **45:** 127-140.

QUINN, G. P., and M. J. KEOUGH. 2002. Experimental design and data analysis for biologists. Cambridge University Press.

RIEDEL, G. F., J. G. SANDERS, and R. W. OSMAN. 1999. Biogeochemical control on the flux of trace elements from estuarine sediments: effects of seasonal and short-term hypoxia. Marine Environmental Research **47:** 349-372.

RIVERA-DUARTE, I., and A. R. FLEGAL. 1997. Porewater gradients and diffusive benthic fluxes of Co, Ni, Cu, Zn, and Cd in San Francisco Bay. Croatica Chemica Acta **70:** 389-417.

ROITZ, J. S., A. R. FLEGAL, and K. W. BRULAND. 2002. The biogeochemical cycling of manganese in San Francisco Bay: Temporal and spatial variations in surface water concentrations. Estuarine Coastal and Shelf Science **54:** 227-239.

RYNEARSON, T. A., J. A. NEWTON, and E. V. ARMBRUST. 2006. Spring bloom development, genetic variation, and population succession in the planktonic diatom *Ditylum brightwellii*. Limnology and Oceanography **51:** 1249-1261.

SAÑUDO-WILHELMY, S. A., A. TOVAR-SANCHEZ, N. S. FISHER, and A. R. FLEGAL. 2004. Examining dissolved toxic metals in U.S. estuaries. Environmental Science and Technology **38:** 34A-38A.

SCHÄFER, J., G. BLANC, S. AUDRY, D. COSSA, and C. BOSSY. 2006. Mercury in the Lot-Garonne River system (France): Sources, fluxes and anthropogenic component. Applied Geochemistry **21:** 515-527.

SCHEFFER, M., S. RINALDI, J. HUISMAN, and F. J. WEISSING. 2003. Why plankton communities have no equilibrium: Solutions to the paradox. Hydrobiologia **491:** 9-18.

SCHWARZBACH, S. E., J. D. ALBERTSON, and C. M. THOMAS. 2006. Effects of predation, flooding, and contamination on reproductive success of California Clapper Rails (*Rallus longirostris obsoletus*) in San Francisco Bay. The Auk **123:** 45-60.

SEDLAK, D. L., J. T. PHINNEY, and W. W. BEDSWORTH. 1997. Strongly complexed Cu and Ni in wastewater effluents and surface runoff. Environmental Science and Technology **31:** 3010-3016.

SHOLKOVITZ, E. R., and D. COPLAND. 1981. The coagulation, solubility and adsorption properties of Fe, Mn, Cu, Ni, Cd, Co and humic acids in a river water. Geochimica et Cosmochimica Acta **45:** 181-189.

SMAYDA, T. J. 1997. What is a bloom? A commentary. Limnology and Oceanography **42:** 1132-1136.

SMITH, S. V., and J. T. HOLLIBAUGH. 2006. Water, salt, and nutrient exchanges in San Francisco Bay. Limnology and Oceanography **51:** 504–517.

SMITHSONIAN ENVIRONMENTAL RESEARCH CENTER. 2007. Phytoplankton Guide, http://www.serc.si.edu/labs/phytoplankton/guide/diatoms/cylindnitz.jsp.

SOBCZAK, W. V., J. E. CLOERN, A. D. JASSBY, and A. B. MULLER-SOLGER. 2002. Bioavailability of organic matter in a highly disturbed estuary: The role of detrital and algal resources. Proceedings of the National Academy of Sciences of the United States of America **99:** 8101-8105.

STEDING, D. J., C. E. DUNLAP, and A. R. FLEGAL. 2000. New isotopic evidence for chronic lead contamination in the San Francisco Bay estuary system: Implications for the persistence of past industrial lead emissions in the

biosphere. Proceedings of the National Academy of Sciences of the United States of America **97:** 11181-11186.

STORDAL, M. C., G. A. GILL, L. S. WEN, and P. H. SANTSCHI. 1996. Mercury phase speciation in the surface waters of three Texas estuaries: Importance of colloidal forms. Limnology and Oceanography **41:** 52-61.

STUMM, W., and J. J. MORGAN. 1996. Aquatic chemistry: Chemical equilibria and rates in natural waters, 3rd ed. John Wiley and Sons, Inc.

SUNDA, W. G., and S. A. HUNTSMAN. 1996. Antagonisms between cadmium and zinc toxicity and manganese limitation in a coastal diatom. Limnology and Oceanography **41:** 373-387.

---. 1998a. Interactions among Cu^{2+}, Zn^{2+}, and Mn^{2+} in controlling cellular Mn, Zn, and growth rate in the coastal alga *Chlamydomonas*. Limnology and Oceanography **43:** 1055-1064.

---. 1998b. Interactive effects of external manganese, the toxic metals copper and zinc, and light in controlling cellular manganese and growth in a coastal diatom. Limnology and Oceanography **43:** 1467-1475.

---. 1998c. Processes regulating cellular metal accumulation and physiological effects: Phytoplankton as model systems. Science of the Total Environment **219:** 165-181.

SUNDERLAND, E. M., F. GOBAS, B. A. BRANFIREUN, and A. HEYES. 2006. Environmental controls on the speciation and distribution of mercury in coastal sediments. Marine Chemistry **102:** 111-123.

THOMAS, M. A., C. H. CONAWAY, D. J. STEDING, M. MARVIN-DIPASQUALE, K. E. ABU-SABA, and A. R. FLEGAL. 2002. Mercury contamination from historic mining in water and sediment, Guadalupe River and San Francisco Bay, California. Geochemistry: Exploration, Environment, Analysis **2:** 211-217.

THOMPSON, B., R. HOENICKE, J. A. DAVIS, and A. GUNTHER. 2000. An overview of contaminant-related issues identified by monitoring in San Francisco Bay. Environmental Monitoring and Assessment **64:** 409-419.

THOMPSON, J. K., and F. H. NICHOLS. 1988. Food availability controls seasonal cycle of growth in *Macoma Balthica* (L.) in San Francisco Bay, California. Journal of Experimental Marine Biology and Ecology **116:** 43-62.

TOVAR-SÁNCHEZ, A., S. A. SAÑUDO-WILHELMY, and A. R. FLEGAL. 2004. Temporal and spatial variations in the biogeochemical cycling of cobalt in two urban estuaries: Hudson River Estuary and San Francisco Bay. Estuarine, Coastal, and Shelf Science **60:** 717-728.

TURNER, A., G. E. MILLWARD, and S. M. LE ROUX. 2004. Significance of oxides and particulate organic matter in controlling trace metal partitioning in a contaminated estuary. Marine Chemistry **88:** 179-192.

TURNER, A., G. E. MILLWARD, and R. S. M. LE. 2001. Sediment-water partitioning of inorganic mercury in estuaries. Environmental Science and Technology **35:** 4648-4654.

WACKER, A., and E. VON ELERT. 2004. Food quality controls egg quality of the zebra mussel *Dreissena polymorpha*: The role of fatty acids. Limnology and Oceanography **49:** 1794-1801.

WATRAS, C. J., and N. S. BLOOM. 1992. Mercury and methylmercury in individual zooplankton: Implications for bioaccumulation. Limnology and Oceanography **37:** 1313-1318.

WETZEL, R. G., and G. E. LIKENS. 1991. Limnological analyses, 2nd ed. Springer-Verlag.

WILKERSON, F. P., R. C. DUGDALE, V. E. HOGUE, and A. MARCHI. 2006. Phytoplankton blooms and nitrogen productivity in San Francisco Bay. Estuaries and Coasts **29:** 401-416.

XU, H., and B. ALLARD. 1991. Effects of a fulvic acid on the speciation and mobility of mercury in aqueous solutions. Water, Air, and Soil Pollution **56:** 709-717.

ZWOLSMAN, J. J. G., and G. T. M. VAN ECK. 1999. Geochemistry of major elements and trace metals in suspended matter of the Scheldt estuary, southwest Netherlands. Marine Chemistry **66:** 91-111.